MINISTRY OF HIGHER EDUCATION AND SCIENTIFIC RESEARCH

UNIVERSITY OF BABYLON
COLLEGE OF ENGINEERING
DEPARTMENT OF CIVIL ENGINEERING

ELASTO-PLASTIC FINITE ELEMENT ANALYSIS OF THICK METAL PLATES UNDER TRANSVERSE DYNAMIC LOADS

A

THESIS

SUBMITTED TO THE COLLEGE OF ENGINEERING OF THE UNIVERSITY OF BABYLON IN PARTIAL FULFILLMENT OF THE REQUIREMENTS FOR THE DEGREE OF MASTER OF SCIENCE IN STRUCTURAL ENGINEERING

By

Abeer Saed Zbala Al-Kraway

B. Sc. 2004

SUPERVISED BY

Asst. Prof. Dr. Nameer A. Alwash

Asst. Prof. Dr. Mustafa B. Dawood

2007

أطروحة
مقدمة إلى جامعة بابل – كلية الهندسة
وهي جزء من متطلبات نيل درجة
ماجستير علوم في الهندسة
المدنيـــــة

من قبل

عيس سعيد زبالة الكرعاوي

باشراف

د. نمير عبد الامير علوش

د. مصطفى بلاسم داود

٢٠٠٧

بسم الله الرحمن الرحيم

﴿ وَيَسْأَلُونَكَ عَنِ الرُّوحِ قُلِ الرُّوحُ مِنْ أَمْرِ رَبِّي وَمَا أُوتِيتُم مِّنَ الْعِلْمِ إِلَّا قَلِيلًا ﴾

صدق الله العظيم

سورة الاسراء /الايه (٨٥)

Abstract

In this study, the analysis of thick plates under transverse dynamic load is performed using the ***incremental finite element method***. The 8 – noded isoparametric quadrilateral element is used for discretization the plates with three degrees of freedom per node ,which are one displacement and two rotations.

For thick plates, the effect of transverse shear stresses as well as transverse direct stress on its behavior is of great importance. In this analysis the effect of transverse shear stresses is included while the transverse direct stress is ignored. Modified expressions for transverse shear strains which permit a parabolic distribution for these strains across the plate thickness are utilized in the present work.

The derivations of the stiffness, mass and damping matrices for plate element is presented in this study. The ***consistent mass matrix*** is adopted. Also, the damping effect is included by using ***Rayleigh type damping***.

The dynamic analysis is performed by using ***Newmark*** method with $\gamma=0.5$ and $\beta=0.25$, i.e., ***constant average acceleration*** method.

A computer program (***EPDATP***) is developed by using ***Fortran 77 language*** to deal with the considered problem (the original version of this program was introduced by Alwash in 1989 for elasto-plastic analysis of thick plates under static loads). This program is used to analyze several examples presented by others. Consequently, it is found that the present study has a good agreement with the previous studies, with maximum difference in the dynamic analysis (as a percentage of the data which was presented by others) is not more than (10%). The effect of several analysis parameters is investigated and it is concluded that the effect of damping in the present problem is significant and can not be neglected.

الخلاصة

في هذا البحث تم دراسة التحليل للصفائح السميكه المعرضة لاحمال ديناميكية باستخدام طريقة العناصر المحددة التزايديه (Incremental Finite elements method). تم توظيف عنصر ذي ثمانية عقد (nodes) لتمثيل الصفائح مع ثلاث درجات حرية لكل عقدة متمثلة بازاحة ودورا نين.
في الصفائح السميكة يكون تاثيركل من اجهادات القص المستعرضة (transverse shear stresses) والاجهاد المباشر المستعرض (transverse direct stress) على نحو كبير من الاهمية,التحليل المستخدم في هذا البحث يتضمن اجهادات القص المستعرضة بينما يهمل الاجهاد المباشر المستعرض. لقد تم استخدام صيغ معدلة لانفعالات القص المستعرضة (transverse shear stains) والتي تسمح بالتوزيع القطعي المكافئ (parabolic distribution) لمثل هذه الانفعالات على سمك الصفيحة.
في هذه الدراسة تم عرض اشتقاق مصفوفات الجسائة (Stiffness matrix) والكتلة (Mass matrix) والاخماد (Damping matrix) لعنصر الصفيحة, حيث تم اعتماد مصفوفة الكتلة المتوافقة (Consistent mass matrix). كذلك تم استخدام مصفوفة اخماد رايلي (Rayleigh type damping matrix) للتعبير عن خواص الاخماد.
من اجل انجاز التحليل الديناميكي تبنت الدراسة اسلوب نيو مارك (Newmark method) وبالتحديد طريقة المعدل الثابت للتعجيل (Constant average acceleration method).
في هذه الدراسة تم تطوير برنامج حاسوب (EPDATP) بلغة فورتران 77 (Fortran 77)(البرنامج الأصلي تم كتابته من قبل نمير عبد الامير علوش -1989 للتحليل المرن اللدن للصفائح السميكة المعرضة لأحمال استاتيكية), ولقد تم تقييم اداء البرنامج عن طريق مقارنة النتائج المستحصلة باستخدام هذا البرنامج مع تلك المستحصلة من دراسات منشورة سابقا لمجموعة من الامثلة. وقد اظهرت المقارنة بين نتائج النظريات والطرق المعتمدة في هذا البحث والنتائج المتوفرة من الدراسات السابقة توافقا جيدا, حيث ان النسبة المئوية للاختلافات بالنسبة للتحليل الديناميكي كانت بحدود (10%).
كذلك فقد تم فحص تاثير بعض معاملات التحليل على النتائج وقد تبين ان تاثير الاخماد في هذه المسالة مهم ولايمكن اهماله.

List of Contents

Acknowledgement

In The Name of Allah, The Gracious, The Merciful

First of all; all thanks to Allah who gave me the power to achieve this study.

I would like to extend my deep thanks, gratitude and appreciation to my supervisors ***Asst. Prof. Dr. Nameer A. Alwash*** and ***Asst. Prof. Dr. Mustafa B. Dawood*** for their invaluable guidance, helpful and encouragement throughout the preparation of this work.

Special thanks is devoted to my family for care, and encouragement during this work.

Finally, thanks to all who helped me in one way or another to bring out this work, specially my friends Zainab Hassan, Abeer Ibrahem, Norus Nomas, Sheren Qassim and Rand Sami.

Abeer Saed
2007

$$
\begin{bmatrix}
m_{11} & 0 & 0 & m_{12} & 0 & 0 & m_{13} & 0 & 0 & m_{14} & 0 & 0 & m_{15} & 0 & 0 & m_{16} & 0 & 0 & m_{17} & 0 & 0 & m_{18} & 0 & 0 \\
0 & m_{11} & 0 & 0 & m_{12} & 0 & 0 & m_{13} & 0 & 0 & m_{14} & 0 & 0 & m_{15} & 0 & 0 & m_{16} & 0 & 0 & m_{17} & 0 & 0 & m_{18} & 0 \\
0 & 0 & m_{11} & 0 & 0 & m_{12} & 0 & 0 & m_{13} & 0 & 0 & m_{14} & 0 & 0 & m_{15} & 0 & 0 & m_{16} & 0 & 0 & m_{17} & 0 & 0 & m_{18} \\
m_{21} & 0 & 0 & m_{22} & 0 & 0 & m_{23} & 0 & 0 & m_{24} & 0 & 0 & m_{25} & 0 & 0 & m_{26} & 0 & 0 & m_{27} & 0 & 0 & m_{28} & 0 & 0 \\
0 & m_{21} & 0 & 0 & m_{22} & 0 & 0 & m_{23} & 0 & 0 & m_{24} & 0 & 0 & m_{25} & 0 & 0 & m_{26} & 0 & 0 & m_{27} & 0 & 0 & m_{28} & 0 \\
0 & 0 & m_{21} & 0 & 0 & m_{22} & 0 & 0 & m_{23} & 0 & 0 & m_{24} & 0 & 0 & m_{25} & 0 & 0 & m_{26} & 0 & 0 & m_{27} & 0 & 0 & m_{28} \\
m_{31} & 0 & 0 & m_{32} & 0 & 0 & m_{33} & 0 & 0 & m_{34} & 0 & 0 & m_{35} & 0 & 0 & m_{36} & 0 & 0 & m_{37} & 0 & 0 & m_{38} & 0 & 0 \\
0 & m_{31} & 0 & 0 & m_{32} & 0 & 0 & m_{33} & 0 & 0 & m_{34} & 0 & 0 & m_{35} & 0 & 0 & m_{36} & 0 & 0 & m_{37} & 0 & 0 & m_{38} & 0 \\
0 & 0 & m_{31} & 0 & 0 & m_{32} & 0 & 0 & m_{33} & 0 & 0 & m_{34} & 0 & 0 & m_{35} & 0 & 0 & m_{36} & 0 & 0 & m_{37} & 0 & 0 & m_{38} \\
m_{41} & 0 & 0 & m_{42} & 0 & 0 & m_{43} & 0 & 0 & m_{44} & 0 & 0 & m_{45} & 0 & 0 & m_{46} & 0 & 0 & m_{47} & 0 & 0 & m_{48} & 0 & 0 \\
0 & m_{41} & 0 & 0 & m_{42} & 0 & 0 & m_{43} & 0 & 0 & m_{44} & 0 & 0 & m_{45} & 0 & 0 & m_{46} & 0 & 0 & m_{47} & 0 & 0 & m_{48} & 0 \\
0 & 0 & m_{41} & 0 & 0 & m_{42} & 0 & 0 & m_{43} & 0 & 0 & m_{44} & 0 & 0 & m_{45} & 0 & 0 & m_{46} & 0 & 0 & m_{47} & 0 & 0 & m_{48} \\
m_{51} & 0 & 0 & m_{52} & 0 & 0 & m_{53} & 0 & 0 & m_{54} & 0 & 0 & m_{55} & 0 & 0 & m_{56} & 0 & 0 & m_{57} & 0 & 0 & m_{58} & 0 & 0 \\
0 & m_{51} & 0 & 0 & m_{52} & 0 & 0 & m_{53} & 0 & 0 & m_{54} & 0 & 0 & m_{55} & 0 & 0 & m_{56} & 0 & 0 & m_{57} & 0 & 0 & m_{58} & 0 \\
0 & 0 & m_{51} & 0 & 0 & m_{52} & 0 & 0 & m_{53} & 0 & 0 & m_{54} & 0 & 0 & m_{55} & 0 & 0 & m_{56} & 0 & 0 & m_{57} & 0 & 0 & m_{58} \\
m_{61} & 0 & 0 & m_{62} & 0 & 0 & m_{63} & 0 & 0 & m_{64} & 0 & 0 & m_{65} & 0 & 0 & m_{66} & 0 & 0 & m_{67} & 0 & 0 & m_{68} & 0 & 0 \\
0 & m_{61} & 0 & 0 & m_{62} & 0 & 0 & m_{63} & 0 & 0 & m_{64} & 0 & 0 & m_{65} & 0 & 0 & m_{66} & 0 & 0 & m_{67} & 0 & 0 & m_{68} & 0 \\
0 & 0 & m_{61} & 0 & 0 & m_{62} & 0 & 0 & m_{63} & 0 & 0 & m_{64} & 0 & 0 & m_{65} & 0 & 0 & m_{66} & 0 & 0 & m_{67} & 0 & 0 & m_{68} \\
m_{71} & 0 & 0 & m_{72} & 0 & 0 & m_{73} & 0 & 0 & m_{74} & 0 & 0 & m_{75} & 0 & 0 & m_{76} & 0 & 0 & m_{77} & 0 & 0 & m_{78} & 0 & 0 \\
0 & m_{71} & 0 & 0 & m_{72} & 0 & 0 & m_{73} & 0 & 0 & m_{74} & 0 & 0 & m_{75} & 0 & 0 & m_{76} & 0 & 0 & m_{77} & 0 & 0 & m_{78} & 0 \\
0 & 0 & m_{71} & 0 & 0 & m_{72} & 0 & 0 & m_{73} & 0 & 0 & m_{74} & 0 & 0 & m_{75} & 0 & 0 & m_{76} & 0 & 0 & m_{77} & 0 & 0 & m_{78} \\
m_{81} & 0 & 0 & m_{82} & 0 & 0 & m_{83} & 0 & 0 & m_{84} & 0 & 0 & m_{85} & 0 & 0 & m_{86} & 0 & 0 & m_{87} & 0 & 0 & m_{88} & 0 & 0 \\
0 & m_{81} & 0 & 0 & m_{82} & 0 & 0 & m_{83} & 0 & 0 & m_{84} & 0 & 0 & m_{85} & 0 & 0 & m_{86} & 0 & 0 & m_{87} & 0 & 0 & m_{88} & 0 \\
0 & 0 & m_{81} & 0 & 0 & m_{82} & 0 & 0 & m_{83} & 0 & 0 & m_{84} & 0 & 0 & m_{85} & 0 & 0 & m_{86} & 0 & 0 & m_{87} & 0 & 0 & m_{88}
\end{bmatrix}
$$

(24x24)

Fig.(B.1): The consistent mass matrix for a plate element with 3 degree of freedom per node.

Appendix – B –

The Consistent Mass Matrix for a Plate Element

The consistent mass matrix for a plate element using 8-noded isoparametric element with 3 degree of freedom per node is given in Fig.(B-1)

Where the values for the symbols in the Figure (B-1), m_{11}, m_{12}, ….m_{88}, are as below:-

$$m_{11} = \rho \int_{vol} N_1 N_1 \, d\,vol$$

$$m_{12} = m_{21} = \rho \int_{vol} N_1 N_2 \, d\,vol$$

$$m_{13} = m_{31} = \rho \int_{vol} N_1 N_3 \, d\,vol$$

.

.

.

$$m_{18} = m_{81} = \rho \int_{vol} N_1 N_8 \, d\,vol$$

or in general form:

$$m_{ij} = m_{ji} = \rho \int_{vol} N_i N_j \, d\,vol$$

Where:

N_1, N_2, N_3, …., N_8: shape function for the plane quadratic isoparametric element[5].

ρ = the mass density .

Appendix – A –

Numerical Integration

It may be noted that there are many formulas to carry out the numerical integration, but one of the most formulas which are used for this purpose is ***Gaussian-Quadrature*** formula.

Let $\int_{x1}^{x2} f(x)\,dx$ an integral having arbitrary limits, this integral can be transformed so that it is limits are form -1 to +1 by substitution $X = f(\zeta)$ where $-1 \le \zeta \le 1$

Then, the integral becomes:-

$$\int_{x1}^{x2} f(x)\,dx = \int_{-1}^{+1} f(\zeta)\, J\, d\xi = \int_{-1}^{+1} \phi\, d\zeta = L \qquad \ldots(A.1)$$

where:

$$\frac{dx}{d\zeta} = J$$

J is called a ***Jacobian***. It can be regarded as a scale factor that describes the physical length dx associated with a reference length dζ, that is, $dx = J\, d\zeta$.

Now, to approximate the integral in the simplest way, one can sample (evaluate) ϕ at the midpoint $\zeta = 0$ and multiply by the length of the interval (Fig.(A.1)(a)).

Thus one approximates the shaded area by a rectangular area of height ϕ_1 and length 2, so that $L \approx 2\phi_1$. This result is exact if $\phi = f(\zeta)$ happens to describe a straight line of any finite slope.

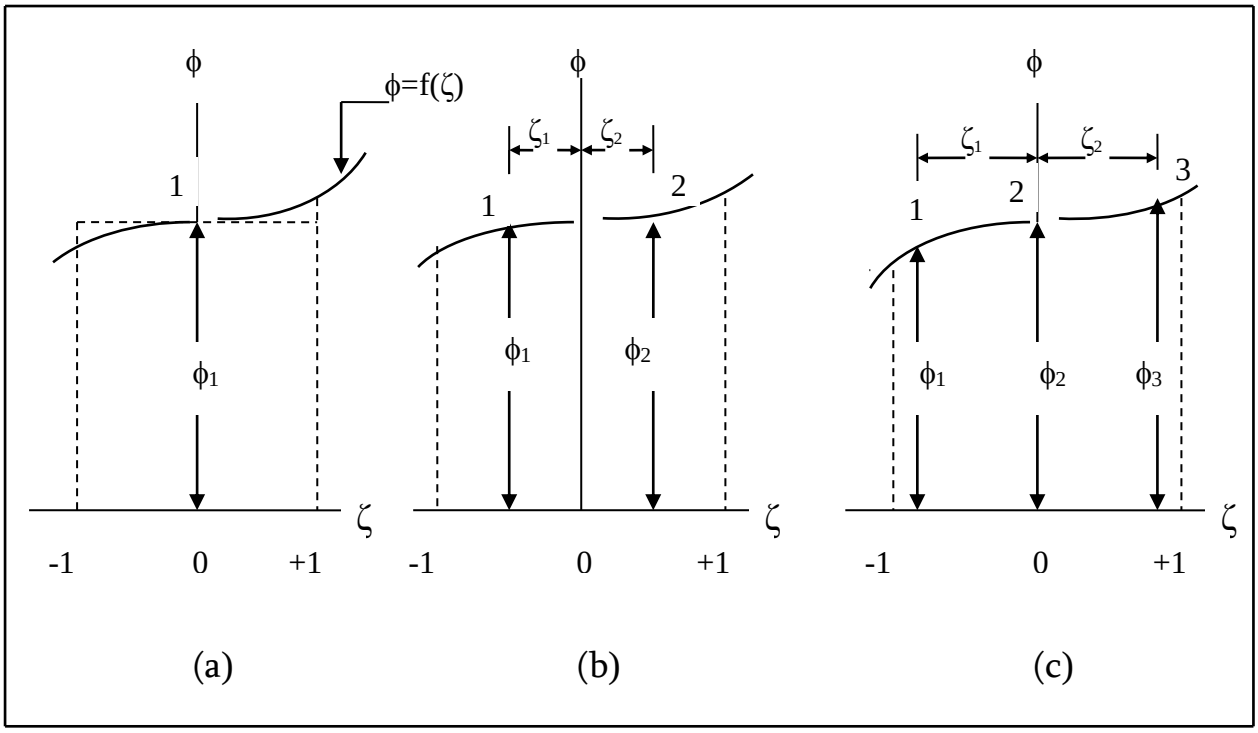

Fig. (A.1) : *Gauss quadrature to compute the shaded area under the curve $\phi = f(\zeta)$, using (a)one, (b)two, (c)three sampling points (also called Gauss points). [17]*

Generalization of the foregoing procedure leads to the quadrature formula

$$L = \int_{-1}^{+1} \phi \, d\zeta = W_1 \, \phi_1 + W_2 \, \phi_2 + \cdots + W_n \, \phi_n \qquad \ldots(A.2)$$

Thus, to approximate L, evaluate $\phi = f(\zeta)$ at each of several locations ζ. To obtain ordinates ϕ_n, multiply each ϕ_n by an appropriate weight W_n and add. For example $L = 2\phi_1$ where n = 1 and $W_n = 2$. Sampling points are located symmetrically with respect to the center of the integration interval.
Symmetrically paired points have the same weight W.

The values of the weight factor W_n, and the location ζ of sampling points for n = 2,3,…..,15 points formulas are shown in table (A-1).

Table (A.1): sampling points and weights for Gauss Quadrature over the interval ζ = -1 to ζ = +1 [24].

Order n	Location ζ of sampling point	Weight Factor (W_i)
2	± 0.57735 02691 89626	1.00000 00000 00000
3	0.00000 00000 00000 ± 0.77459 66692 41483	0.88888 88888 88889 0.55555 55555 555556
4	± 0.33998 10435 84856 ± 0.86113 63115 94053	0.65214 51548 62546 0.34785 48451 37454
5	0.00000 00000 00000 ± 0.53846 93101 05683 ± 0.90617 98459 38664	0.56888 88888 88889 0.47862 86704 99366 0.23692 68850 56189
6	± 0.23861 91860 83197 ± 0.66120 93864 66256 ± 0.93246 95142 03152	0.46791 39345 72691 0.36076 15730 48139 0.17132 44923 79170
10	± 0.14887 43389 81631 ± 0.43339 53941 29247 ± 0.67940 95682 99024 ± 0.86506 33666 88935 ± 0.97390 65285 17172	0.29552 42247 14753 0.26926 67193 09996 0.21908 63625 15982 0.14945 13491 50581 0.06667 13443 08688
15	0.00000 00000 00000 ± 0.20119 40939 97435 ± 0.39415 13470 77563 ± 0.57097 21726 08539 ± 0.72441 77313 60170 ± 0.84820 65834 10427 ± 0.93727 33924 00706 ± 0.98799 25180 20485	0.20257 82419 25561 0.19843 14853 27111 0.18616 10001 15562 0.16626 92058 16994 0.13957 06779 26154 0.10715 92204 67172 0.07036 60474 88108 0.03075 32419 96117

List of Tables

Notation

Symbol	Description
a	Plate dimension in x-direction
b	Plate dimension in y-direction
q	Transverse uniform load
P	Transverse concentrated load
u	Displacement in global x-direction
v	Displacement in global y-direction
w	Displacement in global z-direction
x, y, z	Global Cartesian coordinate system
ξ , η , ζ	Isoperimetric coordinates.
σ_x , σ_y , σ_z	Normal Stresses in Cartesian coordinates
τ_{xy} , τ_{yz} , τ_{zx}	Shear Stresses in Cartesian coordinates
ε_x , ε_y , ε_z	Normal Strain in Cartesian coordinates
γ_{xy} , γ_{yz} , γ_{zx}	Shear Strain in Cartesian coordinates
E	Modulus of elasticity
ν	Poisson's ratio
G	Shear modulus of elasticity
h	Plate thickness
[B]	Strain- nodal variables matrix
$[J]$	Jacobian matrix
$\{d\}$	Nodal displacements vector for an element
[K] , [k]	Global and element Stiffness matrices, respectively
[M] , [m]	Global and element mass matrices, respectively
$\dot{}$ $\ddot{}$ [D] ,[D], [D]	The nodal displacement, velocity and acceleration vectors, respectively
[C]	Global damping matrix
ρ	The mass density for plate material
β, γ	Newmark constants
z_1 , z_2	The proportionality factors that used in Rayleigh damping in the formulation of damping matrix
ξ_i	The ith damping ratio
$d\lambda$	A non-negative scalar
$d\varepsilon_{ep}$	Total strain increments
$d\varepsilon_e$	Elastic strain increments
$d\varepsilon_p$	Plastic strain increments

$d\bar{\sigma}$	Effective stress increment
$d\bar{\varepsilon}_p$	Effective strain increment
σ_1 , σ_2 , σ_3	Principal stresses
ε_1, ε_2, ε_3	Principal strians
$\bar{\sigma}$	Effective stress
ε_y	Yield strain in simple tension(or compression)
σ_Y	Yield stress in simple tension(or compression)
L_0	Plate span to thickness ratio (for rectangle plates)
R_0	Plate radius to thickness ratio (for circular plates)
R	Radius of circular plates

Note: Any other notation may be explained where it appears

List of Figures

CERTIFICATION

We certify that the preparation of this thesis titled **"*Elasto-Plastic Finite Element Analysis Of Thick Metal Plates under Transverse Dynamic Loads*"**, which is being submitted by ***Abeer Saed Zbala Al-Kraway,*** was under our supervision at the University of Babylon in fulfillment of partial requirements for the degree of Master of Science in Civil Engineering (Structural Engineering).

Signature:

Name: ***Asst. Prof. Dr. Nameer A.Alwash***

(Supervisor)

Date: / / 2007

Signature:

Name: ***Asst. Prof. Dr. Mustafa B.Dawood***

(Supervisor)

Date: / / 2007

CERTIFICATION

We certify as an examining committee that we have read this thesis titled "***Elasto-Plastic Finite Element Analysis Of Thick Metal Plates under Transverse Dynamic Loads***", and examined the student ***Abeer Saed Zbala Al-Kraway ,*** in its content and what related to it, and found it meets the standard of a thesis for the degree of Master of Science in Civil Engineering (Structural Engineering).

Signature:

Name: ***Asst. Prof. Dr. Nameer A.Alwash***
(Supervisor)
Date: / / 2007

Signature:

Name: ***Asst. Prof. Dr. Mustafa B.Dawood***
(Supervisor)
Date: / / 2007

Signature:

Name: ***Asst. Prof. Dr. Hyder T. Nimnim***
(Member)
Date: / / 2007

Signature:

Name: ***Asst. Prof. Abdul Ridah Saleh***
(Member)
Date: / / 2007

Signature:

Name: ***Asst. Prof. Dr. Haitham H. Aldaami***
(Chairman)
Date: / / 2007

Approval of the Civil Engineering Department

Signature:

Name: ***Asst. Prof. Dr. Ammar Y. Ali***

Head of the Civil Engineering Department

Date: / / 2007

Approval of the Deanery of the College of Engineering

Signature:

Name: ***Asst. Prof. Dr. Abdul- Wahed K. Rajih***

Dean of the College of Engineering

Date: / / 2007

CHAPTER ONE

INTRODUCTION

1.1 General

Structural components made of plate elements often find applications in the construction of mechanical and nuclear structures dams, footings and other structures. They are, in general, subjected to various types of dynamic loads. So, the prediction of the dynamic analysis of plates is of interest and importance in the design of such structures.

When the thickness of a plate increases with respect to the other dimensions, the effects of transverse shear stresses and strains as well as transverse direct stress and strain on elasto-plastic flexural behavior of the plate become of much greater importance than in thin plates and should be considered in the analysis unlike in thin plates in which they are neglected. This is the main difference between "***thick plate***" and "***thin plate***" analyses.

The finite element method which has been applied with great success to the dynamic analysis of plates is presented in this research for predicting the elasto-plastic behavior of thick plates under transverse dynamic loads.

Consistent with the purpose of this thesis, it is necessary to make a basic reference to the two aspects namely: elasto-plastic analysis, and dynamic analysis of plates.

1.2 Elasto-plastic analysis

A fundamental observation comparing elastic and inelastic analysis is that; in elastic solution, the total stress can be evaluated from the total strain alone whereas in an inelastic behavior, the calculation of the total stress at any step depends on the stress and strain history.

Typical inelastic phenomena are elastoplasticity, creep, and viscoplasticity.[9]

Because of the actual ductility of many engineering materials, such as steel, which permits stresses redistribution and increases the capacity of the plate to carry more loading, the elasto-plastic analysis becomes more realistic in describing the full range of material behavior than the elastic analysis.

Several methods of the elasto-plastic analysis were presented in chapter two. Most of the found previous studies were in reality concern with the analysis of plates subjected to static loading or study the dynamic behavior of thin plates. There are some studies for the dynamic behavior for thick plates but they neglected the elasto-plastic behavior. There is therefore, a real need for a general method for predicting the elasto-plastic behavior of thick plates subjected to transverse dynamic loading.

1.3 Dynamic analysis of plates

Certain civil engineering structures are designed to carry their own dead load plus superimposed loads which are immovable and unvarying with time, that is, superimposed static loads. In such cases, the stress analysis involves only principles of statics. More often, the design of a civil

engineering structure involves not only static loads but also superimposed loads which are either moving or movable and may vary with time as in superimposed dynamic loads. In such cases, the stress analysis properly should involve principles of dynamics to determine the effect of dynamic loading.

However, in many of these cases, experience has shown that the dynamic effect makes a minor contribution to the total load which must be provided for the design and therefore the dynamic effect need not be evaluated precisely. In such cases, the dynamic effect may be handled by the use of an equivalent static load, or by an impact factor or by a modification of the factor of safety [19].

On the other hand, in specific situations it may be of real importance to consider more precisely the response produced by dynamic loading and they are classified as follows [29]:

1. When a structure must be designed to resist transient and /or steady state vibrations produced by operating machinery.
2. When a structure must be designed to resist impact loads and vibrations produced by traffic passing over the structure.
3. When a structure must be designed to resist impulsive loads produced by blasts, wind gusts or water waves.
4. When a structure must be designed to resist vibration developed by oscillating motions of its supports, produced by earthquake shocks.
5. When a protective structure must be designed to resist the impact of striking projectiles.

Since the plates components are widely used in engineering structures which are subjected to dynamic loads as explained above. Then, it is of interest to study the dynamic behavior of plates.

1.4 Objectives of Study

The basic objectives of the present work are summarized as follows:

1. Studying the behavior of thick plates under different dynamic loads, step load or impact load.
2. Studying the effect of the elasto-plastic behavior on the plates under dynamic loads.
3. Studying the effect of some analysis parameters such as the boundary condition, the dimensions aspect ratio on the dynamic response for the plate.

1.5 Layout of the thesis

This thesis is organized in six chapters:

Chapter one: introduces and explains briefly the problem within hand, the aim of the study and the subjects included in other chapters.

Chapter two: a review of previous studies on analysis of plates is presented. The review contains studies of nonlinear analysis of plates under static loads and the analysis of plates under dynamic loads.

Chapter three: contains a formulation of the stiffness, mass and damping matrices in case of plate bending element. Also, it includes a discussion of the solution techniques which are adapted to solve the eignvalue problems as well as the dynamic equilibrium equations.

Chapter four: describes the elasto-plastic analysis of plates.

Chapter five: describes the flow chart of the computer program (***EPDATP***) which has been developed in this study by using ***Fortran-77*** language. It, also includes a parametric study that was done on different variables which affect the dynamic response of plates.

Chapter six: gives a summary of the conclusions which can be drawn from this study and the suggestions for future related works.

CHAPTER TWO

REVIEW OF LITERATURE

2.1 Nonlinear analysis of plates subjected to transverse static loads

The nonlinear behaviour of plates subjected to transverse static loading has been the subject of several studies; in this section some of these studies are presented.

Reddy and ***Haung*** [36] in ***1981*** analyzed axisymmetric annular plates with varying thickness using large deflection bending by annular finite-element. The more general Reissner plate equations were used in the formulation. Shear deformation, geometrical nonlinearity and material orthotropy were included in that work. Both static and free vibration analysis were preformed.

Owen and ***Figueiras*** [30] in ***1983*** employed a semiloof curved shell element for the elastic-plastic analysis of plates and shells by means of the finite element displacement method. In that work, the elasto-plastic analysis was based on the Huber-Mises criterion, which was extended for anisotropic materials. The yield function was generalized by introducing anisotropic

parameters of plasticity, which were updated during the material strain hardening history. The analysis was applicable to both perfectly plastic and work hardening materials. The middle surface of the structure was assumed to be a surface of material symmetry and linear geometrical behaviour was assumed.

In their second paper, ***Owen*** and ***Figueiras*** [31] in ***1983*** studied the anisotropic elasto-plastic finite element analysis of thick and thin plates and shells using a degenerate three-dimensional continuum element and a thick shell formulation accounting for shear deformation. A layered approach was used. Plastic yielding was based on the Huber-Mises yield surface. The assumption of a constant transverse shear strain was made, and a correction shear factor was used to approximate the real shear strain energy component.

Striz et al. in ***1988*** [40] presented a paper to study the behavior of thin circular isotropic plates with immovable edges and undergoing large deflections by using the numerical technique of differential quadrature. Approximate results were determined with the aid of a symbolic manipulation computer program and a Newton-Raphson technique to solve the nonlinear systems of equations. Bending stresses, membrane stresses, and deflections were calculated for clamped and simply supported flexural edge conditions and for a uniform pressure load and a concentrated load at the center.

In ***1989 Bert et al.*** [10] presented a study about the behavior of thin, rectangular, orthotropic plates, with immovable edges and undergoing large deflections. The numerical technique of differential quadrature was used.

Approximate results were obtained, using the Newton-Raphson method and, alternatively, a finite-difference-based method to solve the nonlinear systems of equations. Bending stresses, membrane stresses, and deflections were calculated for plates with fully clamped and simply supported flexural edge conditions under uniform pressure loading. Results were compared with existing analytical, numerical, and experimental ones.

In ***1989 Alwash*** [5] presented two methods of evaluating the limit load (Collapase load) for thick plates. The first method was an incremental finite element method by which a complete elasto-plastic behavior of thick plates of any shape with various boundary conditions can be studied. The effect of transverse shear stress was included while the transverse direct stress was ignored. The second method was a lower bond limit analysis , this method includes all stress components. It was used for the analysis of thick annular plates and thick rectangular plates with two type of boundary conditions; simple support and clamped support. The stresses were expressed in terms of an independent set of parameters and a non-linear programming method called (SUMT) method was used to optimize these parameters to get the best lower bound limit load. Among other conclusions it was found that the limit load of very thick plates is drastically smaller than that estimated by thin plate limit analyses which ignore shear and direct transverse stresses.

In ***1994*** an approach of the incompatible elements with additional internal shear strain was suggested and applied to geometrically nonlinear analysis of Mindlin plate bending problem by ***Zhao-ping et al*** [42]. It provided a quite convenient way to avoid the shear locking troubles. The nonlinear element formulations and some numerical results were presented.

In ***1995 Chen*** and ***Austin*** [12] introduced a report described the nonlinear finite element analysis of shell structures. The finite elements were based on a three-dimensional continuum formulation, and were simplified by assuming a flat element geometry. Numerical experiments were presented for in-plane displacements of a flat plate, and out-of-plane bending of a cantilever structure. In each case, material nonlinearities are modeled with bi-linear and Ramberg-Osgood stress-strain curves.

In ***2003*** a C^0 finite element was introduced by ***Kocak*** **and** ***Hassis*** [25] for the analysis of thick plates with transverse shear and normal strain and nonlinear in-plane displacement distribution with respect to the plate thickness. Based on higher order shear deformation theory, an eight-node finite element was introduced for thick plates and a computer program was developed. The warping functions used in the formulations presented simpler equations than the other higher order homogeneous models. Some example problems were solved and the results were compared with the exact and other mathematical solutions. For comparison, both stress and displacement results were investigated. The results of the proposed element were found to be in a good agreement with the literature.

Al-Saeq [4] in ***2005*** introduced a research deals with the optimal elastic-plastic design of plate and shell structures based on elastic-plastic geometrically nonlinear incremental-iterative finite element analysis. The nine-node degenerated curved shell element was used in which five degrees of freedom are specified at each nodal point, which are three displacements and two rotations of the normal at the node. In the case of the material nonlinearity, an elastic-plastic analysis was employed using a generalization of Huber-Mises law as the yield criterion. In his study a layered model was

employed to determine the stress profile through the thickness direction. The transverse shear deformation was permitted and taken into account. The formulation of the geometrical nonlinearity problem was carried out using the well-known total Lagrangian principle. For the structural optimization problem, which was dealt with as a constrained nonlinear optimization, the so-called Modified Hooke and Jeeves method was employed by considering the volume of the structure as the objective function. The results show good agreement especially with experimental works with maximum difference of 7%. Also the results show that the optimal design based on nonlinear analysis gives optimal volume smaller than that based on linear analysis may reach to 25 %.

2.2 Dynamic analysis of plates

The analysis of dynamically loaded structures has received a continuous but varying level of attention over the past 50 years. Due to the infinite number of permutations of structural parameters and due to the costs of performing tests on such structures, there is difficult in find experimental data. So, the theatrical data is used for comparing.

In this section a review of theoretical studies on the dynamic analysis of plates is presented.

Raghavan and ***Rao*** [34] presented a paper in ***1978*** deals with a study of the significance of elasto-plastic transition state in the dynamic response of Euler beams and thin plates. The study was based on a comparative evaluation of the response predicted by two independent approaches that use: (i) stress-strain relation and basic plasticity theory and (ii) moment-

curvature relation; assuming the shape factor to be unity. Responses were evaluated by the way of finite-element idealization followed by numerical integration. It was found that the simplified model, based on moment-curvature relation, underestimates the response by a significant amount for longer durations of the applied load.

Cheung and ***Chan*** [15] developed two and three-dimensional finite strips in ***1981*** for the static and dynamic analysis of thin and thick sectorial plates. The plates can be isotropic or orthotropic, of constant or variable thickness, and can have different combinations of boundary conditions. The displacement functions for the finite strips were made up of polynomial shape functions and beam eigenfunctions. The 2-*D* finite strips were derived based on plate bending theory and have as nodal degrees of freedom, the out-of-plane displacement and the slope. The 3-*D* finite strips were formulated using three-dimensional elasticity constitutive equations, and the three displacement components in a cylindrical co-ordinate system were chosen as the nodal degrees of freedom. Numerical results involving various boundary conditions, radii and subtended angles were presented. Comparisons were made with existing solutions whenever available. Close agreements were noted.

In ***1994 Providakis et al*** [33] was developed the direct boundary element method for the dynamic analysis of thin inelastic flexural plates of arbitrary plan form and boundary conditions. It employes the static fundamental solution of the associated elastic problem and involves not only boundary integrals but domain integrals as well. Thus, boundary as well as interior elements are employed in the numerical solution. Time integration was accomplished by the explicit algorithm of the central difference

predictor method. A viscoplastic constitutive theory with state variables was employed to model the material behavior. Numerical results were also presented to illustrate quantitatively the proposed method of solution.

The effects of different types of variations in the thickness profile on the dynamic displacements and the dynamic stresses of a square plate had been investigated by ***Roy*** and ***Ganesan*** [38] in ***1995***. The plate was assumed to be clamped or simply supported at the edges and excited by a point harmonic load at resonance. For the analysis, a four-noded plate bending element had been used. The response had been determined for the first three modes of vibration. The results obtained for different thickness variations were compared with those obtained for a uniform thickness plate. It was observed that considerable reductions in dynamic displacements and/or stresses can be achieved by proper selection of the thickness variation.

The spline finite strip method and the incremental time–space finite element procedure were used by ***Cheung et al***. [14] in ***1998*** to analyze large amplitude vibration of thin plates with initial stresses. Two improvements for the procedure were presented. The free vibration and the internal resonance of plates with initial stress as well as the forced vibration of plates with damping and initial stress were computed.

In ***2002 Argyris et al.*** [7] extended the implementation of the natural mode method for finite element analysis to the dynamic analysis, linear and nonlinear, of shell structures by formulating the kinematically consistent mass matrix of a model three-node multilayered triangular element(TRIC). Both translational and rotational inertia are included in the mass matrix which is generated using kinematic and geometric arguments consistent with

the assumed natural rigid-body and straining modes of the element. Subsequently, numerical examples were performed to demonstrate the efficiency of the formulation and the potential of the natural mode method to deal efficiently with intricate time dependent phenomena of shell structures.

Also, in ***2002 Zhou*** [43] introduced a paper to study the stiffening effect of dead loads on dynamic behaviors of plates analyzed using the finite-element method. The element stiffness matrices that include the effect of dead loads were derived. It was shown that the stiffness of plates increases when the effect of dead loads is included in the calculation and that the effect is more significant for plates with a smaller stiffness. The validity of the proposed procedure is confirmed by numerical examples. The results show that although the finite-element results obtained were in agreement with the approximate closed-form solutions, the proposed method based on a finite-element formulation was more easily applied to practical structures under various support conditions and various types of dead loads.

In ***2003 Sladek et al.*** [39] introduced a paper in which simply supported and clamped thin elastic plates under dynamic loads were analyzed. Both harmonic and impact load were considered, also the viscous damping is taken into account. The governing partial differential equation (PDE) of fourth order is decomposed into two coupled PDEs of second order for the deflection and its Laplacian**.** Both equations contain time-dependent variables. The Laplace transform was used to eliminate the time dependence of the variables. Unknown Laplace transforms were computed from the local boundary integral equations. The meshless approximation based on the moving least square method is employed for the implementation. Time-dependent values were obtained by the Durbin inversion technique.

Chen et al. [13] in ***2004*** studied the dynamic response behavior of the delaminated composite plates considering progressive failure process. A formula of element stiffness and mass matrices for the composite laminates was deduced by using the first-order shear deformation theory combined with the selecting numerical integration scheme. A damping model was constituted by a generalized orthogonal damping model. A virtual interface linear spring element was also employing for avoiding the overlap and penetration phenomenon between the upper and lower sublaminates at the delamination region. The failure analysis method for the delaminated plates under dynamic loading was established by a modified Newmark direct integral method in conjunction with Tsai's failure criterion and corresponding stiffness degradation scheme. By some numerical examples, the effects of frequency of dynamic load, delamination length and location, and reduction of structure stiffness during the progressive failure process upon dynamic behavior of the delaminated composite thin plates were discussed.

In ***2004 Ali*** [3] present a research about the dynamic analysis for laminated fiber–reinforced composite materials and sandwich constructions by using the finite element method. This study was depended on the Higher order shear deformation theory for two dimensional layered approach with 7 and 9 degrees of freedom per node. The 9-noded Lagrangian isoparanetric quadrilateral element was used for discretrzation of layered plates.

In the dynamic analysis, Newmark method was used to solve the dynamic equilibrium equation. The consistent mass matrix was considered; also the damping effect was considered in the study by using Rayleigh type damping matrix. Two method were presented to find the natural frequencies; there are the inverse iteration method and matrix deflection method.

The results showed that the best angle at which one gets minimum deflection, minimum summation of normal stresses and minimum shear stresses in plates is 45^0.

In ***2006, Albarwary*** [2] introduced a study about the dynamic analysis of plates. In this study, the lower and higher order finite layer method was used for both free and forced vibration analysis of plates. Many plates were used and having different material properties as homogeneous plates which may be isotropic or orthotropic. In this study it was also used the plate consists of layers, each layer has an independent material properties from the others. These types of plate known as laminated plates. The effect of various boundary conditions of plate on dynamic analysis results had been considered.The study focuses on the dynamic analysis of plates in two stages: the first stage included the free vibration analysis, which has been performed by using the Jacobi's iterative method which can find all eigen values of a plate. In the second stage, the forced vibration of the plates was performed by investigating the dynamic response of plates by using Newmark method which is an implicit time integration method.
The consistent mass matrix had been used in the general equation of plate movement. The damping matrix was founded by using the form that given by Rayleigh in which the damping matrix is depended on the stiffness and mass matrix.

2.3 Summary

From the preceding review of literature, it is clear that there is a need for study considers the elasto-plastic dynamic analysis of thick plates by

taking into account the effect of damping. Also, there is a little literature that takes into account the effect of the transverse shear deformation of the plate, different boundary conditions and aspect ratio effect. Thus, the present study will cover the above research fields.

CHAPTER THREE

FINITE

ELEMENT FORMULATION AND

NUMERICAL SOLUTION

3.1 Introduction

The finite element method can be defined as a general method of structural analysis in which a continuum is replaced by finite number of elements interconnected at finite number of nodal points. The shape, size and the number of elements are related to the geometry of the body, material properties and loading condition **[26]**.

The finite element method is the most powerful numerical technique, which offers approximate solution to realistic types of structures such as plates. However, the term "finite elements" was first used by **Clough** in **1960** (mentioned by ***Reddy, 1984***) [35].

In the present study, the 8 – noded isoparametric quadrilateral element is used for discretization of plates. The derivations of the stiffness matrix [**K**] of plates are presented. Also the formulation of the element mass matrix [**M**] and damping matrix [**C**] of plates are introduced.

Finally, the numerical solutions which are used to solve the basic dynamic equilibrium equation and the eigenvalue problem are presented.

3.2 Formulation of the stiffness matrix

An 8 – nodded isoparametric element (serendipity element) which is shown in Fig. (3.1.b) is used. This element contains four nodes at the corners and four nodes at the mid – side of the element boundaries.

It is assumed, the degrees of freedom at any node are:- w, θ_x, θ_y.

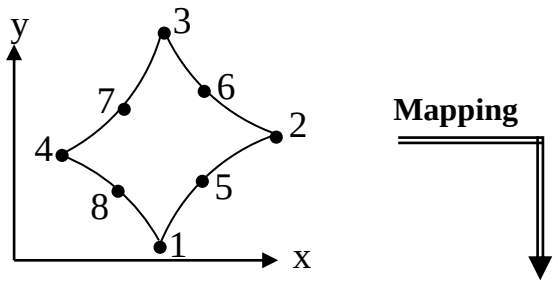

a. *element of general shape*

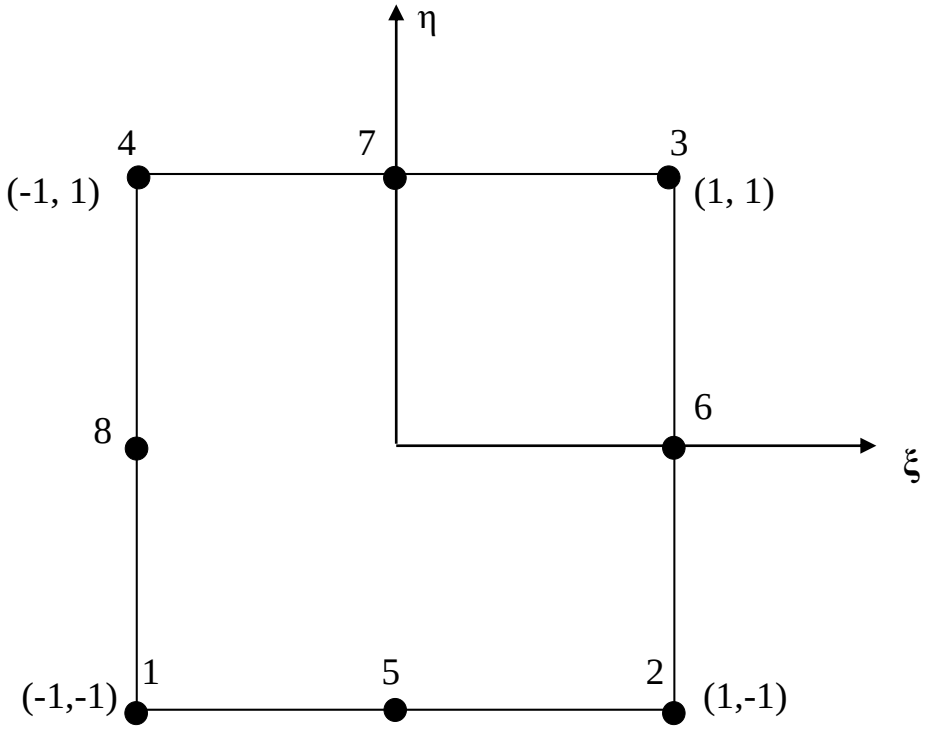

b .*Eight – noded quadrilateral isoparametric element.*

Fig.(3.1) :*Plane view showing isoparametric coordinates ξ-η and element of general form.*

The basic assumptions adopted in this analysis are based on Mindlin's assumptions **[17]**, which are:

a. Displacements are small compared with the plate thickness.
b. The stress normal to the midsurface of the plate (σ_z) is negligible.
c. Normal to the midsurface before deformation remains straight (but not necessarily normal to the midsurface) after deformation. However, this assumption is modified so that cross-sectional warping is permitted through the proposed expressions for the transverse shear strains, with using a shear correction factor, as it will be seen later in this chapter.

The shape function, Ni(ξ, η), at the i- th node of this element are given in table (3.1).

Table (3.1): *shape function for the plane quadratic isoparametric element[5].*

Node (i)	Corresponding shape function
1	$-0.25 (1-\xi) (1-\eta) (1+\xi+\eta)$
2	$-0.25 (1+\xi) (1-\eta) (1-\xi+\eta)$
3	$-0.25 (1+\xi) (1+\eta) (1-\xi-\eta)$
4	$-0.25 (1-\xi) (1+\eta) (1+\xi-\eta)$
5	$0.5 (1-\xi^2) (1-\eta)$
6	$0.5 (1-\eta^2) (1+\xi)$
7	$0.5 (1-\xi^2) (1+\eta)$
8	$0.5 (1-\eta^2) (1-\xi)$

Where ξ and η are the isoperimetric coordinates.

3.2.1: The displacement field:-

The displacement field of the element which is described above could be given as follows:-

$$\left.\begin{aligned} w &= \sum_{i=1}^{8} N_i \; w_i \\ \theta_x &= \sum_{i=1}^{8} N_i \; \theta_{xi} \\ \theta_y &= \sum_{i=1}^{8} N_i \; \theta_y i \end{aligned}\right\} \qquad \ldots(3.1)$$

$$\left.\begin{aligned} u &= -z \; \theta_x \\ v &= -z \; \theta_y \end{aligned}\right\} \qquad \ldots(3.2)$$

where:-

- w transverse displacement.
- u displacement in x-direction.
- v displacement in y-direction.
- θ_x average rotation in x- direction.
- θ_y average rotation in y-direction.

3.2.2: The stress-strain relationship:-

In the present analysis, the considered strains are the two direct strains ε_x and ε_y and the in plane shear strain γ_{xy} and the transverse shear strains γ_{yz} and γ_{zx} (the transverse direct stress σ_z and strain ε_z are negligible) and this reflects the second assumption of ***Mindlin's theory*** on which the 8-noded finite element is used.

The stress-strain relationship within the elastic range; in matrix form is:

$$\{\sigma\}_{5*1} = [E]_{5*5} \; \{\varepsilon\}_{5*1} \qquad \ldots\ldots(3.3)$$

Where: $\{\sigma\} = \{\sigma_x \ \sigma_y \ \tau_{xy} \ \tau_{yz} \ \tau_{zx}\}$

$$\{\varepsilon\} = \{\varepsilon_x \ \varepsilon_y \ \gamma_{xy} \ \gamma_{yz} \ \gamma_{zx}\}$$

$$[E] = \begin{bmatrix} \lambda & \lambda\upsilon & 0 & 0 & 0 \\ \lambda\upsilon & \lambda & 0 & 0 & 0 \\ 0 & 0 & G & 0 & 0 \\ 0 & 0 & 0 & G & 0 \\ 0 & 0 & 0 & 0 & G \end{bmatrix}$$

$\lambda = E / (1 - \upsilon^2)$

$G = E / 2(1+ \upsilon)$ = Shear modulus of elasticity.

E = Modulus of elasticity.

υ = Poission ’s ratio.

3.2.3: The strain – displacement matrix [B]:-

The strain-displacement matrix [B] is derived in the following steps:-

- Utilizing eq. (3.2)

$$\left.\begin{aligned} \varepsilon_x &= \partial u / \partial x = -z \ \partial \theta_x / \partial x \\ \varepsilon_y &= \partial v / \partial y = -z \ \partial \theta_y / \partial y \\ \gamma_{xy} &= \partial u / \partial y + \partial v / \partial x = -z \ (\partial \theta_x / \partial y + \partial \theta_y / \partial x) \end{aligned}\right\} \quad \ldots(3.4)$$

$$\left.\begin{aligned} \gamma_{yz} &= \partial w / \partial y + \partial v / \partial z = (\partial w / \partial y) - \theta_y \\ \gamma_{zx} &= \partial w / \partial x + \partial u / \partial z = (\partial w / \partial x) - \theta_x \end{aligned}\right\} \quad \ldots(3.5)$$

In the present analysis eqs. (3.5) given uniform transverse shear strains across the thickness of the plate as a result from the assumed

displacement field. However, these strains are modified to the following from presented:-

$$\left.\begin{aligned}\gamma_{yz} &= 5/6 * \left[(3/2) \left[\left(\partial w / \partial y \right) - \theta_y \right] \left[1 - \left(z^2 / (0.5\,h)^2 \right) \right] \right] \\ \gamma_{zx} &= 5/6 * \left[(3/2) \left[\left(\partial w / \partial x \right) - \theta_x \right] \left[1 - \left(z^2 / (0.5\,h)^2 \right) \right] \right]\end{aligned}\right\} \quad \ldots(3.6)$$

Where:-

5/6 : is the shear correction factor to allow for cross-sectional warping . These modified expressions for (γ_{yz}) and (γ_{zx}) produce a parabolic distribution for the shear strains and their corresponding stresses (τ_{yz} and τ_{zx}) across the thickness of the plate such parabolic distribution seems to be more accurate and realistic especially when the transverse shear stresses are to be included in the yield criterion as in the present work.

The properties of this modified expression for (γ_{yz}) and (γ_{zx}) are given by ***Alwash (1989)*** **[5].**

- Then, rewriting eqs. (3.4) and (3.6) in a matrix form:-

$$\{\varepsilon\}_{5*1} = \begin{Bmatrix} \varepsilon_x \\ \varepsilon_y \\ \gamma_{xy} \\ \gamma_{yz} \\ \gamma_{zx} \end{Bmatrix} = \underbrace{\begin{bmatrix} 1 & 0 & 0 & 0 & 0 & 0 & 0 & 0 & 0 \\ 0 & 0 & 0 & 0 & 1 & 0 & 0 & 0 & 0 \\ 0 & 1 & 0 & 1 & 0 & 0 & 0 & 0 & 0 \\ 0 & 0 & 0 & 0 & 0 & b & 0 & b & 0 \\ 0 & 0 & b & 0 & 0 & 0 & b & 0 & 0 \end{bmatrix}}_{[H]_{5*9}} \begin{Bmatrix} \partial u/\partial x \\ \partial u/\partial y \\ \partial u/\partial z \\ \partial v/\partial x \\ \partial v/\partial y \\ \partial v/\partial z \\ \partial w/\partial x \\ \partial w/\partial y \\ \partial w/\partial z \end{Bmatrix} \quad \ldots(3.7)$$

Where:-

$$b = \frac{5}{6} \left[\frac{3}{2} \left(1 - \frac{z^2}{(0.5h)^2}\right) \right]$$

Since the shape functions $\mathbf{N_i}$ are functions of the natural coordinates rather than Cartesian coordinates, a relationship needs to be established between the derivatives in the two coordinates systems. By using the chain rule, the partial differential relation can be expressed in a matrix form as:

$$\begin{bmatrix} \frac{\partial u}{\partial \xi} \\ \frac{\partial u}{\partial \eta} \\ \frac{\partial u}{\partial z} \end{bmatrix} = \underbrace{\begin{bmatrix} \frac{\partial x}{\partial \xi} & \frac{\partial y}{\partial \xi} & 0 \\ \frac{\partial x}{\partial \eta} & \frac{\partial y}{\partial \eta} & 0 \\ 0 & 0 & 1 \end{bmatrix}}_{[J]_{3*3}} \begin{bmatrix} \frac{\partial u}{\partial x} \\ \frac{\partial u}{\partial y} \\ \frac{\partial u}{\partial z} \end{bmatrix} \qquad \ldots(3.8)$$

where [J] is the **Jacobian** matrix and the elements of this matrix can be obtained by differentiating the following equations:

$$\begin{aligned} x(\xi,\eta) &= \sum_{i=1}^{8} N_i(\xi,\eta)\ x_i \\ y(\xi,\eta) &= \sum_{i=1}^{8} N_i(\xi,\eta)\ y_i \end{aligned} \qquad \ldots(3.9)$$

Hence, the **Jacobian** matrix can be expressed as:

$$[J]_{3*3} = \begin{bmatrix} \sum_{i=1}^{8} \frac{\partial N_i}{\partial \xi} x_i & \sum_{i=1}^{8} \frac{\partial N_i}{\partial \xi} y_i & 0 \\ \sum_{i=1}^{8} \frac{\partial N_i}{\partial \eta} x_i & \sum_{i=1}^{8} \frac{\partial N_i}{\partial \eta} y_i & 0 \\ 0 & 0 & 1 \end{bmatrix} \qquad \ldots(3.10)$$

Then, the derivatives of the shape functions with respect to Cartesian coordinates can be given as:

$$\begin{bmatrix} \frac{\partial u}{\partial x} \\ \frac{\partial u}{\partial y} \\ \frac{\partial u}{\partial z} \end{bmatrix} = [J]^{-1}{}_{3*3} \begin{bmatrix} \frac{\partial u}{\partial \xi} \\ \frac{\partial u}{\partial \eta} \\ \frac{\partial u}{\partial z} \end{bmatrix} \qquad \ldots(3.11)$$

where $[J]^{-1}$ is the inverse of **Jacobian** matrix.

So, the transformation from(x-y) coordinates to isoparametric coordinales (ξ-η) gives:-

$$\begin{Bmatrix} \frac{\partial u}{\partial x} \\ \frac{\partial u}{\partial y} \\ \frac{\partial u}{\partial z} \\ \frac{\partial v}{\partial x} \\ \frac{\partial v}{\partial y} \\ \frac{\partial v}{\partial z} \\ \frac{\partial w}{\partial x} \\ \frac{\partial w}{\partial y} \\ \frac{\partial w}{\partial z} \end{Bmatrix} = \underbrace{\begin{bmatrix} & & & 0 & 0 & 0 & 0 & 0 & 0 \\ & [J]^{-1}_{3*3} & & 0 & 0 & 0 & 0 & 0 & 0 \\ & & & 0 & 0 & 0 & 0 & 0 & 0 \\ 0 & 0 & 0 & & & & 0 & 0 & 0 \\ 0 & 0 & 0 & & [J]^{-1}_{3*3} & & 0 & 0 & 0 \\ 0 & 0 & 0 & & & & 0 & 0 & 0 \\ 0 & 0 & 0 & 0 & 0 & 0 & 0 & 0 & 0 \\ 0 & 0 & 0 & 0 & 0 & 0 & & [J]^{-1}_{3*3} & \\ 0 & 0 & 0 & 0 & 0 & 0 & & & \end{bmatrix}}_{[\Gamma\ \Gamma\ \Gamma]_{9*9}} \begin{Bmatrix} \frac{\partial u}{\partial \xi} \\ \frac{\partial u}{\partial \eta} \\ \frac{\partial u}{\partial z} \\ \frac{\partial v}{\partial \xi} \\ \frac{\partial v}{\partial \eta} \\ \frac{\partial v}{\partial z} \\ \frac{\partial w}{\partial \xi} \\ \frac{\partial w}{\partial \eta} \\ \frac{\partial w}{\partial z} \end{Bmatrix} \qquad \ldots(3.12)$$

-Substituting form eq. (3.1) in eq. (3.2) and differentiating with respect to (ξ, η, z) give (in matrix form):-

$$\begin{Bmatrix} \frac{\partial u}{\partial \xi} \\ \frac{\partial u}{\partial \eta} \\ \frac{\partial u}{\partial z} \\ \frac{\partial v}{\partial \xi} \\ \frac{\partial v}{\partial \eta} \\ \frac{\partial v}{\partial z} \\ \frac{\partial w}{\partial \xi} \\ \frac{\partial w}{\partial \eta} \\ \frac{\partial w}{\partial z} \end{Bmatrix} = \begin{bmatrix} 0 & -z\frac{\partial N_i}{\partial \xi} & 0 \\ 0 & -z\frac{\partial N_i}{\partial \eta} & 0 \\ 0 & -Ni & 0 \\ 0 & 0 & -z\frac{\partial N_i}{\partial \xi} \\ 0 & 0 & -z\frac{\partial N_i}{\partial \eta} \\ 0 & 0 & -N_i \\ \frac{\partial N_i}{\partial \xi} & 0 & 0 \\ \frac{\partial N_i}{\partial \eta} & 0 & 0 \\ 0 & 0 & 0 \end{bmatrix} \begin{Bmatrix} w_i \\ \theta x_i \\ \theta y_i \end{Bmatrix} = \left[\overline{N}\right]_{9*24} \quad \{d\}_{24*1} \qquad \ldots(3.13)$$

- Substitution from eq. (3.12) and eq. (3.13) in eq. (3.7) leads to:-

$$\{\varepsilon\}_{5*1} = [B]_{5*24} \quad \{d\}_{24*1} \qquad \ldots(3.14)$$

or; in other form

$$\lfloor \varepsilon \rfloor_{1*5} = \lfloor d \rfloor_{1*24} \quad [B]^T_{24*5} \qquad \ldots(3.15)$$

$$\text{Where: } [B]_{5*24} = [H]_{5*9} \quad [\Gamma\Gamma\Gamma]_{9*9} \quad \left[\overline{N}\right]_{9*24} \qquad \ldots(3.16)$$

then, the stiffness matrix at the element level could be derived from the strain energy:

$$\textit{strain energy} = U = 1/2 \int_V \lfloor \sigma_x \ \sigma_y \ \tau_{xy} \ \tau_{yz} \ \tau_{zx} \rfloor \{\varepsilon_x \ \varepsilon_y \ \gamma_{xy} \ \gamma_{yz} \ \gamma_{zx}\} dV$$

$$= 1/2 \int_V \lfloor \sigma \rfloor_{1*5} \ \{\varepsilon\}_{5*1} \ dV \qquad \ldots(3.17)$$

Substitute from eq. (3.3), eq. (3.14) and eq. (3.15) in eq. (3.17) to get:-

$$U = 1/2 \lfloor d \rfloor \left[\int_V [B]^T [E] [B] \, dV \right] \{d\}$$

But, in general, it is well-known that

$$U = 1/2 \ \lfloor d \rfloor \ [k] \ \{d\}$$

Hence,

$$stiffness\ matrix\ at\ element\ level = [k]_{24*24} = \int_V [B]^T_{24*5} \ [E]_{5*5} \ [B]_{5*24} \ dV$$

$$[k]_{24*24} = \int_{-1}^{+1} \int_{-1}^{+1} \int_{-h/2}^{h/2} [B]^T [E] [B] |J| \ d\xi \ d\eta \ dZ \qquad \ldots(3.18)$$

where $|J|$ is the determinant of the ***Jacobian*** matrix.

In finding [k] from eq. (3.18), the integration with respect to (ξ and η) is carried out numerically (by reduced integration, see ref**. [17]**) using 2-by-2 ***Gauss rule***. 6-point ***Gauss rule*** is applied to integrate numerically in z-direction after transforming z-coordinate to isoparametric coordinate ζ (see *Appendix(A)*).

3.3 Dynamic Analysis

In this section, the dynamic equilibrium equation of motion is stated. Then, the mass matrix for plate element is derived. Finally the damping properties of structures and the formulation of damping matrix are described.

3.3.1:Dynamic Equation of Motion

The equation of motion for a nonlinear system can be formulated by expressing the equilibrium of the effective forces associated with each of

it's degrees of freedom. In general, four types of forces will be involved at any point i , the externally applied load, $F_i(t)$, and the forces resulting from the motion that is, inertia, f_{Ii} , damping, f_{Di} , and internal forces, f_{Si}. Thus, the dynamic equilibrium may be expressed as **[16]**:-

$$f_{Ii} + f_{Di} + f_{Si} = F_i(t) \quad \ldots(3.19)$$

or in a matrix form :-

$$\{f_I\} + \{f_D\} + \{f_S\} = \{F(t)\} \quad \ldots(3.20)$$

In which:-

$$\{f_I\} = [M] \{\ddot{D}\} \quad \ldots(3.21)$$

$$\{f_D\} = [C] \{\dot{D}\} \quad \ldots(3.22)$$

$$\{f_S\} = [K] \{D\} \quad \ldots(3.23)$$

Where: [M], [C] and [K] = mass, damping and stiffness matrices respectively, and: $\{\ddot{D}\}$, $\{\dot{D}\}$ and $\{D\}$ = acceleration, velocity and displacement vectors of the nodal points of the system, respectively

Substituting Eqs. (3.21), (3.22) and (3.23) into Eq.(3.20) gives the complete dynamic equilibrium of the system, i.e :-

$$[M] \{\ddot{D}\} + [C] \{\dot{D}\} + [K] \{D\} = \{F(t)\} \quad \ldots(3.24)$$

3.3.2:Formulation of Mass Matrix

The mass proportion of an element can be defined in two ways, either lumped or consistent.

The consistent mass matrix (or the elemental mass matrix), which is always symmetrical, is a matrix of equivalent nodal masses that dynamically represent the actual distributed mass of the element **[37].**

An alternative approximation to the consistent mass matrix is the lumped mass matrix.

The usual process adopted in deriving the latter is to distribute the mass of the element evenly between its nodal points in the form of concentrated of lumped masses **[37].**

In the present study only the consistent mass matrix is considered.

3.3.2.1:Derivation of the consistent mass matrix

For a plate element the inertia force per unit area due to acceleration is:-

Inertia force = mass per unit area * acceleration

The acceleration may be expressed by the same function for the displacement, so:

$$\ddot{w}_{(x,y)} = \ddot{w}_1 N_1 + \ddot{w}_2 N_2 + \ddot{w}_3 N_3 + \ddot{w}_4 N_4 + \ddot{w}_5 N_5 + \ddot{w}_6 N_6 + \ddot{w}_7 N_7 + \ddot{w}_8 N_8 = \sum_{i=1}^{8} N_i \ddot{w}_i \quad \ldots(3.25)$$

$$\ddot{\theta}_x(x,y) = \sum_{i=1}^{8} N_i \ddot{\theta}_{xi} \quad \ldots(3.26)$$

$$\ddot{\theta}_y(x,y) = \sum_{i=1}^{8} N_i \ddot{\theta}_y i \quad \ldots(3.27)$$

Now, if $\ddot{w}(x,y)$ is considered only:-

let a unit nodal acceleration is applied at node 1 then, $\ddot{w}_1 = 1$ and,

$\ddot{w}_2 = \ddot{w}_3 = \ddot{w}_4 = \ddot{w}_5 = \ddot{w}_6 = \ddot{w}_7 = \ddot{w}_8 = 0$

so:-

$$\ddot{w}(x,y) = N_1 * 1 + (N_2 + N_3 + N_4 + N_5 + N_6 + N_7 + N_8) * 0 = N_1 \quad \ldots(3.28)$$

To determine the mass matrix coefficients m_{11}, m_{12}, m_{13}, ….., $m_{24\ 24}$ the principle of virtual work is applied. For example the coefficient m_{21} may be found by applying a virtual displacement δw_2 at node 2 ($\delta w_2 = 1$), therefore, the external work done by this virtual displacement is:-

External work $= P\ \delta w_2$ …(3.29)

Where P is the real inertia force existed before the applying of the virtual displacement. Then the external work becomes.

$$External\ work = m_{21}\ \ddot{w}_1 w_2 = m_{21} * 1 * 1 = m_{21} \quad \ldots(3.30)$$

and the internal virtual work

Internal work $= F_{int}\ w(x,y)$ …(3.31)

where:-

w(x,y) : the virtual displacement function and it is obtained by using the displacement field:-

$w(x,y) = \sum_{i=1}^{8} N_i\ w_i$ so:-

$$w(x,y) = N_1 w_1 + N_2 w_2 + N_3 w_3 + N_4 w_4 + N_5 w_5 + N_6 w_6 + N_7 w_7 + N_8 w_8 = N_2 \quad \ldots(3.32)$$

and F_{int} : is the inertia force = $\int_{vol} \rho\ d(vol)\ \ddot{w}(x,y)$ …(3.33)

the substitution of equation (3.28), (3.32) and (3.33) in to equation (3.31) leads to:

$$Internal\ work = \int_{vol} \rho\ N_1 N_2\ d(vol) \quad \ldots(3.34)$$

now: external work = internal work, leads to:

$$m_{21} = \int_{vol} \rho\ N_1 N_2\ d(vol) \quad \ldots(3.35)$$

eq. (3.35) can be put in a general form to express any coefficient m_{ij} in the mass matrix:-

$$mi_j = \rho \int_{vol} N_i \, N_j \; d(vol) \qquad \ldots(3.36)$$

using eq. (3.36), the general equation for consistent mass matrix for a plate element (with one degree of freedom) is:-

$$\begin{aligned} [m]_{8*8} &= \rho \int_{vol} \lfloor N \rfloor^T \; \lfloor N \rfloor d(vol) \\ &= \rho \int_{-1}^{+1} \int_{-1}^{+1} \int_{-h/2}^{h/2} \lfloor N \rfloor^T \lfloor N \rfloor \, |J| \; d\xi \; d\eta \; dz \end{aligned} \qquad \ldots(3.37)$$

where: $|J|$ is the determinant of the ***Jacobian*** matrix.

The integration with respect to (ξ and η) is carried out numerically using 2*2 ***Gauss*** rule. 6-point ***Gauss*** rule is applied to integrate numerically in z-direction after transforming z-coordinate to isoperimetric coordinate ξ (see ***Appendix A***).

Now, if the same steps (to find $[m]_{8*8}$ for w) are repotting with θ_x, θ_y then, the total matrix for the plate element will be $[m]_{24*24}$.

To show the final form for the consistent mass matrix (see ***Appendix (B)*).**

3.3.3:Formulation of Damping Matrix

In the analysis of dynamic problems, it is noticed that the amplitude of the free vibration remains constant with time, but in actual structures such a vibration without decrease in amplitude is never realized. This is occurred because of the presence of the damping forces. These forces cause the dissipation of energy that progressively reduces the amplitude of vibration and ultimately stops the motion when all energy initially stored in the system has been dissipated **[22].**

Damping in structures may be of several different forms. It is in part due to the internal molecular friction of the material. It is also due to the loss of energy associated with the slippage of structural connections either between members or between the structure and the supports. In some cases it may be due to the resistance to motion provided by air or other fluids surrounding the structure. In any case, the effect is one of forces opposing the motion, and hence the amplitude of the response is decreased **[11].**

Although research studies have proposed numerous ways of mathematically describing damping, the exact nature of damping in structure is usually impossible to determine. The most common analytical model of damping employed in structural dynamics analyses is the linear viscous dashpot model (***viscous damping***), **[18].**

3.3.3.1: Effect of Damping

All structural dynamic systems contain damping to some degree, but the effect may not be significant if the load duration is short and only the maximum dynamic response is of interest. On the other hand, if a continuing state of vibration is being investigated, damping may be of primary importance. In fact, if enough damping is present, vibration may be completely eliminated **[11].**

Because the damping effect is usually not known in advance, it should ordinarily be included in the vibrational analysis until its importance is found out **[1].**

3.3.3.2:Damping Matrix

In practice it is difficult, if not impossible, to determine for general finite element assemblages, the element damping parameters. In particular,

this is because the damping properties are frequency dependent. For this reason, the damping matrix is in general not assembled from elements damping matrices but is constructed by using the mass matrix and stiffness matrix of the complete element assemblage together with experimental results on the amount of damping **[9].**

Viscous type damping can be used whatever the form of the excitation is, the most common form of such damping is the so-called ***Rayleigh- type damping* ,[32],** given by:

$$[C] = Z_1 [M] + Z_2 [K] \quad \ldots(3.38)$$

In which Z_1 and Z_2 are arbitrary proportionality factors.

Then, by making benefit of ***Mode Analysis,*** Eq. (3.38) can be reduced to:

$$2 \zeta_r \omega_r = Z_1 + \omega_r^2 Z_2 \quad \ldots(3.39)$$

Where ζ_r , ω_r are the modal damping ratio and the natural frequency for the mode r respectively (a typical variation of the damping ratio with the natural frequency is illustrated in Fig.(3.2)).

The two factors Z_1 and Z_2 can be determined by specifying the damping ratio for two modes, for example, 1 and 2, and substituting them into Eq. (3.39):

$$\left.\begin{aligned} 2\zeta_1 \omega_1 &= Z_1 + \omega_1^2 Z_2 \\ 2\zeta_2 \omega_2 &= Z_1 + \omega_2^2 Z_2 \end{aligned}\right\} \quad \ldots(3.40)$$

The solution of these two equations gives:

$$Z_1 = 2\omega_1\omega_2 (\omega_2\zeta_1 - \omega_1\zeta_2) / (\omega_2^2 - \omega_1^2) \quad \ldots(3.41)$$

$$Z_2 = 2 (\omega_2 \zeta_2 - \omega_1\zeta_1) / (\omega_2^2 - \omega_1^2) \quad \ldots(3.42)$$

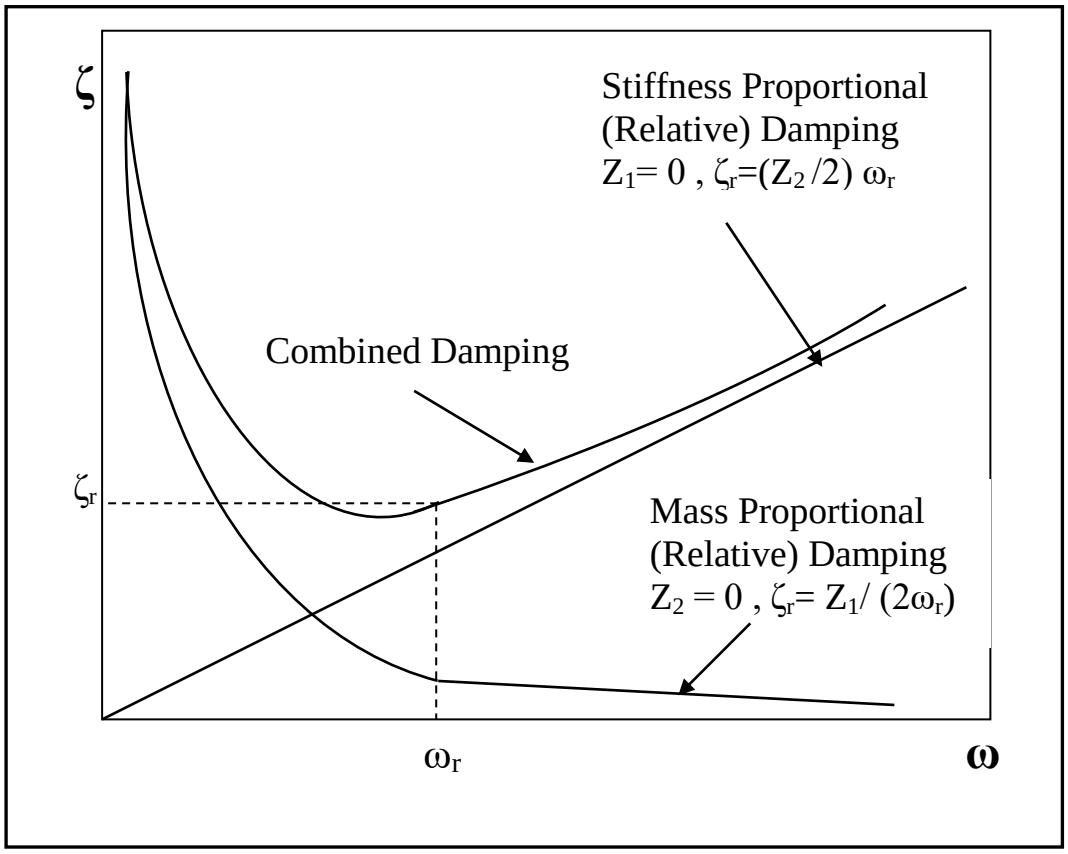

Fig .(3.2) *: Relationship between damping ratio and frequency for Rayleigh damping[32].*

Now, by substituting the values of Z_1 and Z_2 into Eq. (3.38) the damping matrix is obtained.

Natural frequencies, ω_1 and ω_2 used in the above equations are obtained from the solution of eigenvalue problem for undamped case (this will be discussed later in this chapter). The corresponding damping ratios can be obtained by finding the damping ratio ζ_1 which is related to the first mode of vibration using field testing of a structure or from the previous experience or by assuming it within an acceptable range according to the

type of the structure. With the value of ζ_1 on hand, any other value ζ_r can be obtained using the approximate formula **[1],**

$$\zeta_r \approx \zeta_1 (\omega_r/\omega_1)^{el} \quad ; \quad (0.5 \le el \le 0.7) \qquad \ldots(3.43)$$

Structures generally have a value of the first mode damping ratio in the range of **0.02** to **0.1**, **[20].**

3.4 Numerical methods for the dynamic analysis

The dynamic equilibrium equation, equation (3.24), represents a system of linear differential equations of second order and, in principle; the solution of the equations can be obtained by standard procedures for the solution of differential equations with constant coefficients. However, the procedures proposed for the solution of general system of differential equations become very expensive if the order of the matrices is large. In practical finite element analysis, there are few effective methods. These are mainly, direct time-integration and mode superposition. In the present work, the direct integration method is used.

In direct integration methods the dynamic equilibrium equations are integrated using a numerical step-by-step procedure. The term "direct" meaning that prior to the numerical integration, no transformation of the equation into different form is carried out.

In essence, direct numerical integration is based on two ideas. First, instead of trying to satisfy the equation of motion at any time t, it is aimed to satisfy this equation only at discrete time intervals Δt apart. The second idea on which a direct integration method based is that the variation of

displacements, velocities and accelerations within each time interval Δt is assumed, **[9].**

Basically there are two general classes of algorithms for dynamics problems, ***explicit*** and ***implicit.*** For ***explicit*** methods the solution at time $t+\Delta t$ is obtained by considering the equilibrium condition at time t. While for ***implicit*** methods the solution at time $t+\Delta t$ is obtained if the equilibrium condition at time $t+\Delta t$ is considered.

The ***implicit*** algorithms are more effective for structural dynamic problems, in which the response is controlled by a relatively small number of low frequency modes, while ***explicit*** algorithms are very efficient for wave propagation problems, in which the contribution of intermediate and high frequency structural modes to response is important **[41].**

Many explicit and implicit methods for direct integration are available. However, in the present study, only the ***implicit Newmark method*** is adopted.

3.4.1: The Newmark family methods

The most widely used family of implicit methods of direct time integration for solving the dynamic equation of motion is the ***Newmark's family of methods***.

In 1959 ***Newmark*** **[28]**, presented equations for approximating the velocity and the displacement of a single degree of freedom system at time $t+\Delta t$ as follows:–

$$\dot{D}_{t+\Delta t} = \dot{D}_t + \Delta t\,[(1-\gamma)\,\ddot{D}_t + \gamma\,\ddot{D}_{t+\Delta t}] \quad \ldots(3.44)$$

$$D_{t+\Delta t} = D_t + \Delta t\,\dot{D}_t + (\Delta t)^2\,[((1/2)-\beta)\,\ddot{D}_t + \beta\,\ddot{D}_{t+\Delta t}] \quad \ldots(3.45)$$

where, γ and β are parameters which determine the stability and accuracy of the algorithm.

Assuming different values for γ and β, gives different formulas within the ***Newmark*** family of methods. This method is unconditionally stable if $\gamma \geq 1/2$ and $\beta \geq (2\gamma+1)^2/16$.

Unless γ is taken to be **0.5**, the method introduces artificial damping which can be negative when $\gamma < 0.5$ **[32]**. Therefore, as remarked by ***Newmark***, all schemes for which

$$\gamma \geq 1/2\ ,\ \beta \geq 1/4 \quad \ldots(3.46)$$

are unconditionally stable and indeed show no artificial damping, **[44].**

In the present study, values of γ and β are (0.5 and o.25), respectively. Newmark method with these values of γ and β is called ***constant average acceleration method***. This method is generally used in structural dynamics because it has been shown to have high degree of numerical stability, **[20].**

3.4.1.1:Basic Equations

Equations (3.44) and (3.45) can be rewritten for multi-degree of freedom system in the following matrix form:

$$\{\dot{D}\}_{t+\Delta t} = \{\dot{D}\}_t + \Delta t\ [\ (1-\gamma)\ \{\ddot{D}\}_t + \gamma\ \{\ddot{D}\}_{t+\Delta t}\ ] \quad \ldots(3.47)$$

$$\{D\}_{t+\Delta t} = \{D\}_t + \Delta t\ \{\dot{D}\}_t + (\Delta t)^2[((1/2) - \beta)\ \{\ddot{D}\}_t + \beta\ \{\ddot{D}\}_{t+\Delta t}\ ] \quad \ldots(3.48)$$

New, by considering the dynamic equilibrium at time t+Δt Eq.(3.24) becomes:

$$[M]_{t+\Delta t}\ \{\ddot{D}\}_{t+\Delta t} + [C]_{t+\Delta t}\ \{\dot{D}\}_{t+\Delta t} + [K]_{t+\Delta t}\ \{D\}_{t+\Delta t} = \{F(t)\}_{t+\Delta t} \quad \ldots(3.49)$$

Where $\{\ddot{D}\}_{t+\Delta t}$,$\{\dot{D}\}_{t+\Delta t}$,$\{D\}_{t+\Delta t}$ and $\{F(t)\}_{t+\Delta t}$ are acceleration, velocity, displacement and dynamic applied load vectors at time t+Δt, respectively.

In order to solve Eq.(3.49) it is necessary first to write in terms of one unknown, $\{D\}_{t+\Delta t}$. By solving Eq. (3.48) for $\{\ddot{D}\}_{t+\Delta t}$ in terms of $\{D\}_{t+\Delta t}$ and then substituting for $\{\ddot{D}\}_{t+\Delta t}$ into Eq.(3.47), the following equations for $\{\ddot{D}\}_{t+\Delta t}$ and $\{\dot{D}\}_{t+\Delta t}$ in term of $\{D\}_{t+\Delta t}$ are obtained:

$$\{\ddot{D}\}_{t+\Delta t} = (1/\beta\Delta t^2)[\{D\}_{t+\Delta t} - \{D\}_t] - (1/\beta\Delta t)\{\dot{D}\}_t - ((1/2\beta) - 1)\{\ddot{D}\}_t \quad \ldots(3.50)$$

$$\{\dot{D}\}_{t+\Delta t} = (\gamma/\beta\Delta t)[\{D\}_{t+\Delta t} - \{D\}_t] + (1 - (\gamma/\beta))\{\dot{D}\}_t - \Delta t((\gamma/2\beta) - 1)\{\ddot{D}\}_t \quad \ldots(3.51)$$

If equations (3.50) and (3.51) are substituted into Eq.(3.49) then:

$$[\ (1/\beta\Delta t^2)\ [M]_{t+\Delta t} + (\gamma/\beta\Delta t)\ [C]_{t+\Delta t} + [K]_{t+\Delta t}\ ]\ \{D\}_{t+\Delta t} = \{F(t)\}_{t+\Delta t} +$$
$$[M]_{t+\Delta t}\ [(1/\beta\Delta t^2)\ \{D\}_t + (1/\beta\Delta t)\ \{\dot{D}\}_t + [(1/2\beta) - 1]\ \{\ddot{D}\}_t\ ] +$$
$$[C]_{t+\Delta t}[(\gamma/\beta\Delta t)\ \{D\}_t - [1-(\gamma/\beta)]\ \{\dot{D}\}_t + \Delta t\ [(\gamma/2\beta) - 1]\ \{\ddot{D}\}_t] \quad \ldots(3.52)$$

Let $[K^{\bullet}] = (1/\beta\Delta t^2)[M]_{t+\Delta t} + (\gamma/\beta\Delta t)[C]_{t+\Delta t} + [K]_{t+\Delta t}$ …(3.53)

And

$$\{F^{\bullet}(t)\} = \{F(t)\}_{t+\Delta t} + [M]_{t+\Delta t}\left[(1/\beta\Delta t^2)\{D\}_t + (1/\beta\Delta t)\{\dot{D}\}_t + [(1/2\beta)-1]\{\ddot{D}\}_t\right] + [C]_{t+\Delta t}\left[(\gamma/\beta\Delta t)\{D\}_t - [1-(\gamma/\beta)]\{\dot{D}\}_t + \Delta t\,[(\gamma/2\beta)-1]\{\ddot{D}\}_t\right] \quad \ldots(3.54)$$

Hence Eq. (3.52) becomes:

$$[K^{\bullet}]\{D\}_{t+\Delta t} = \{F^{\bullet}(t)\} \quad \ldots(3.55)$$

The Eq. (3.55) can be used for linear systems, where $[K^{\bullet}]$ will be constant during the analysis at any time. And, since the present problem is nonlinear due to the material nonlinearity, therefore, the incremental form will be adopted in the analysis, where $[K^{\bullet}]$ is changed with time.

The complete steps for putting Eq. (3.55) in an incremental form are given by (***Alwash, 2002***) **[6]** as below:

If Eq. (3.52) rewritten in an incremental form, then:

$$[(1/\beta\Delta t^2)[M]_{t+\Delta t} + (\gamma/\beta\Delta t)[C]_{t+\Delta t} + [K]_{t+\Delta t}]\,(\{D\}_{t+\Delta t} - \{D\}_t) = \{F(t)\}_{t+\Delta t} - [K]_{t+\Delta t}\{D\}_t + [M]_{t+\Delta t}\left[(1/\beta\Delta t)\{\dot{D}\}_t + [(1/2\beta)-1]\{\ddot{D}\}_t\right] + [C]_{t+\Delta t}\left[[(\gamma/\beta)-1]\{\dot{D}\}_t + \Delta t[(\gamma/2\beta)-1]\{\ddot{D}\}_t\right] \quad \ldots(3.56)$$

Now let $[K^{\bullet}] = (1/\beta\Delta t^2)[M]_{t+\Delta t} + (\gamma/\beta\Delta t)[C]_{t+\Delta t} + [K]_{t+\Delta t}$ …(3.57)

$$\{\Delta D\} = \{D\}_{t+\Delta t} - \{D\}_t \quad \ldots(3.58)$$

$$\{\Delta F^{\bullet}(t)\} = \{F(t)\}_{t+\Delta t} - [K]_{t+\Delta t}\{D\}_t + [M]_{t+\Delta t}\left[(1/\beta\Delta t)\{\dot{D}\}_t + [(1/2\beta)-1]\{\ddot{D}\}_t\right] + [C]_{t+\Delta t}\left[[(\gamma/\beta)-1]\{\dot{D}\}_t + \Delta t\,[(\gamma/2\beta)-1]\{\ddot{D}\}_t\right] \quad \ldots(3.59)$$

At the beginning of the analysis, the matrices $[K]_{t+\Delta t}$, $[M]_{t+\Delta t}$, and $[C]_{t+\Delta t}$ are taken at time t as an approximation.

Since [M] will be constant at all time steps, then $[M]_{t+\Delta t} = [M]$. Consequently Eq. (3.56) may be written as:

$$[K^{\bullet}]\{\Delta D\} = \{\Delta F^{\bullet}(t)\} \quad \ldots(3.60)$$

Where:

$$[K^{\bullet}] = (1/\beta\Delta t^2)[M] + (\gamma/\beta\Delta t)[C]_{t+\Delta t} + [K]_{t+\Delta t} \quad \ldots(3.61)$$

$$\{\Delta F^{\bullet}(t)\} = \{F(t)\}_{t+\Delta t} - \{f\}_t + [M]\,[(1/\beta\Delta t\{\dot{D}\}_t + [(1/2\beta)-1]\{\ddot{D}\}_t]$$

$$+ [C]_{t+\Delta t}[\,[\,(\gamma/\beta)-1]\{\dot{D}\}_t + \Delta t\,[(\gamma/2\beta)-1]\{\ddot{D}\}_t] \quad \ldots(3.62)$$

Where $\{f\}_t$ is the internal force vector at time t (for nonlinear solution).

Now by solving Eq.(3.60) for $\{\Delta D\}$, approximate values for accelerations, velocities and displacements may be given as follows:

$$\{\ddot{D}\}_{t+\Delta t} = (1/\beta\Delta t^2)\{\Delta D\} - (1/\beta\Delta t)\{\dot{D}\}_t - [(1/2\beta)-1]\{\ddot{D}\}_t \quad \ldots(3.63)$$

$$\{\dot{D}\}_{t+\Delta t} = (\gamma/\beta\Delta t)\{\Delta D\} + [1-(\gamma/\beta)]\{\dot{D}\}_t - \Delta t\,[(\gamma/2\beta)-1]\{\ddot{D}\}_t \quad \ldots(3.64)$$

$$\{D\}_{t+\Delta t} = \{D\}_t + \{\Delta D\} \quad \ldots(3.65)$$

3.5 Calculation of natural frequencies

In the dynamic analysis, the natural frequency, ω (radian/sec),of the vibration is required to formulate the damping matrix as shown previously.

Also, in order to determine the critical time step for direct integration the ***smallest natural period*** T (sec) is required, which is related to the natural frequency as follows:

$$T = \frac{2\pi}{\omega} \qquad ...(3.66)$$

Therefore, in order to perform the analysis, the evaluation of natural frequencies is necessary to accomplish first.

The undamped free vibration is represented by Eq.(3.24) with no damping (i.e., [C]=0) and no external force (i.e., {F(t)}=0). The result is an equation of motion of the form, **[18]:**

$$[M]\{\ddot{D}\} + [K]\{D\} = 0 \qquad \ldots(3.67)$$

Harmonic motion is given by:

$$\{D\} = \{\bar{U}\}\cos(\omega t - \delta) \qquad \ldots(3.68)$$

Where:

$\{\bar{U}\}$: is the nodal amplitudes vector,

δ : is the phase angle,

It is may by substituted into Eq.(3.67) to give the n th-order ***algebraic eigenvalue problem*** ($K\phi = \lambda M\phi$):

$$\left([K] - \omega^2 [M]\right)\{\bar{U}\} = 0 \qquad \ldots(3.69)$$

For a nontrivial solution, Eq.(3.69) must be written in the following form:

$$\left| [K] - \omega^2 [M] \right| = 0 \qquad \ldots(3.70)$$

This is called the ***characteristic equation***. When the determinant of Eq.(3.70) is expanded, the result is a polynomial equation of degree n in ω^2 whose roots are the eigenvalues, or squared natural frequencies, ω_r^2. These can be ordered from the lowest to the highest:

$$0 \le \omega_1^2 \le \omega_2^2 \le \cdots \le \omega_r^2 \le \cdots \le \omega_n^2 \qquad ...(3.71)$$

Corresponding to each eigenvalue ω_r^2, there will be an ***eigenvector***, or ***natural mode*** $\{\overline{U_r}\}$, where

$$\{\overline{U_r}\} = \begin{Bmatrix} \overline{U_1} \\ \overline{U_2} \\ \vdots \\ \overline{U_n} \end{Bmatrix} \quad r = 1,2,\ldots,n \qquad \ldots(3.72)$$

Texts are involved many techniques for solving the eigenvalue problem. However in the present work only two methods are adopted, ***inverse iteration method*** and ***Gram- Schmidt method***.

3.5.1:Inverse Iteration Method

This technique is very effective in calculating the smallest eigenvalue and the corresponding eigenvector which are the most important eigenpair in structural dynamics.

The basic steps for solving the eigenvalue problem of the form ($K\phi=\lambda M\phi$)using the inverse iteration method are **[8]**:-

1- Assuming a starting iteration vector, $\{X_1\}$, almost with all terms equal to one

2- Assuming that:-

$$\{Y_1\} = [M]\{X_1\} \qquad \ldots(3.73)$$

3- Evaluating, for each iteration step k=1,2,……,

$$\{\overline{X}_{k+1}\} = [K]^{-1}\{Y_k\} \qquad \ldots(3.74)$$

$$\{\overline{Y}_{k+1}\} = [M]\{\overline{X}_{k+1}\} \qquad \ldots(3.75)$$

$$\rho\left(\{\overline{X}_{k+1}\}\right) = \frac{\{\overline{X}_{k+1}\}^T\{Y_k\}}{(\{\overline{X}_{k+1}\}^T\{\overline{Y}_{k+1}\})} \qquad \ldots(3.76)$$

$$\{Y_{k+1}\} = \frac{\{\overline{Y}_{k+1}\}}{(\{\overline{X}_{k+1}\}^T\{\overline{Y}_{k+1}\})^{1/2}} \qquad \ldots(3.77)$$

Where the superscript T denotes transpose.

4- The value of $(\{\overline{X}_{k+1}\})$ in Eq.(3.76) represents an approximation to the eigenvalue, λ_1. Denoting the current approximation for λ_1 by $\lambda_1^{(k+1)}$, i.e., $\lambda_1^{(k+1)} = \rho\left(\{\overline{X}_{k+1}\}\right)$, the convergence will occur when:-

$$\frac{\left|\lambda_1^{(k+1)} - \lambda_1^{(k)}\right|}{\lambda_1^{(k+1)}} \le 10^{-S} \qquad \ldots(3.78)$$

Where s is the number of significant digits of the desired accuracy.

5- If m is the last iteration cycle, then the smallest eigenvalue, λ_1, and the corresponding eigenvector, $\{\phi_1\}$, will be respectively:-

$$\lambda_1 = \rho\left(\{\overline{X}_{m+1}\}\right) \qquad \ldots(3.79)$$

$$\{\phi_1\} = \frac{\{\overline{X}_{m+1}\}}{(\{\overline{X}_{m+1}\}^T \{\overline{Y}_{m+1}\})^{1/2}} \qquad \ldots(3.80)$$

3.5.2:Gram-Schmidt Method

The other eigenpair can be obtained by the inverse iteration method through choosing the trial vector form a space M-orthogonal to the calculated eigenvector. A particular vector orthogonalization procedure that is employed extensively is the ***Gram-Schmidt method.***

In order to consider a general case **[9]**, assume that the eigenvectors $\{\phi_1\}$, $\{\phi_2\}$,…, $\{\phi_m\}$ are calculated by inverse iteration and that it is wanting now to M-orthogonalize {X} (the trial vector) to these eigenvectors. In Gram-Schmidt orthogonalization a vector $\{\tilde{X}\}$, which is M-orthogonal to the eigenvectors $\{\phi_i\}$, i = 1,…,m, is calculated by using:

$$\{\tilde{X}\} = \{X\} - \sum_{i=1}^{m} \vartheta_i \{\phi_i\} \qquad \ldots(3.81)$$

Where the coefficients ϑ_i are obtained by using the conditions that

$$\{\phi_i\}^T [M] \{\tilde{X}\} = 0 \qquad i = 1,\ldots,m \qquad \ldots(3.82)$$

and $$\{\phi_i\}^T [M] \{\phi_j\} = \delta_{ij} \qquad \ldots(3.83)$$

where δ_{ij} is Kronecker delta, $\delta_{ij} = 1$ for $i = j$ and $\delta_{ij} = 0$ for $i \neq j$.

Premultiplying both sides of Eq.(3.81) by $\{\phi_i\}^T$ [M], one may obtain:

$$\vartheta_i = \{\phi_i\}^T [M] \{X\} \qquad i = 1,\ldots,m \qquad \ldots(3.84)$$

Now the inverse iteration is started using the vector $\{\tilde{X}\}$ instead of {X}.

CHAPTER FOUR

ELASTO-PLASTIC ANALYSIS

4.1 Introduction

In this chapter, an elasto-plastic analysis of thick plates of arbitrary shape and support condition subjected to dynamic transverse loading is presented. Derivation is presented of the basic equations relating to the incremental approach

The approach which is followed in this study for the analysis of isotropic plates of elastic - perfectly plastic material with the assumed stress –strain relationship is shown in Fig.(4.1). However, this approach is equally applicable to plates of other inelastic solids. ***von Mises'*** yield criterion and the associated flow rule (***Prandtle –Reuss relation***) are used here.

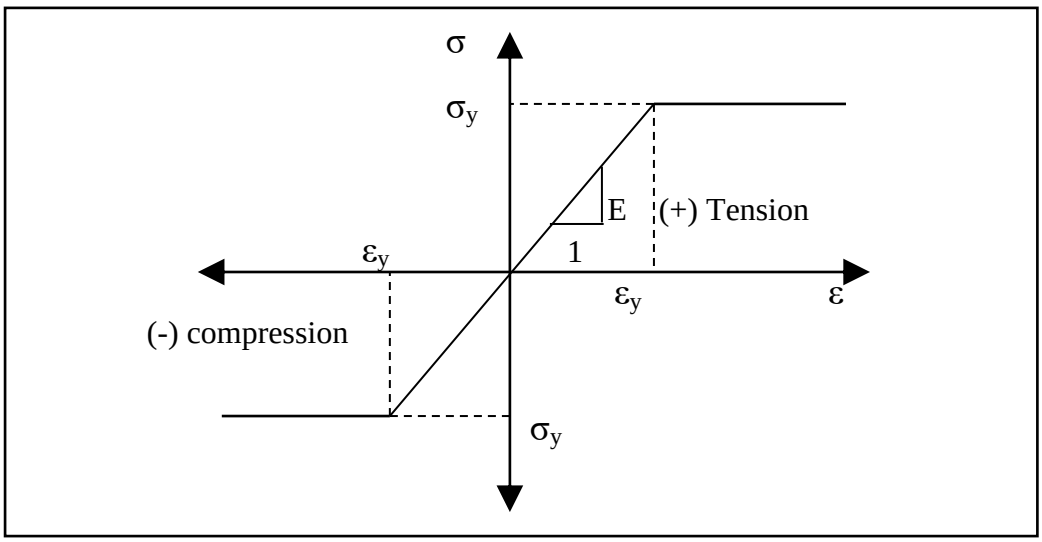

Fig.(4.1) : *The assumed stress – strain relationship in uniaxial loading.*

4.2 Flow Theory of Plasticity

A yield criterion is a hypothesis concerning the limit of elasticity under any state of stresses [23]. The yield criterion employed in the present work for an isotropic materials will be a generalization of ***von-Mises'*** plasticity theory. According to this criterion, yielding begins under any state of stress when the effective stress $(\bar{\sigma})$ exceeds the yield strength in uniaxial tension or compression (σ_y).

$$\bar{\sigma} = \frac{\sqrt{2}}{2}\left[(\sigma_x - \sigma_y)^2 + (\sigma_y - \sigma_z)^2 + (\sigma_z - \sigma_x)^2 + 6(\tau_{xy}^2 + \tau_{yz}^2 + \tau_{zx}^2)\right]^{1/2} \quad \ldots(4.1)$$

More refined tests certify that the circular cylinder of ***von-Mises'*** yield criterion gives a more exact yield surface for most metals than hexagonal prism considered in ***Tresca's*** yield criterion [23].

4.3 Formulation of the basic elasto-plastic equations

Through neglecting the transverse direct stress (σ_z) and squaring both sides of Eq.(4.1), ***von-Mises'*** yield criterion can be written as follows [17,23]:

$$\bar{\sigma}^2 = \frac{1}{2}\left[(\sigma_x - \sigma_y)^2 + \sigma_y^2 + \sigma_x^2 + 6(\tau_{xy}^2 + \tau_{yz}^2 + \tau_{zx}^2)\right] \quad \ldots(4.2)$$

Eq.(4.2) may be expressed in terms of principal stresses as follows:

$$\bar{\sigma}^2 = \frac{1}{2}\left[(\sigma_1-\sigma_2)^2+(\sigma_2-\sigma_3)^2+(\sigma_3-\sigma_1)^2\right] \quad \ldots(4.3)$$

According to ***von-Mises'*** theory, the effective plastic strain increment $d\,\bar{\varepsilon}_p$ is defined as a combination of the separate plastic strain increments (neglecting ε_z) **[**17,23**]**

$$d\,\bar{\varepsilon}_p = \frac{\sqrt{2}}{3}\,[(d\,\varepsilon_{xp}-d\,\varepsilon_{yp})^2+(d\,\varepsilon_{yp})^2+(d\,\varepsilon_{xp})^2+\frac{3}{2}(d\gamma_{xyp})^2 + \frac{3}{2}(d\gamma_{yzp})^2+\frac{3}{2}(d\gamma_{zxp})^2\,]^{1/2} \quad \ldots(4.4)$$

and in terms of principal plastic strain increments:-

$$d\,\bar{\varepsilon}_p = \frac{\sqrt{2}}{3}\,[(d\,\varepsilon_{p1}-d\,\varepsilon_{p2})^2+(d\,\varepsilon_{p2}-d\,\varepsilon_{p3})^2+(d\,\varepsilon_{p3}-d\,\varepsilon_{p1})^2\,]^{1/2} \quad \ldots(4.5)$$

by differentiating Eq.(4.2), one gets

$$d\,\bar{\sigma} = \{Q\}^T_{1*5}\ \{d\,\sigma\}_{5*1} \quad \ldots(4.6)$$

Where:-

$$\{Q\} = \frac{3}{\bar{\sigma}}\left\{\frac{\sigma'_x}{2}\ \frac{\sigma'_y}{2}\ \tau'_{xy}\ \tau'_{yz}\ \tau'_{zx}\right\} \quad \ldots(4.6a)$$

$$\{d\,\sigma\} = \{d\,\sigma_x\ \ d\,\sigma_y\ \ d\,\tau_{xy}\ \ d\,\tau_{yz}\ \ d\,\tau_{zx}\}$$

$$\sigma'_x = \sigma_x - \sigma_a \quad ;\ \sigma'_y = \sigma_y - \sigma_a \quad ;\ \sigma_a = \frac{\sigma_x+\sigma_y}{3}$$

$$\tau'_{xy} = \tau'_{xy} \quad ;\ \tau'_{yz} = \tau'_{yz} \quad ;\ \tau'_{zx} = \tau'_{zx}$$

The mathematical form of flow rule (***Pradtle-Reuss*** relation)**[**23**]** is:

$$\frac{d\,\varepsilon_{xp}}{\sigma'_x} = \frac{d\varepsilon_{yp}}{\sigma'_y} = \frac{d\gamma_{xyp}}{2\tau'_{xy}} = \frac{d\gamma_{yzp}}{2\tau'_{yz}} = \frac{d\gamma_{zxp}}{2\tau'_x} = d\,\lambda \quad \ldots(4.7)$$

(d λ : instantaneous non-negative constant of proportionality)

and in the form of principal stress directions:

$$\frac{d\varepsilon_{p1}-d\varepsilon_{p2}}{\sigma_1-\sigma_2}=\frac{d\varepsilon_{p2}-d\varepsilon_{p3}}{\sigma_2-\sigma_3}=\frac{d\varepsilon_{p3}-d\varepsilon_{p1}}{\sigma_3-\sigma_1}=d\lambda \qquad \ldots(4.8)$$

then:-

$$d\lambda\sqrt{(\sigma_1-\sigma_2)^2+(\sigma_2-\sigma_3)^2+(\sigma_3-\sigma_1)^2}= \sqrt{(d\varepsilon_{p1}-d\varepsilon_{p2})^2+(d\varepsilon_{p2}-d\varepsilon_{p3})^2+(d\varepsilon_{p3}-d\varepsilon_{p1})^2} \qquad \ldots(4.9)$$

and from the principle terms for the stresses and strains in eqs.(4.3),(4.5) and (4.9):-

$$d\lambda\sqrt{2}\ \bar{\sigma}=\frac{3}{\sqrt{2}}\,d\bar{\varepsilon}_p$$

and in another form:

$$d\lambda=\frac{3}{2}\frac{d\bar{\varepsilon}_p}{\bar{\sigma}} \qquad \ldots(4.10)$$

By substituting from Eq.(4.10) in Eq.(4.7) and put the result in a matrix form:-

$$\begin{Bmatrix} d\varepsilon_{xp}\\ d\varepsilon_{yp}\\ d\gamma_{xyp}\\ d\gamma_{yzp}\\ d\gamma_{zxp}\end{Bmatrix}=\frac{3}{2}\frac{d\bar{\varepsilon}_p}{\bar{\sigma}}\begin{Bmatrix}\sigma'_x\\ \sigma'_y\\ 2\tau'_{xy}\\ 2\tau'_{yz}\\ 2\tau'_{zx}\end{Bmatrix}$$

or, in other form:

$$\{d\varepsilon_p\}_{5*1}=\{Q\}_{5*1}\quad d\bar{\varepsilon}_p \qquad \ldots(4.11)$$

Where:-

$$\{d\varepsilon_p\}=\{d\varepsilon_{xp}\quad d\varepsilon_{yp}\quad d\gamma_{xyp}\quad d\gamma_{yzp}\quad d\lambda_{zxp}\}$$

Form Fig. (4.2), one can get:-

$$\{d\sigma\}_{5*1}=[E]_{5*5}\quad\{d\varepsilon_e\}_{5*1} \qquad \ldots(4.12)$$

or $\{d\sigma\} = [E]\ \left(\{d\varepsilon_{ep}\} - \{d\varepsilon_p\}\right)$ …(4.13)

where: $\{d\varepsilon_e\}$: elastic strain increments.

$\{d\varepsilon_p\}$: plastic strain increments.

$\{d\varepsilon_{ep}\}$: total strain increments.

Multiply both sides of Eq.(4.13) by $\{Q\}^T$ and substituting from Eq.(4.6) and Eq.(4.11) in the resulting equation give:-

$$d\bar{\sigma} = \{Q\}^T\ [E]\ \left(\{d\varepsilon_{ep}\} - \{Q\}\, d\bar{\varepsilon}_p\right) \quad \ldots(4.14)$$

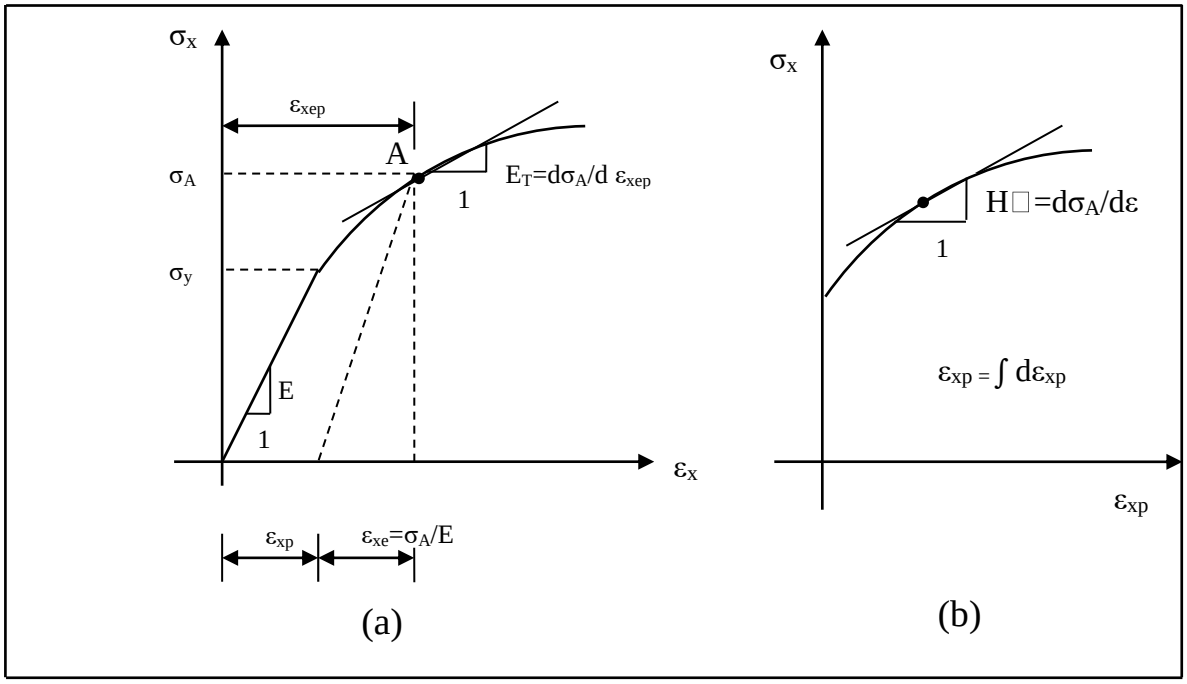

Fig.(4.2) : *General stress-strain relations in uniaxial tension. (E: elastic modulus, E_T: tangent modulus). The second plot is obtained from the first by subtracting the elastic strains.[5]*

but form Fig.(4.2):

$$d\bar{\sigma} = H'\ d\bar{\varepsilon}_p \quad \ldots(4.15)$$

$$\{Q\}^T\ [E]\ \left(\{d\varepsilon_{ep}\} - \{Q\}\, d\bar{\varepsilon}_p\right) = H'\, d\bar{\varepsilon}_p$$

$$\left(H' + \{Q\}^T\ [E]\{Q\}\right)\, d\bar{\varepsilon}_p = \{Q\}^T\ [E]\ \{d\varepsilon_{ep}\}$$

$$d\bar{\varepsilon}_p = \frac{\{Q\}^T [E]}{H' + \{Q\}^T [E]\{Q\}} \{d\varepsilon_{ep}\} \quad \ldots(4.16)$$

$H' = 0$ (for elastic-perfectly plastic material [5])

Let $\lfloor W \rfloor = \frac{\{Q\}^T [E]}{\{Q\}^T [E] \{Q\}}$ …(4.17)

Then, Eq.(4.16) becomes:-

$$d\bar{\varepsilon}_p = \lfloor W \rfloor_{1*5} \{d\varepsilon_{ep}\}_{5*1} \quad \ldots(4.18)$$

Then, to find the elasto-plastic stress-strain matrix [E_{ep}], the stress increments {dσ} could be expressed in terms of total strain increments {$d\varepsilon_{ep}$} as follows:-

$$\{d\sigma\} = \lfloor E_{ep} \rfloor \{d\varepsilon_{ep}\} \quad \ldots(4.19)$$

But from Eq.(4.11) and Eq.(4.18), one can relate the plastic strain increments {$d\varepsilon_p$} with the total strain increments {$d\varepsilon_{ep}$} by the following equation:

$$\{d\varepsilon_p\} = \{Q\} \lfloor W \rfloor \{d\varepsilon_{ep}\} \quad \ldots(4.20)$$

Then, substituting Eq.(4.20) in Eq.(4.13) gives:

$$\{d\sigma\} = ([E] - [E] \{Q\} \lfloor W \rfloor) \{d\varepsilon_{ep}\} \quad \ldots(4.21)$$

By comparing Eq.(4.19) with Eq.(4.21), one deduces that

$$\lfloor E_{ep} \rfloor_{5*5} = [E] - [E] \{Q\} \lfloor W \rfloor \quad \ldots(4.22)$$

CHAPTER FIVE

COMPUTER PROGRAM TESTING AND DISCUSSION OF RESULTS

5.1 Introduction

An algorithm for the method which is used and the computer program ***EPDATP*** (Elasto-Plastic Dynamic Analysis of Thick Plates) which is developed in the present study will be described in this chapter.

Then, the results that obtained from the application of the proposed analysis and the prepared computer program ***EPDATP*** to several theoretical problems is presented.

A convergence study is carried out in order to select a suitable mesh with minimum number of elements that indicates a convergence in results.

In order to verify the reliability of the computer program, some examples reported in previous researches are considered.

Finally, the effect of some analysis parameters such as the boundary conditions, the dimensions aspect ratio and the effect of damping are studied.

5.2 An algorithm for the present study

An algorithm for the elasto-plastic analysis of plate under transverse dynamic load by the finite element method is presented in this section:-

For each time interval:-

1. Compute the mass matrix $[M] = \sum [m_e]$.
2. For each time step (i):
   a. If i = 1, 1. find the elastic stiffness matrix $[K_e] = \sum [k_e]$.
      2.compute the first and second natural frequency by using the ***inverse iteration method*** and ***Gram-Schmidt method*** respectively.
      3.find the damping factors: Z_1 and Z_2.
   b. If $i \neq 1$ find $[E_{epi}]$ using Eq.(4.22) at each Gauss point in each element, corresponding to stress history $\{\sigma_{i-1}\}$ of that point. Then find the elastic-plastic total stiffness matrix of the plate $[K_{epi}]=\sum[K_{epi}]$ where

$$[K_{epi}] = \int_V [B]^T [E_{epi}] [B]\, dV \qquad \text{for an element.}$$

   Such updated total stiffness matrix $[K_{epi}]$ at the beginning of each time step will be used in all iterations in that time step.
3. Compute the damping matrix from the equation: $[C] = Z_1[M] + Z_2[K]$
4. At iteration (j);
   a. if (j=1) apply the load step p_i for $\{\Delta R_j\}$ but,
   b. if (j≠1) apply the residual forces from previous iteration to be $\{\Delta R_j\}$(see step 9 for the mathematical expression for the residual forces).

Then, find the $[K^\bullet]$ and $[F^\bullet]$ from equations :

$$[K^\bullet] = (1/\beta\Delta t^2)[M] + (\gamma/\beta\Delta t)[C]_{t+\Delta t} + [K]_{t+\Delta t}$$

$$\{\Delta F^{\bullet}(t)\} = \{F(t)\}_{t+\Delta t} - \{f\}_t + [M]\,[(1/\beta\Delta t\{\dot{D}\}_t + [(1/2\beta)-1]\{\ddot{D}\}_t\,]$$

$$+ [C]_{t+\Delta t}\,[\,[\,(\gamma/\beta)-1]\{\dot{D}\}_t + \Delta t\,[(\gamma/2\beta)-1]\{\ddot{D}\}_t]$$

and compute the corresponding $\{\Delta D_j\}$ from equilibrium:

$[K^{\bullet}]\ \{\ \Delta D_j\ \} = \{F^{\bullet}(t)\}$

5. Update acceleration, velocity and displacement vectors from the equations :

$$\{\ddot{D}\}_{t+\Delta t} = (1/\beta\Delta t^2)\{\Delta D\} - (1/\beta\Delta t)\{\dot{D}\}_t - [(1/2\beta)-1]\{\ddot{D}\}_t$$

$$\{\dot{D}\}_{t+\Delta t} = (\gamma/\beta\Delta t)\{\Delta D\} + [1-(\gamma/\beta)]\{\dot{D}\}_t - \Delta t\,[(\gamma/2\beta)-1]\{\ddot{D}\}_t$$

$$\{D\}_{t+\Delta t} = \{D\}_t + \{\Delta D\}$$

6. Extract the element's $\{\Delta d_j\}$ form $\{\Delta D_j\}$ and compute the resulting strain increments $\{\Delta\ \varepsilon_{epj}\} = [B]\ \{\Delta d_j\}$ (at each Gauss point). After that, find the effective elastic-plastic strain increment $\Delta\bar{\varepsilon}_{epj}$ from Eq. (4.4) putting the subscript (ep) instead of (p) in all terms of that equation. Then, subdivide such strain increments into subincrements, where for each subincrement (m):
$\{\Delta\varepsilon_{epm}\} = \{\Delta\varepsilon_{epj}\}\ /\ (\Delta\bar{\varepsilon}_{epj} / 0.0002)$. The factor (0.0002) is suitable for ductile metals .[5]
7. In each subincrement (m); at a certain Gauss point in an element from the plate, find the effective plastic strain increment $\Delta\bar{\varepsilon}_{pm}$ from Eq. (4.18). Then, compute the plastic strain increments $\{\Delta\varepsilon_{pm}\}$ from Eq. (4.11). The stress increments $\{\Delta\sigma_m\}$ are found from Eq.(4.13) to be added to the total stress vector from previous subincrement(or iteration) $\{\sigma_{m-1}\}$ to find $\{\sigma_m\}$ at the end of subincrement (m). Then compute the effective stress $\bar{\sigma}_m$ from Eq.(4.1). The subscript (m) is put in each term in each one of the preceding indicated equations in

this step. In the present elasto-plastic analysis, the normality condition and incompressibility condition are satisfied through utilizing the ***Prandtle-Reuss*** relation (***flow rule of von Mises'*** plasticity theory) in deriving the preceding equations as introduced in the previous section. Although, a finite sized stress increments, which result from each subincrement within iteration within load time step, may depart the final stress point, corresponding to such stress increments at the end of that subincrement, from the yield surface as shown in Fig.(5.1). This discrepancy can be particularly eliminated by insuring that the subincrements in each iteration are sufficiently small. However, the point of final stress can be reduced to the yield surface simply by scaling the stress vector $\{\sigma_m\}$ as given in Fig.(5.1) .

At the end of subincrement (m), the updated $\{Q_{m+1}\}$ and $\lfloor W_{m+1} \rfloor$ are found using Eq.(4.6a) and (4.17) respectively utilizing the stress history $\{\sigma_m\}$ for the considered Gauss point.

Fig.(5.1): *Scaling the stress vector $\{\sigma_m\}$ at the end of each subincrement (m) in order to satisfy the yield condition.[5]*

8. If subincrements have completed go to the next Gauss point and repeat the subincrement process (steps: 6,7) at the same iteration. Otherwise, go to the next subincrement for the same Gauss point repeating step (7) for subincrement (m+1) …etc.
9. If the subincrement are completed for all Gauss points in the plate within iteration (j), find the residual forces in the whole plate $\{\Delta R_{j+1}\}$ to be used in the next iteration (j+1):

$$\{\Delta R_{j+1}\} = \{R_j\} - \sum \int_V [B]^T \{\sigma_j\} \, dV$$

where the vector $\{R_j\}$ of equivalent nodal forces corresponds to the

load increment (i), and { σ_j } is the total stresses vector, evaluated at each Gauss point, which equals to total stresses vector {σ_m} at the last subincrement in the considered Gauss point within iteration (j).

10. Find the (norm) of residual forces at the end of iteration (j) as follows:

$$(norm)_j = \left[\sqrt{\sum \left(\Delta R_{j+1}\right)^2} \; / \; \sqrt{\sum \left(R_j\right)^2} \right] * 100$$

where: R_j represented the load at the considered time step(p_i).

Then;

a. If $(norm)_j \leq (norm)_{j-1}$ and $(norm)_j \leq 0.1$, print the total nodal displacements $\{D_j\} = \{D_{j-1}\} + \{\Delta D_j\}$ which represent $\{D_i\}$ at the end of the time step t . Then, go to step (2) with the next load step(i+1) at time $t+\Delta t$.

b. If $(norm)_j \leq (norm)_{j-1}$ and $(norm)_j > 0.1$, go to step (4) for the next iteration (j+1).

c. Otherwise (i.e. norm $)_j > (norm)_{j-1}$, the analysis reach to the failure stage, stop the analysis.

5.3 Computer program

This section presents a description of the computer program ***EPDATP*** (elasto-plastic dynamic analysis of thick plates) developed in the present study. The computer program which is coded in ***Fortran-77*** language was first introduced by ***Alwash*** in ***1989*** [5], and it was designed to deal with elasto-plastic analysis of thick plates under static loads.

In the present study, the previous version of the computer program has been modified to deal with the analysis of plates under dynamic loads. The dynamic part of this program is designed to deal with the dynamic response

using Newmark's integration method. Also, the program is developed to find the natural frequencies. In addition, the damping effect on the dynamic behavior of plates is included in the program.

The properties and abilities of this program may be summarized as:

1. The program can be used for the analysis for thin as well as thick plates with constant and varying thickness.
2. Also, it can be used for linear and nonlinear(elasto-plastic) analysis with static and dynamic loads.
3. The program is capable of dealing with the eigenvalue problem, in order that two eigenvalues are obtained. The first one represents the lowest natural frequency of the system obtained by using ***the inverse iteration method*** while the other represents the second natural frequency and it is obtained using ***Gram-Sehmidt method.***
4. Including damping properties using ***Rayleigh*** type damping.
5. In the dynamic analysis, the program can be used for any function of loading such as step, triangle impact or impulse loading.

The structure of the flow chart of the present program is given in figure (5.2).

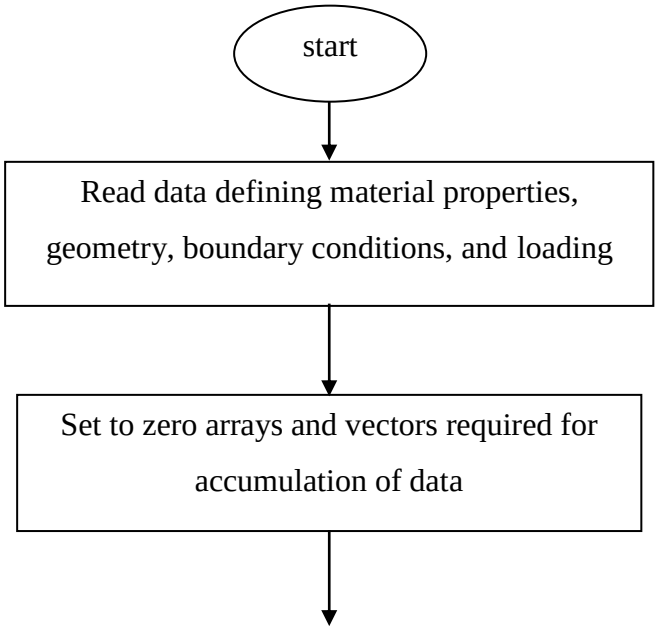

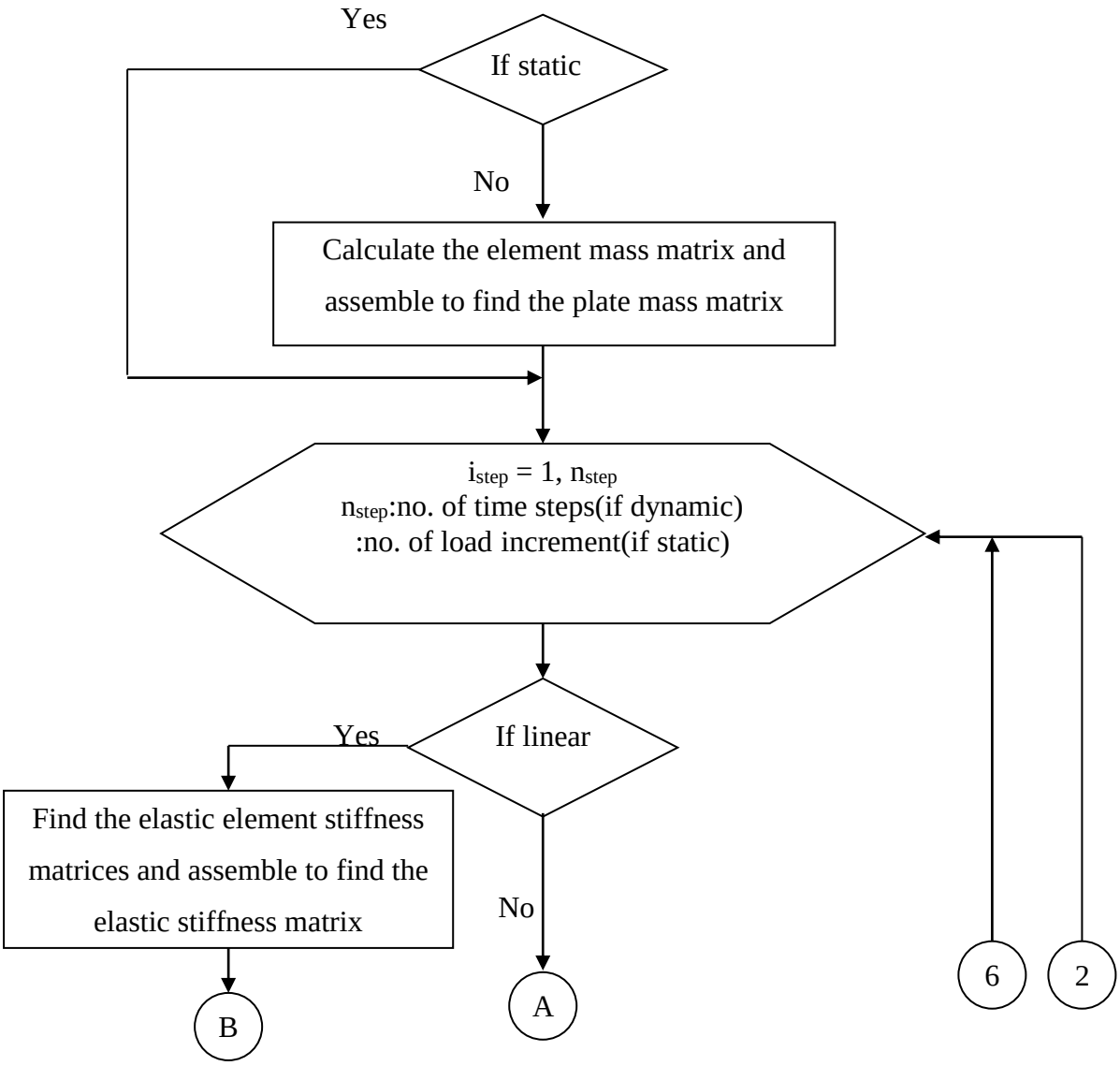

Fig.(5.2):*flow chart for program of incremental F.E.M analysis for plates*

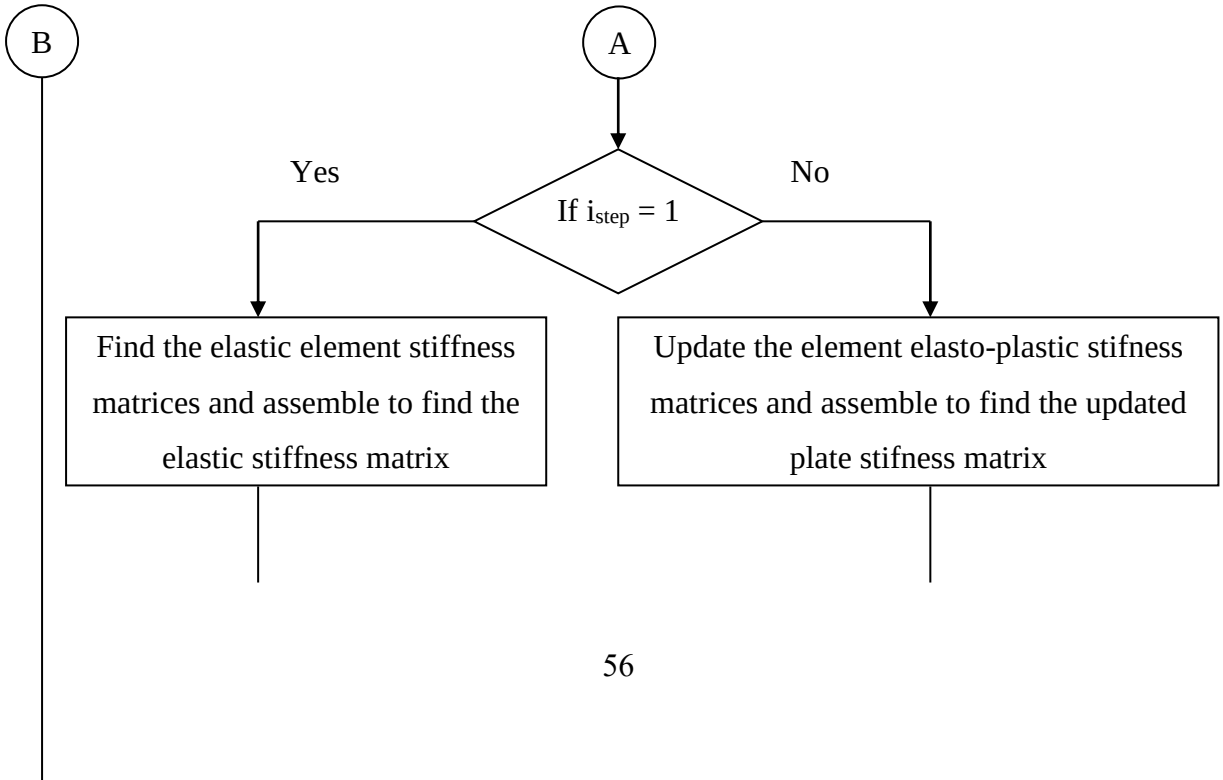

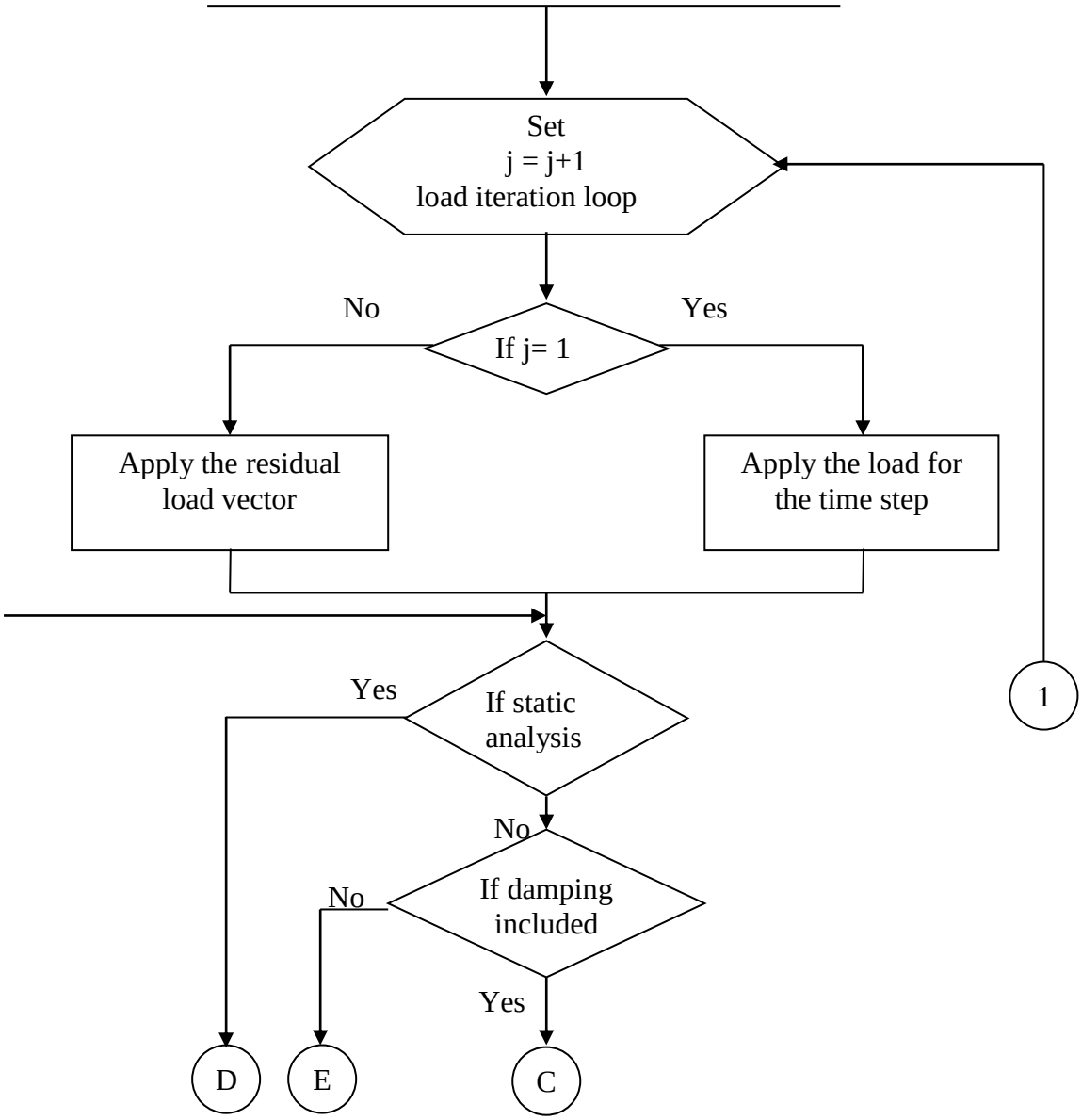

Fig.(5.2): *continued*

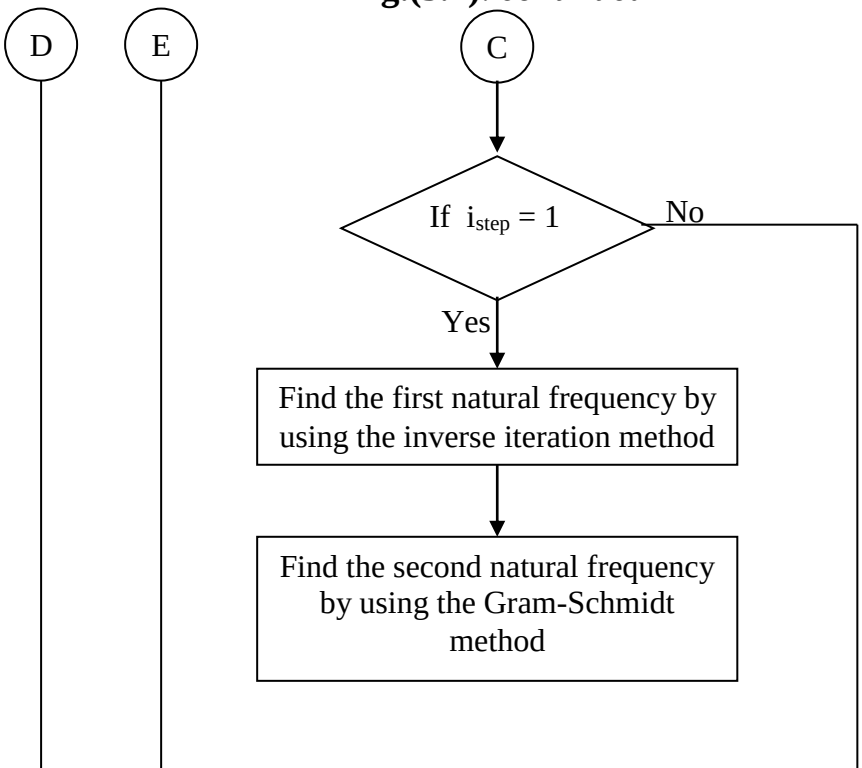

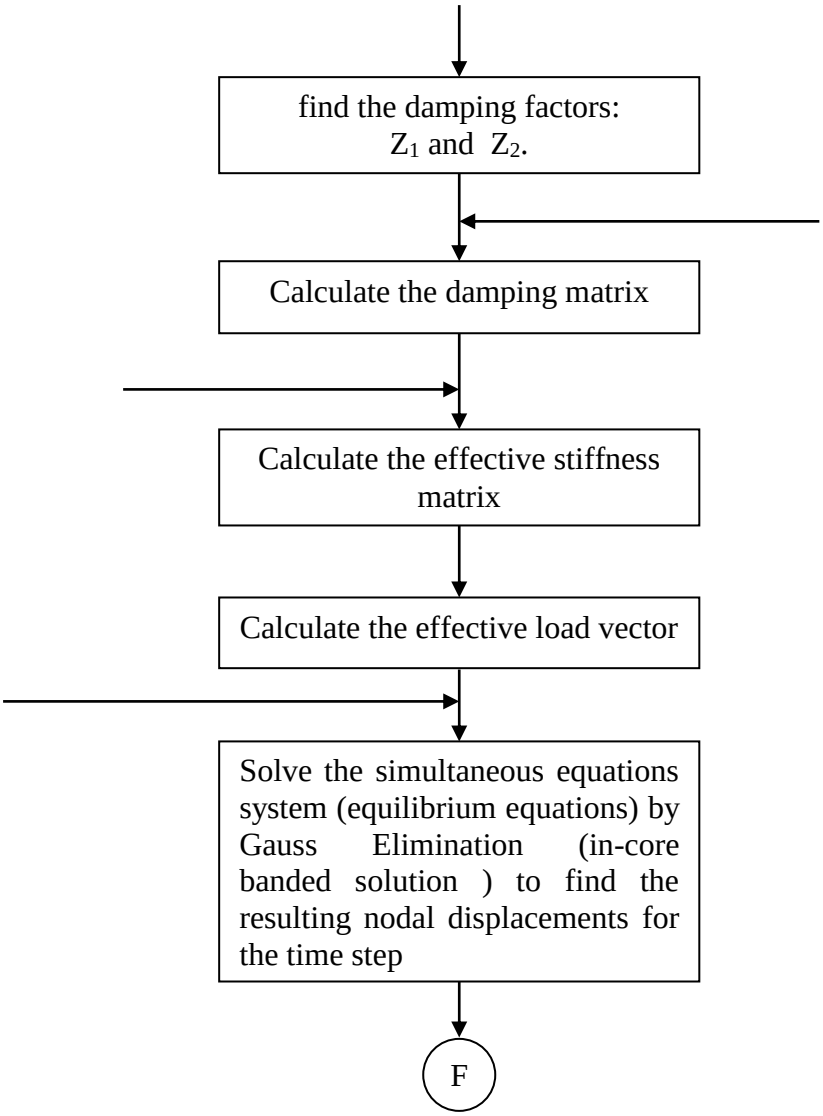

Fig(5.2): *continued*

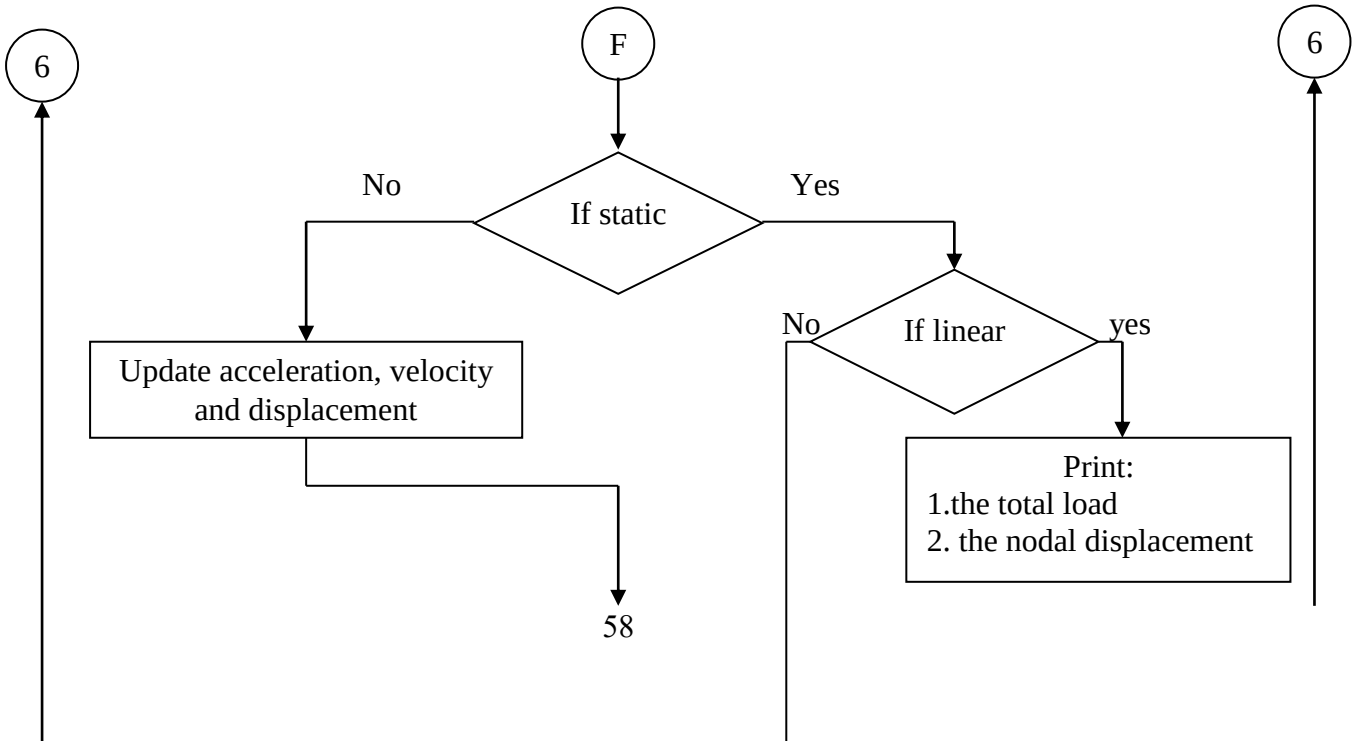

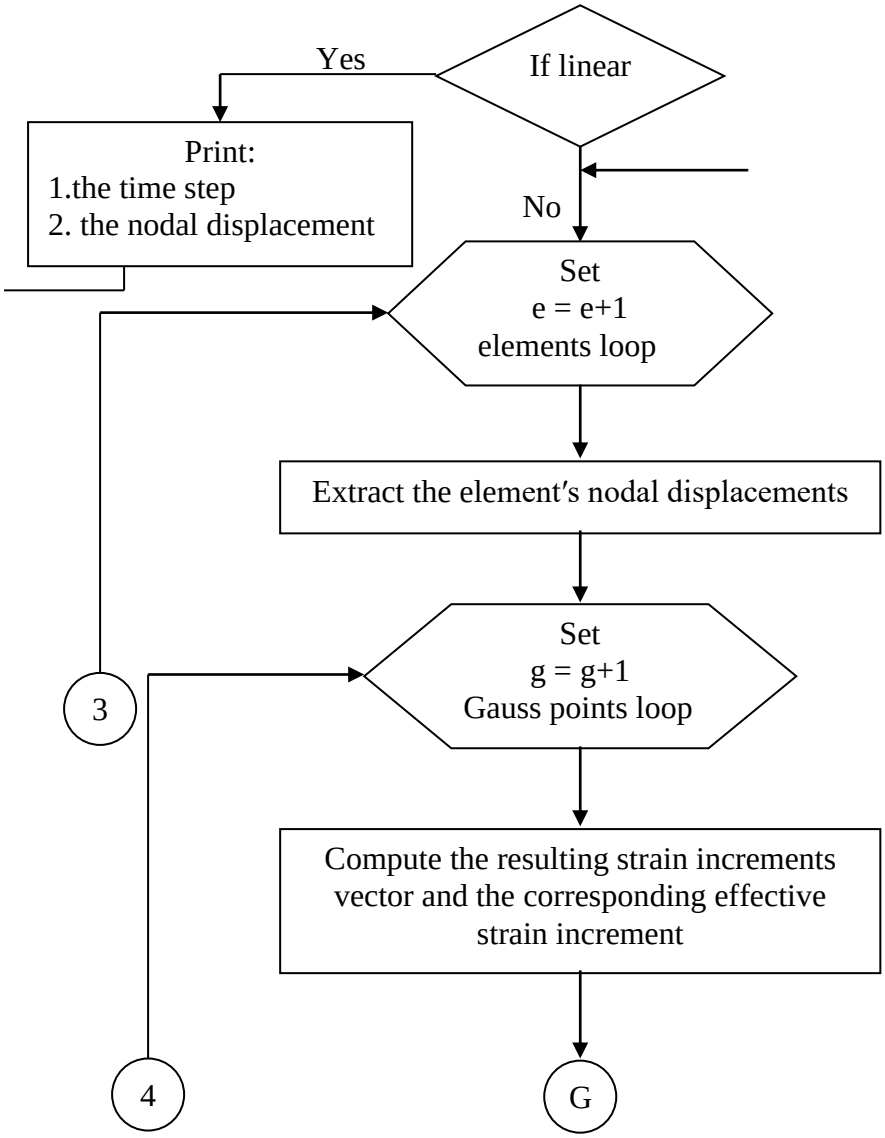

Fig.(5.2): *continued*

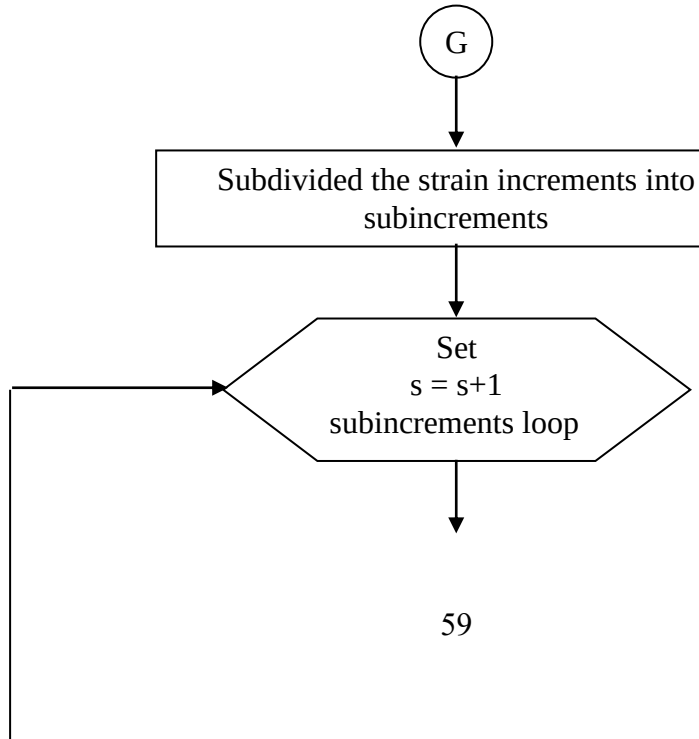

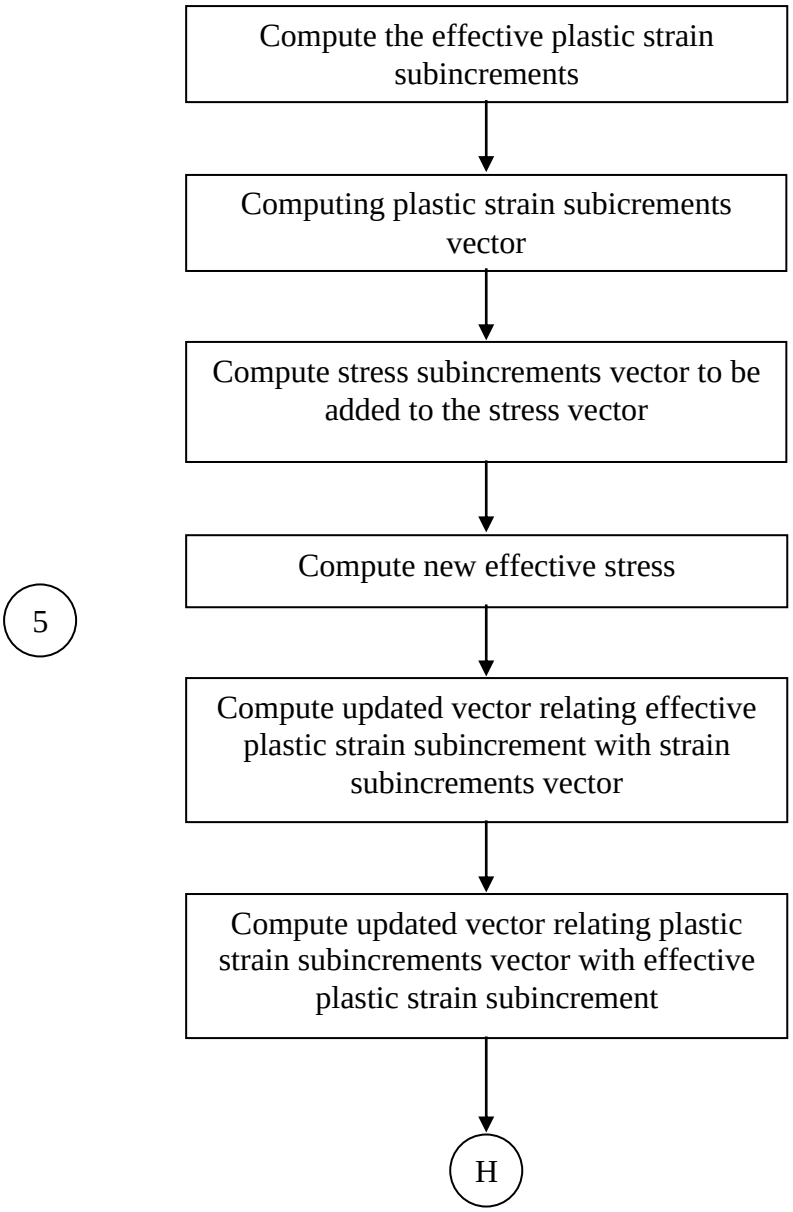

Fig.(5.2): *continued*

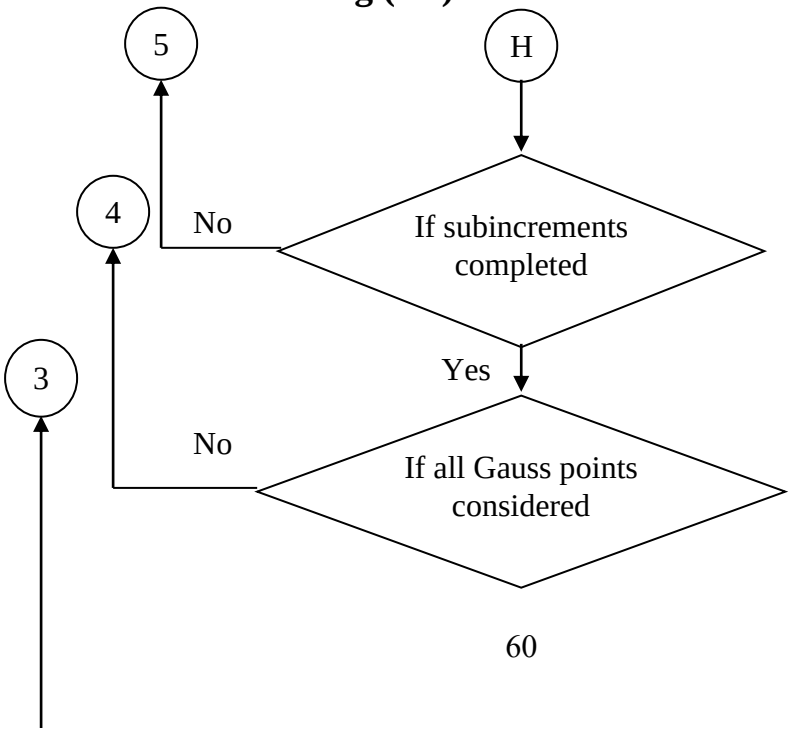

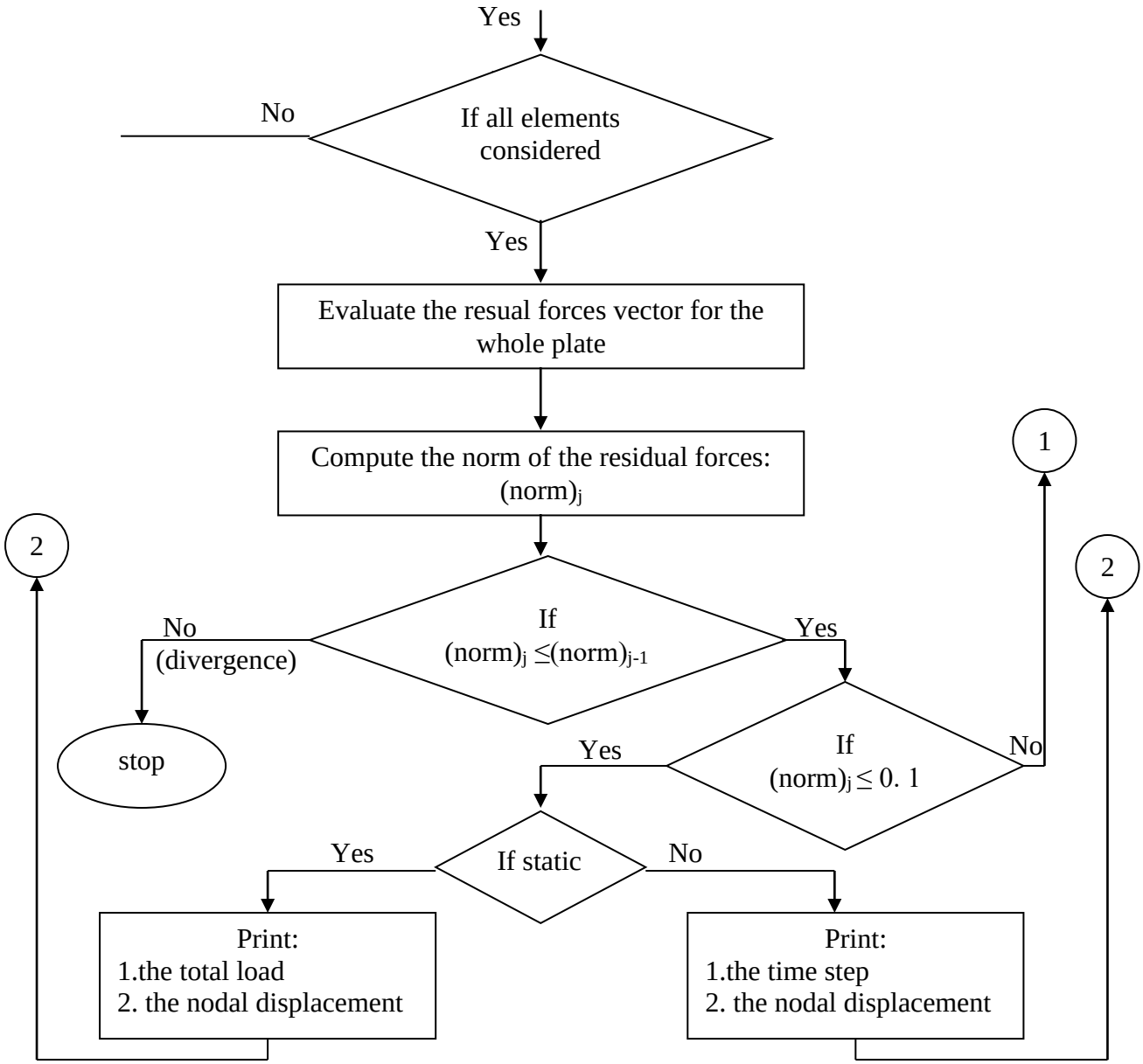

Fig.(5.2): *continued*

5.4 Numerical examples

In order to verify the reliability of the computer program, some examples are considered. These examples are varied among static and dynamic analysis :

5.4.1: Static Analys

Print:
1.the time step
2. the nodal displacement

5.4.1.1:Example No.1 : ***Clamped square plate subjected to***

transverse static uniformly distributed load

A clamped square plate (Fig.(5.3)) subjected to an increasing uniform load is studied as example to validate the static part of the computer program. The plate geometry and material properties are as follows:-

thickness (h) = 0.2m

length (a) = 6.0m

modulus of elasticity (E) = 30000.0MPa

Poisson's ratio (υ) = 0.3

the yield stress= 30.0MPa.

$\theta_y = 0$

Fig .(5.3) : *Clamped support square plate.*

The problem was analyzed by ***Al-Saeg*** [4] in ***2005*** by using elastic-plastic geometrically nonlinear finite element analysis using the degenerated shell element with 5 degree of freedom per node (u, v, w, θ_x ,θ_y). Due to symmetry of loading, geometry and boundary condition, only one quarter of the plate was analyzed using 9 elements. Number of load increment was 20 and 6 layers are used to represent the material through the thickness.

In the present analysis, also one quarter is used utilizing the symmetry, and the number of load increments is 20.

The convergence of the results of the finite element method, for the mesh size, was tested by Alwash[5] for square plate subjected to static load and it was showed that the 9 elements mesh size was the suitable mesh. So 9 elements mesh size will be used in this example.

The results of the deflection at the plate center vs. the uniformly distributed load are plotted in Fig.(5.4). From this figure, and by comparing the results of the present study with that results which are obtained by ***Al-Saeq*** , it is clear that the difference between the two curves is vary small in first loads (to about q = 0.15MPa), but after that (when the loads increase) the difference increases (reach to about 7%), where the effect of the nonlinearity appear. Also, the results explain that the load capacity for the plate decreases when the geometrical nonlinearity included, and the deflection for the plate under the same amount and type of load become greater (by about 7%) when the geometrical nonlinearity considered.

The load versus central deflection curves are shown in Fig.(5.5) for different values of span to thickness ratio L_0($L_0 < 3$ for thick plates [5]) using 9 elements (mesh(3) in Fig.(5.9)). As expected, the load capacity for the plate is increasing when the plate become more thick, and the deflection reduced for the plate which is subjected to same amount and type of loading when the plate thickness increases because the plate become more stiff.

Fig.(5.4) *: Load versus central deflection for a clamped square plate.*

Fig.(5.5) : *Load versus central deflection for a clamped square plate for different values of L_0 (the symbol * represent the collapse point)*

5.4.1.2:Example No.2 : Clamped circular plate subjected to transverse static concentrated load

A clamped circular plate (Fig.(5.6)) subjected to concentrated load at the center of the plate (p = 4Ib = 17.8N) is analyzed in the present study as another example for the static part of the computer program.

The plate geometry and material properties are as follows:

the radius(R) = 5 in (0.127m)

the thickness(h) = 2 in (0.0508m)

modulus of elasticity(E) = $1.09*10^6$ psi (7521MPa)

Poisson's ratio (υ) = 0.3

the yield stress = 57971.0149 psi = 400MPa

Fig .(5.6) : *Clamped support circular plate.*

The following formula is used to generate the analytical results [21]:

$U(r) = PR^2 [1-(r/R)^2-2(r/R)^2 \ln(R/r)-8D \ln(r/R)/(K G t R^2)]/16\pi D$

where:

U(r) = the displacement at distance r from the plate center

R = the radius of the plate

P = the force value

$D = \frac{E_x t^3}{12*(1-\upsilon^2)}$, where E_X and υ are the modulus of elasticity and the Poisson's ratio of the plate and t is the thickness of the plate.

$G = \frac{E_x}{2*(1+\upsilon)}$

K = 0.8333 (shear correction factor)

In the present analysis, one quarter is used utilizing the symmetry using 16 elements mesh size (mesh(4) in Fig.(5.22)), [16 elements mesh size is used here instead of 12 elements for comparing with the analytical study which gave the deflection for five points along the radius as in table (5.1)] . Table (5.1) shows the deflection for the plate with different distance from the center and from this table ,one can show that the present study has a

very good agreement with the analytical solution with difference not exceeded (1.58 %).

The load versus central deflection curves are shown in Fig.(5.7) for different values of radius to thickness ratio R_0 ($R_0 < 2$ for thick plates [5]) using 12 elements (mesh(3) in Fig.(5.22)),(the convergence of the results of the finite element method, for the mesh size, was tested by Alwash[5] for circular plate subjected to static load and it was shown that the 12 elements mesh size was the suitable mesh). The figure explain that the load capacity for the plate increases when the plate become more thick (R_0 decreases) and that was expected as discussion in example no.1.

Table (5.1) *: deflection for the circular plate in example no. 2*

Distance from the plate center, r	Deflection		% difference
	Analytical solution	Present study	
0	___	$6.407199*10^{-06}$in ($16.2743*10^{-08}$ m)	___
1 in (0.0254 m)	$3.53748*10^{-06}$ in ($8.9852*10^{-08}$ m)	$3.489087*10^{-06}$ in ($8.86427*10^{-08}$ m)	1.36
2 in (0.0508 m)	$2.19719*10^{-06}$ in ($5.58086*10^{-08}$ m)	$2.232036*10^{-06}$ in ($5.66937*10^{-08}$ m)	1.58
3 in (0.0762 m)	$1.14364*10^{-06}$ in ($2.90485*10^{-08}$ m)	$1.131385*10^{-06}$ in ($2.87372*10^{-08}$ m)	1.1
4 in (0.1016 m)	$3.88628*10^{-07}$ in ($0.98712*10^{-08}$ m)	$3.937136*10^{-07}$ in ($1*10^{-08}$ m)	1.31
5 in (0.127 m)	0	0	0

Fig.(5.7) : *load versus central deflection for a clamped circular plate for*

*different values of R_0 (the symbol * represent the collapse point)*

5.4.2: Dynamic Analysis:

5.4.2.1:ExampleNo.3 : *Square plate subjected to suddenly applied uniformly distributed load*

A simply supported square plate (Fig.(5.8)) subjected to suddenly applied load is selected to be solved in the present study as example for the dynamic part of the computer program.

The intensity of the uniformly distributed load is equal 300 psi ($2.07*10^6 N/m^2$) (Fig.(5.8-b)).

The geometry and material properties are:

the length (a) = 10 in = 0.254m

the thickness (h) =0.5 in =0.0127m

modulus of elasticity (E) = $0.1 * 10^8$ psi =$69*10^3$ MPa

the mass density (ρ) = 0.2589 Ib/in^3 = $7.157*10^3$ Kg/m^3

Poisson's ratio (υ) = 0.3

the yield stress = 57971.0149 psi = 400MPa

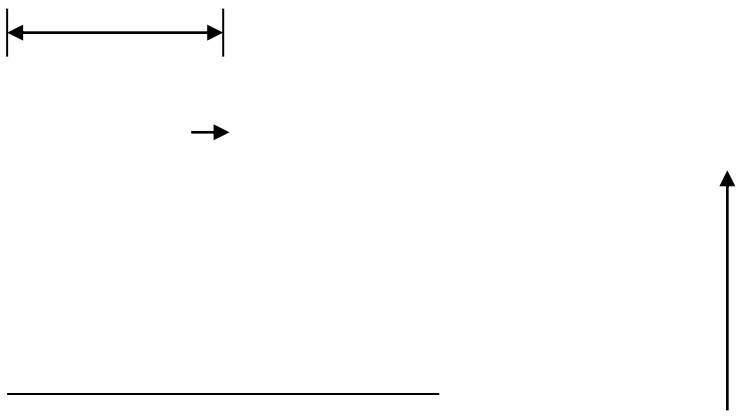

Fig. (5.8)*:Boundary condition for the plate and the dynamic characteristic.*

5.4.2.1.a : Convergence study

A convergence study for the mesh size is presented in Fig.(5.10) using the four meshes in Fig.(5.9) ,where one quarter of the plate is considered with time step equal to (0.00001 sec). From Fig.(5.10) one can show that the percentage difference for the 4 elements mesh size with respect to the 9 elements mesh size is really small (less than 0.1%) ,so, 4 elements mesh can be adopted.

But, when the convergence study repeated for the same plate by using clamped support instead of simply support as in Fig.(5.11) the percentage difference(at the third peak value) for the 4 elements mesh size with respect to the 9 elements mesh size was about 7%(amplitude difference), while this percentage was less than 1% when the 16 elements comparing with the 9 elements.

So, in the present study the 9 elements mesh size can be considered as a suitable mesh which is indicated a convergence in results with minimum number of elements .

5.4.2.1.b :Comparison with pervois studies

Sladek et al. [39] in ***2003*** solved this example by using the ***LBIE*** (local boundary integral equations) method with a meshless approximation. They analyzed the plate as a thin elastic plate with ***Kirchhoff theory***.

Also , in ***2006 Albarwary***[2] solved this example using the lower and higher order finite layer method with time step equal to ($0.223*10^{-4}$sec).

In the present study, the time step is equal to (0.00001 sec) and one quarter of the plate is used with 9 elements mesh. Also, the Mindlin plate theory is used, where the plate is analyzed as a thick plate.

Fig. (5.12) shows the dynamic response curves of the central deflection for the present study comparing with the study of ***Sladek et al.*** , from this figure one can noticed that the linear behavior has an amplitude difference by about 6.66% and a period difference by about 10% when the meshless approach is used comparing with the finite element method .The same figure shows that the central deflection for the present analysis using the linear behavior increasing by about 3.3% when the nonlinear behavior is used. This is due to the relatively low load is applied and mainly the whole plate is remain within elastic range throughout the analysis.

Fig.(5.13) shows that the result of the present study for the linear behavior has a good agreement with the corresponding results reported by ***Albarwary*** with maximum difference in the period 10%.

The time histories of the displacement at the center of the plate for various levels of yield stress are depicted in Fig.(5.14). As expected, the oscillations of displacement waves reduce further as the values of yield stress increase.

From this figure it is clear that the difference between the linear and the nonlinear behavior can be greater when the yield stress value reduced.

5.4.2.1.c: The damping effect

The effect of including the damping on the dynamic response is shown in Fig. (5.15) using different damping ratios (ζ_1).

It is clear that the increasing in the damping ratio leads to decreasing in the vibration and this effect becomes greater with time increasing.

Also, it should be noted that the effect of damping on the first peak of response is not great. However, this effect becomes considerable at the second positive peak, and becomes greater as time increases.

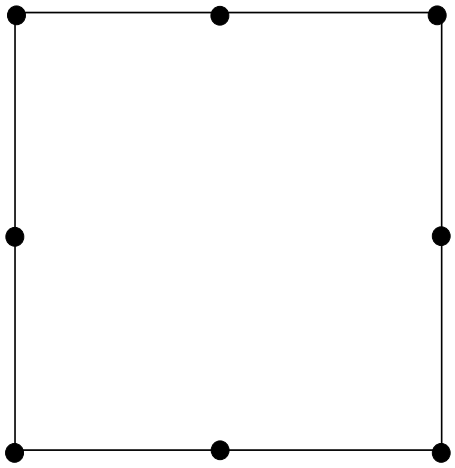

Mesh (1) : 1 element

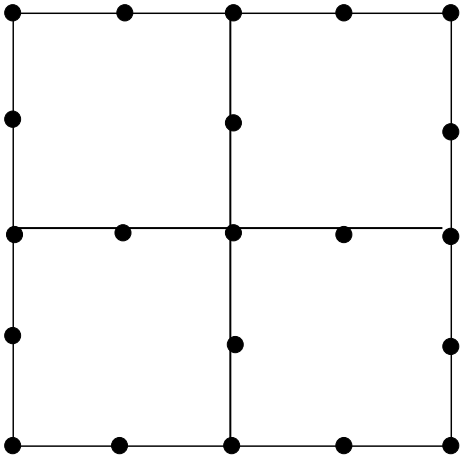

Mesh (2) : 4 elements

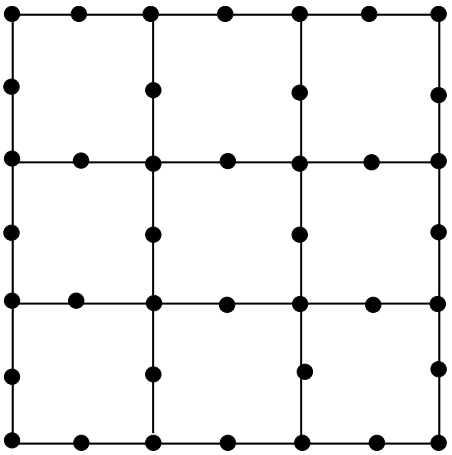

Mesh (3) : 9 elements

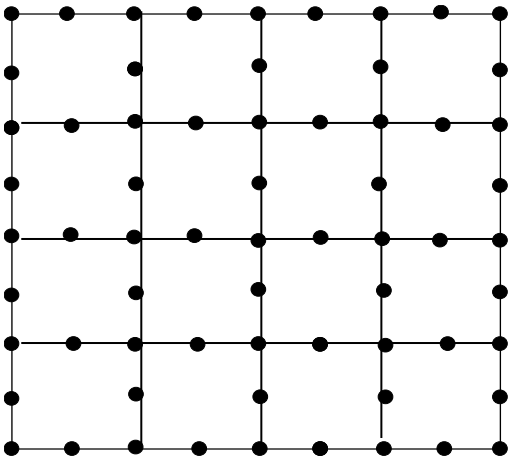

Mesh (4) : 16 elements

Fig. (5.9): *Finite element meshes for square plate due to symmetry only one quadrant is discredited*

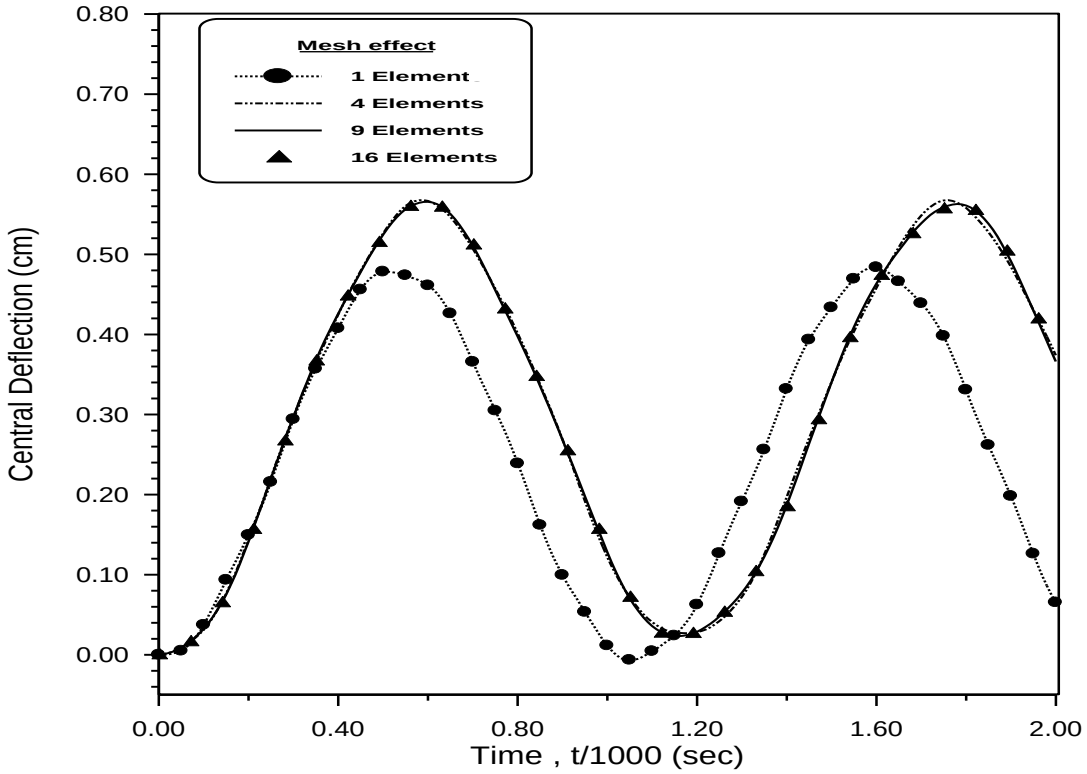

Fig.(5.10)*: Nonlinear transient response for a simply supported square plate subjected to suddenly applied uniformly distributed load for different mesh size.*

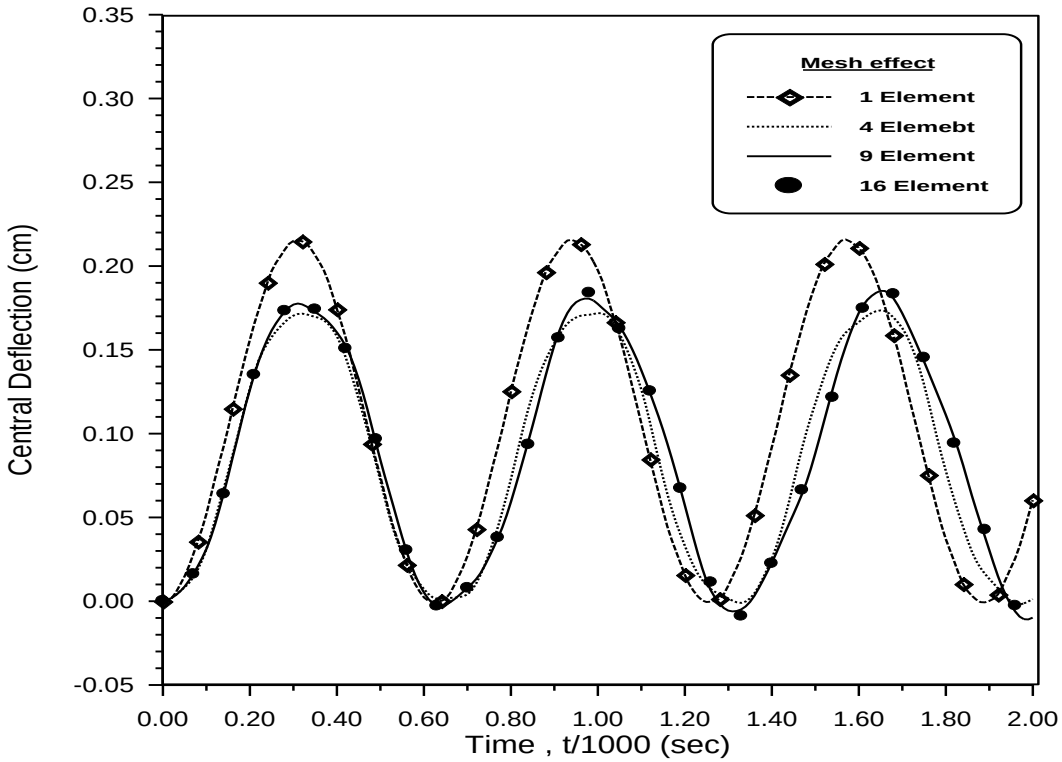

Fig.(5.11) : *Nonlinear transient response for a clamped supported square plate subjected to suddenly applied uniformly distributed load for different mesh size.*

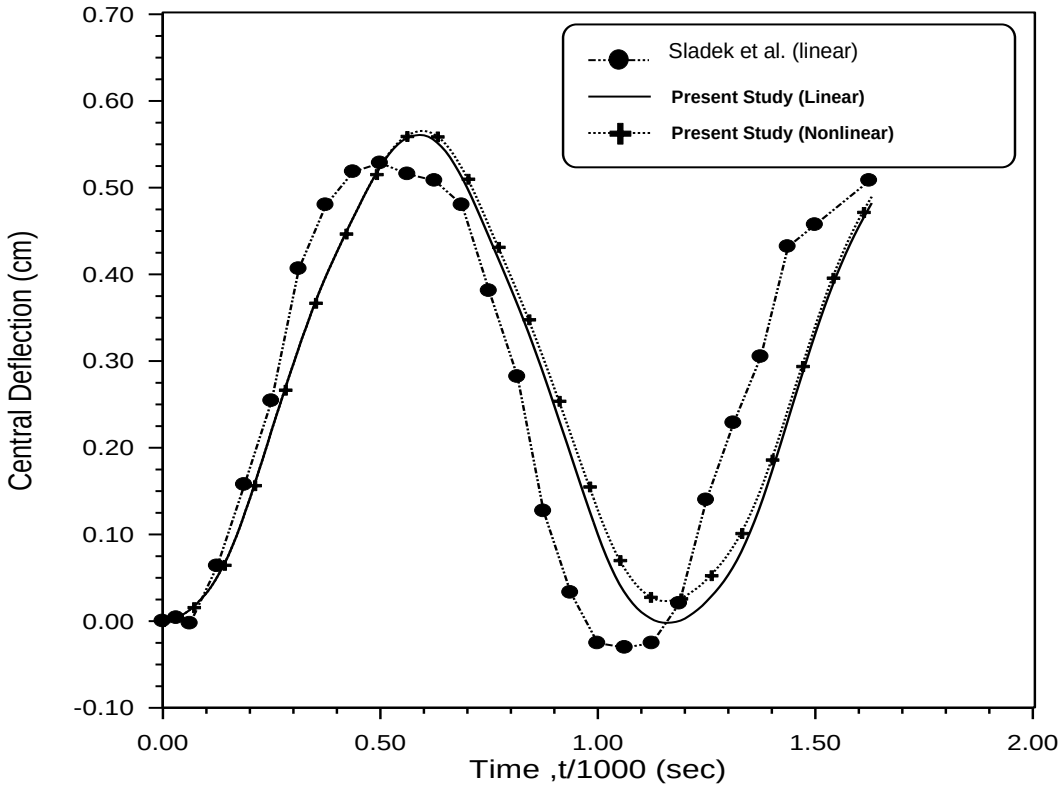

Fig.(5.12) : *Linear and nonlinear transient response of a simply supported square plate subjected to suddenly applied uniformly distributed load.*

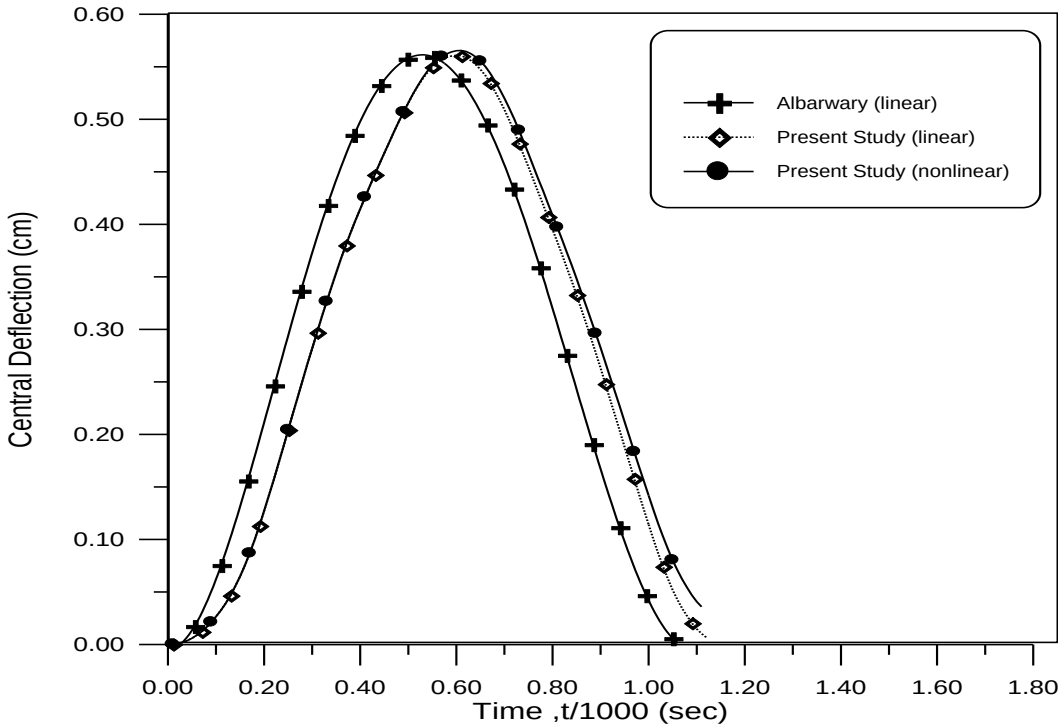

Fig.(5.13):*Linear and nonlinear transient response of a simply supported square plate subjected to suddenly applied uniformly distributed load.*

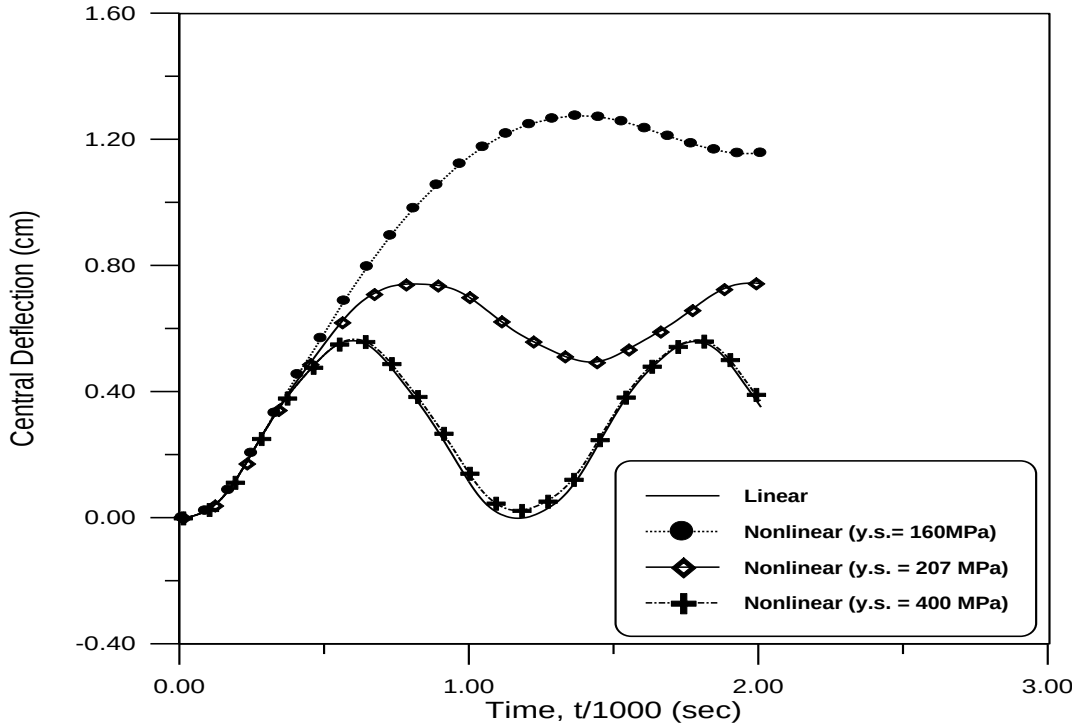

Fig.(5.14):*Linear and nonlinear transient response of a simply supported square plate subjected to suddenly applied uniformly distributed load (using different values of the yield stress(y.s.))*

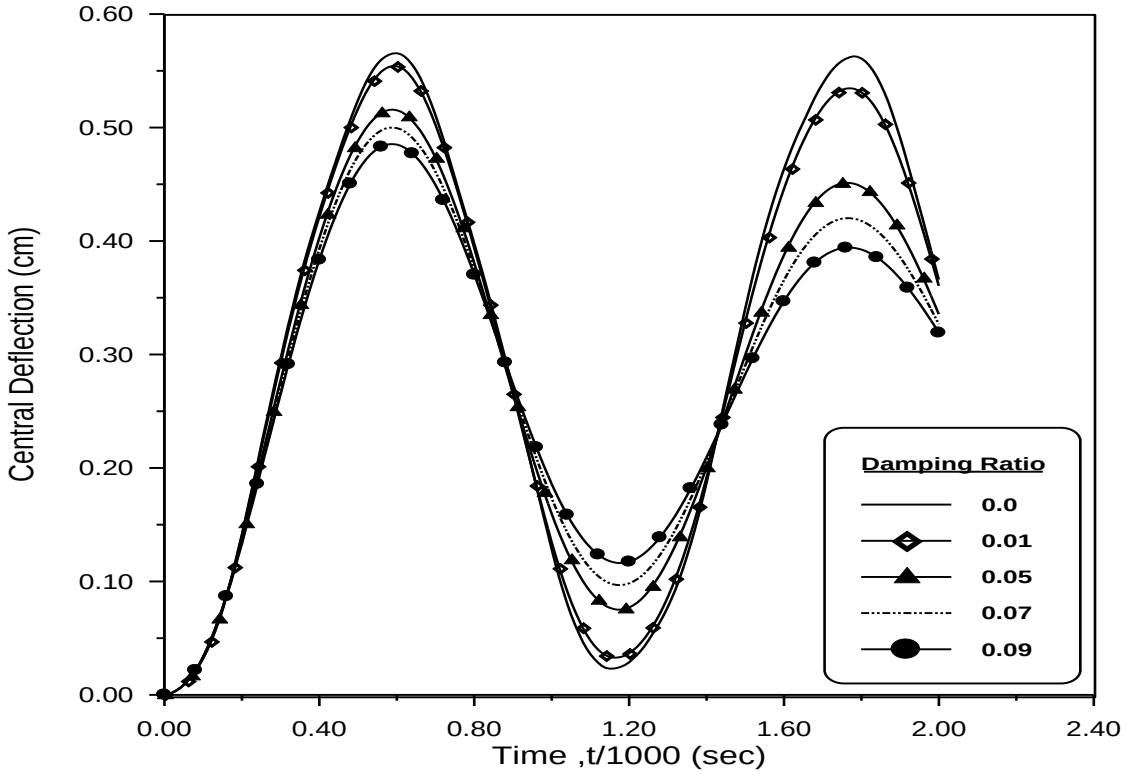

Fig.(5.15) : *Effect of damping on the transient response of a simply supported square plate subjected to suddenly applied uniformly distributed load using different damping ratios (ζ_1).*

5.4.2.2:ExampleNo.4 : ***Simply supported rectangular plate subjected to suddenly applied uniformly distributed load***

A flat, simply supported, rectangular steel plate having the following dimensions and parameters:-

length (a) = 60 in = 1.524 m

width (b) = 40 in = 1.016 m

thickness (h) = 1 in = 0.0254 m

modulus of elasticity (E) = $30 * 10^6$ psi =$20.685*10^4$ MPa

Poisson's ratio (υ) = 0.25

mass density (ρ) = 0.00073 Ib-sec² / in³ = $20.18*10^3$ Kg/m^3

yield stress = 57971.0149 psi = 400MPa

is chosen to be analyzed in the present study to assess the dynamic part of the computer program. The plate is subjected to uniformly distributed blast pressure. All the boundary conditions for the plate and the dynamic characteristic are given in Fig. (5.16).

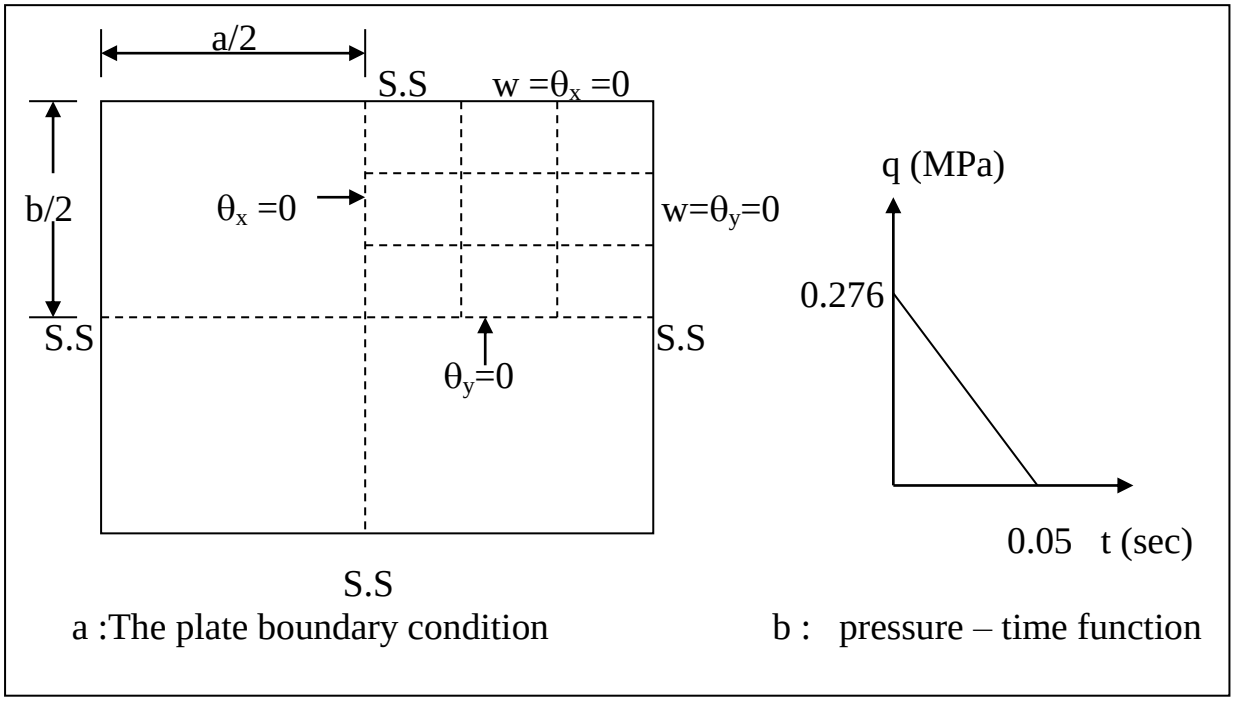

Fig. (5.16):*Boundary condition for the plate and the dynamic characteristic*.

The problem has been solved by ***Biggs*** in ***1964*** [11] with exact solution using the dynamic load factor (which defined as the ratio of the dynamic deflection at any time to the deflection which would have resulted from the static application of load, which is used in specifying the load time vibration) to determine the maximum linear dynamic deflection at the center of the plate.

In the present study, only one quarter of the plate is used with 9 elements mesh size, utilizing the symmetry. The time step is (0.001sec).

The results of the present study have a good agreement with the corresponding result reported by ***Biggs***, where the percentage difference for the maximum linear deflection at the center of the plate was equal to 5 % as shown in table (5.2).

In order to show the effect of increasing the value of the load on nonlinear behavior of the plate, the problem is reanalyzed by using load (q = 0.483 MPa) . Fig.(5.17) shows the linear and nonlinear dynamic response for the plate in this example with load equals (40psi = 0.276 MPa) and (70 psi = 0.483 MPa). From this figure one can noticed that the increasing of load by about 42.8% leads to increasing the difference between the linear and nonlinear central deflection from 0% to 13% (as amplitude difference)and this explains that the elasto-plastic behavior has a clear effect on the response of plates when subjected to large loads.

Table (5.2) : *The maximum central deflection for linear analysis*.

Linear analysis	The maximum central deflection	% difference
Biggs	0.575 in (1.4605 cm)	5%
Present study	0.546 in (1.38684 cm)	

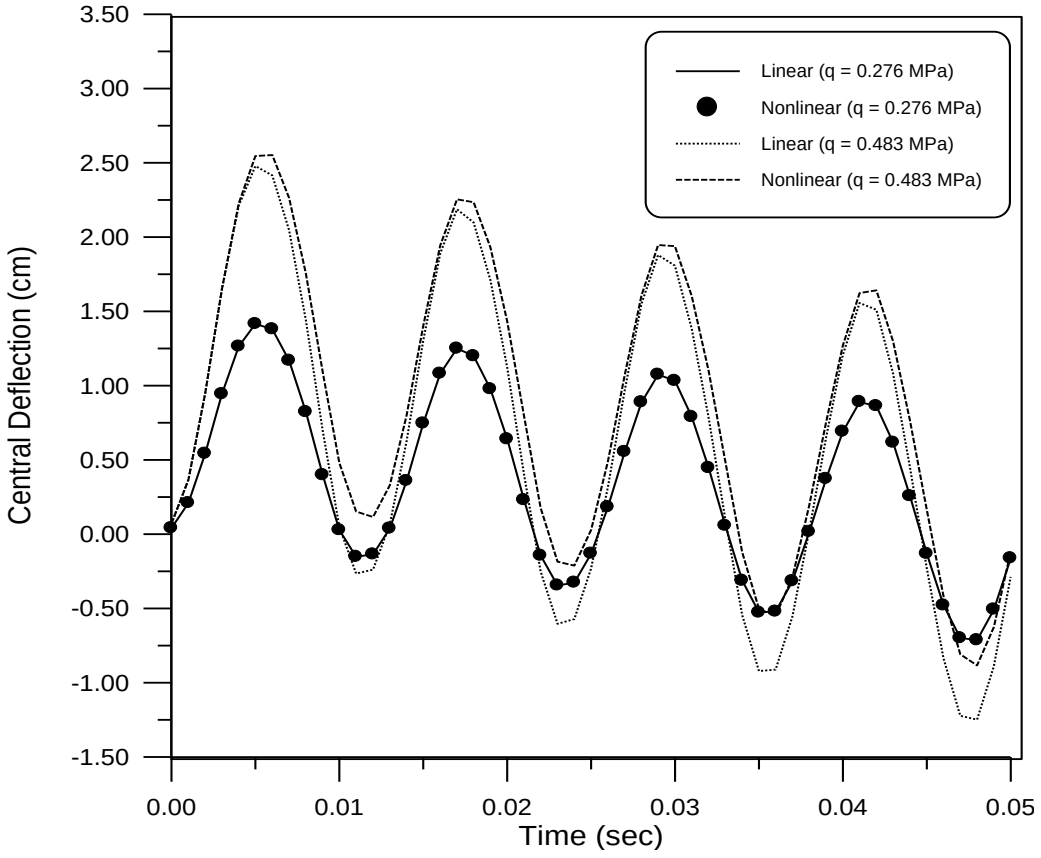

Fig.(5.17):*Linear and nonlinear transient response for a simply supported rectangular plate subjected to suddenly triangular pulse loading*.

5.4.2.3:ExampleNo.5 : ***Simply supported square plate subjected to sinusoidal uniformly distributed load***

A simply supported isotropic square plate (see Fig.(5.8.a)) with length (a =200 mm) and thickness (h = 10 mm) is excited by a sinusoidal uniform distributed load(see Fig.(5.18)):-

q = 530 sin ($\alpha\omega_o t$) kPa, in which:-

ω_o = 678 Hz (natural frequency in the first mode of plate)

α = 0.74 (specified constant).

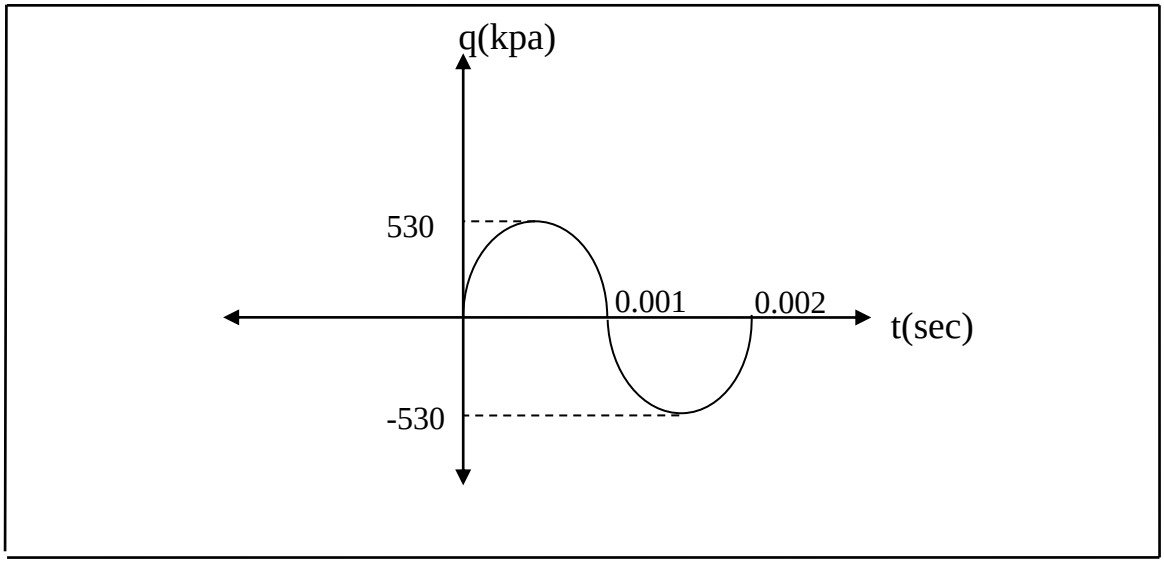

Fig.(5.18): *Sinusoidal load function*.

The material properties for the plate are:-

modulus of elasticity (E) =210 GPa

Poisson's ratio (υ) = 0.30

tension strength = 160 MPa

mass density (ρ) =7800 Kg / m^3

damping ratio (ζ_1) = 0.02

Chen et al. in ***2004*** [13] solved this example considering progressive failure process using the first-order shear deformation theory with 5 degrees of freedom per node(u, v, w, θ_x ,θ_y). The failure analysis method for the delaminated plate under dynamic loading is established by a modified Newmark direct integral method in conjunction with Tsai 's failure criterion and corresponding stiffness degradation scheme. The damping effect was considered by using a generalized orthogonal damping modle on basis of an approximate strain energy method.

In the present study, the time step is equal to (0. 0001 sec) and also one quarter of the plate is used with 9 elements mesh.

Fig.(5.19) plots the normalized dynamic midpoint deflections (w/h) versus the normalized time (t/T) within half of the first period, where T is the time period of the plate ($T=2\pi/\omega_0$). It can be noticed that the results obtained in the present study using the nonlinear analysis is agree well with the results reported by ***Chen et al***. where the maximum percentage difference between the two studies is about 10% in amplitude and 7% in the time period. This difference occurred because the differences in the methods which were used in the analysis and studying the nonlinearity as explained above. Where, ***Tsia*** failure criterion used a degradation rules to evaluate the reduced material properties. While, in the present study the reduced in the material properties(modulus of elasticity, Shear modulus of elasticity) is updated in each time step for all elements depending on ***von-Mises'*** plasticity theory. So, the present study is more accurate.

Fig.(5.20) shows the dynamic deflection of middle point for plate using different values of L_0 ($L_0 < 3$ for thick plates [5]). As expected the deflection reduced when L_0 (a/h ratio) increases, where the plate becomes more stiff.

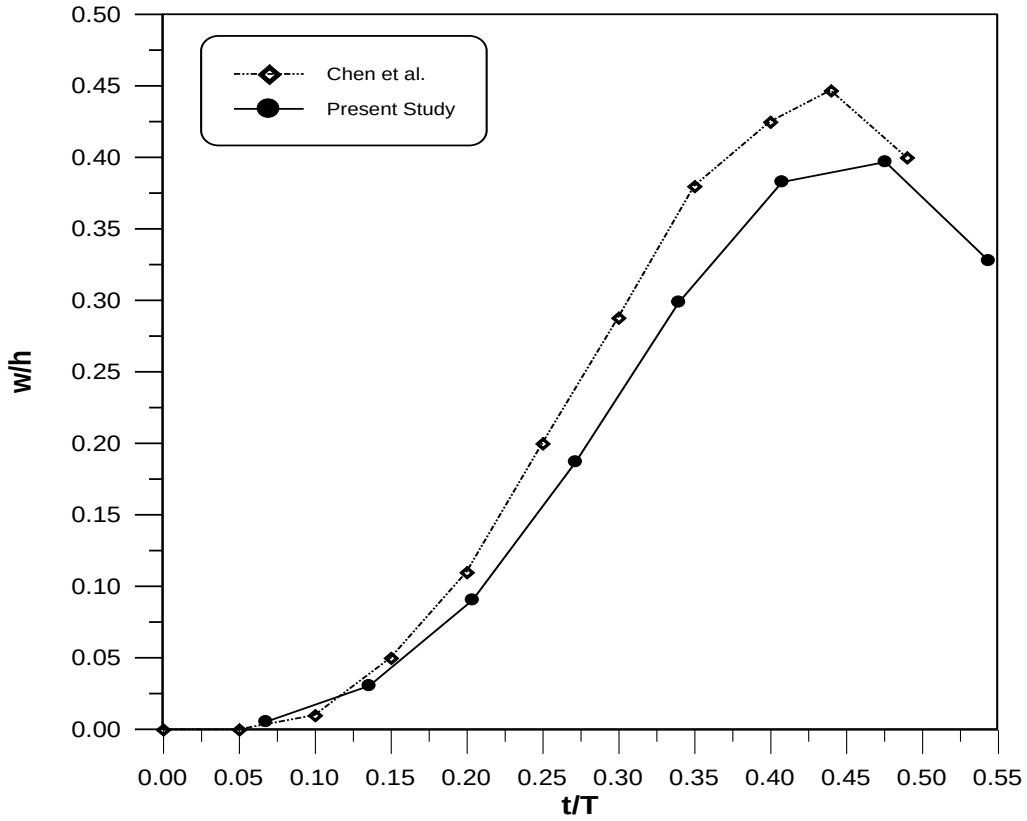

Fig.(5.19): *Dynamic deflection of middle point for a simply supported square plate subjected to a sinusoidal uniform distributed load.*

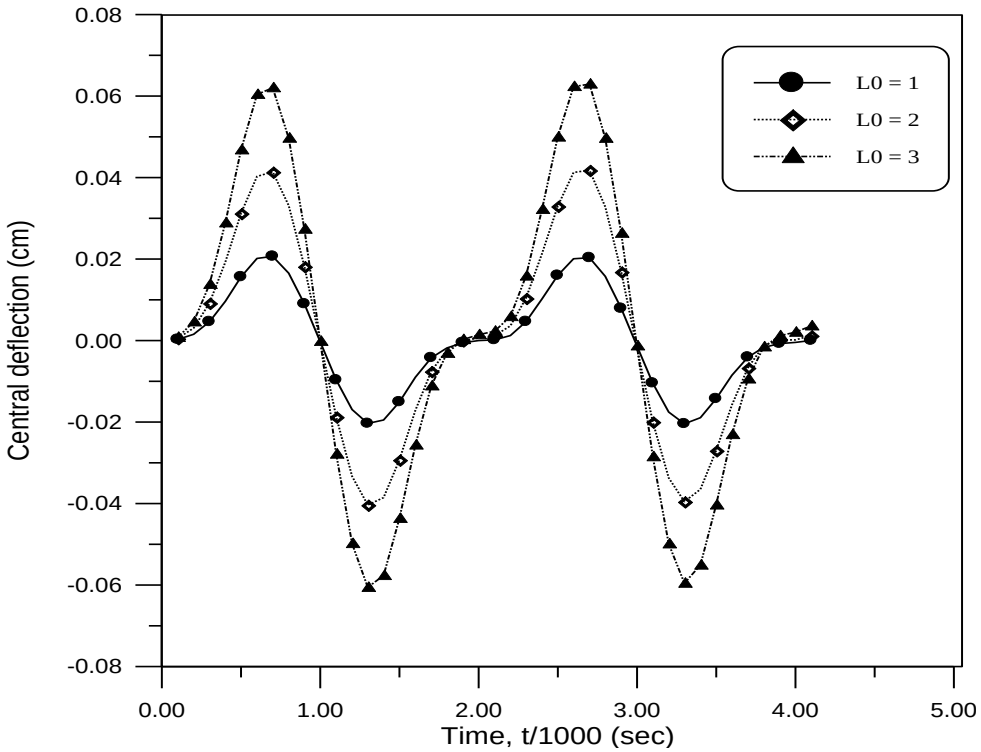

Fig.(5.20): *Dynamic deflection of middle point for a simply supported square plate subjected to a sinusoidal uniform distributed load for different values of* L_0.

5.4.2.4:Example No.6 : Clamped circular plate subjected to suddenly applied concentrated load

A clamped circular plate (the same plate which is used in example No.2(the mass density (ρ) = 0.2589 Ib/in^3 = 7.157*10^3 Kg/m^3)) subjected to suddenly applied concentrated load at the center of the plate (p= 1200Ib =5.34*10^{3}MN)(see Fig.(5.21))is presented in this example.

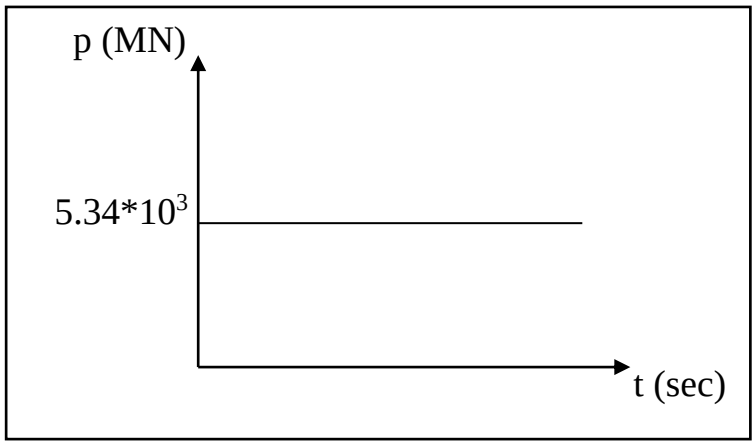

Fig.(5.21) : *Suddenly applied load***.**

Only one quarter of the plate is used , utilizing the symmetry. The time step is (0.00001sec).

The convergence with mesh refinement is indicated from the figures (5.23.a) and (5.23.b) for R_0=2.5 using the different meshes shown in Fig.(5.22). From this figure , it is clear that the 12 elements mesh size (mesh(3)) is the suitable mesh.

Nonlinear transient response for the plate is shown in Fig.(5.24) for different values of R_0 (R_0 < 2 for thick plates [5]) using 12 elements (mesh(3) in Fig.(5.22)). As expected, the deflection reduced when R_0 (R/h ratio) decreases, where the plate becomes more stiff.

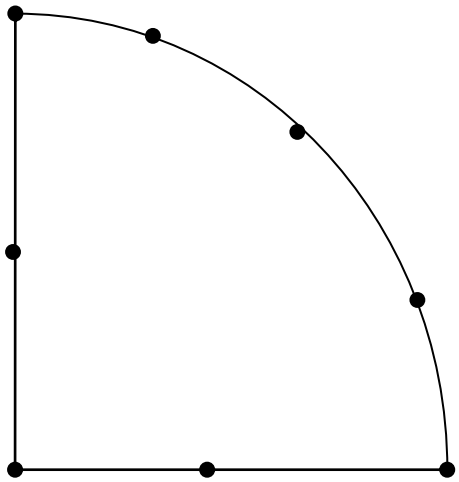

Mesh (1): 1 element

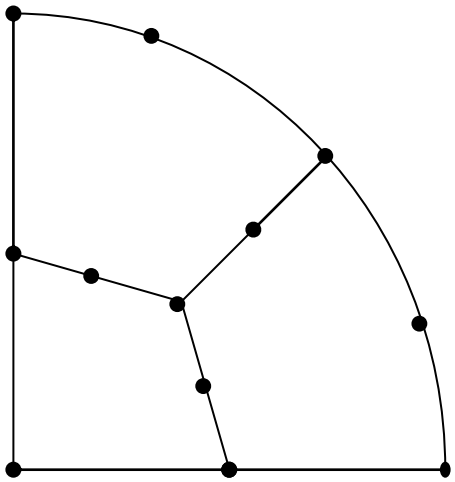

Mesh (2): 3 elements

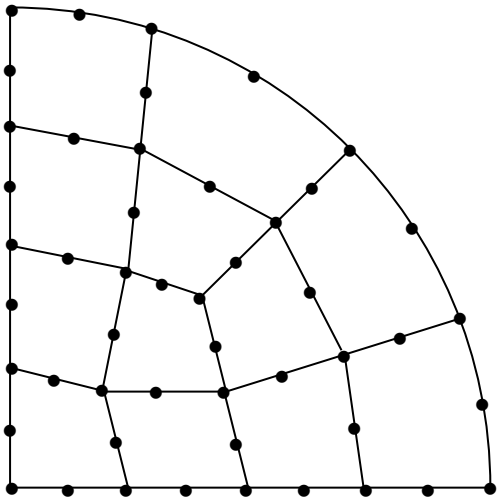

Mesh (3): 12 elements

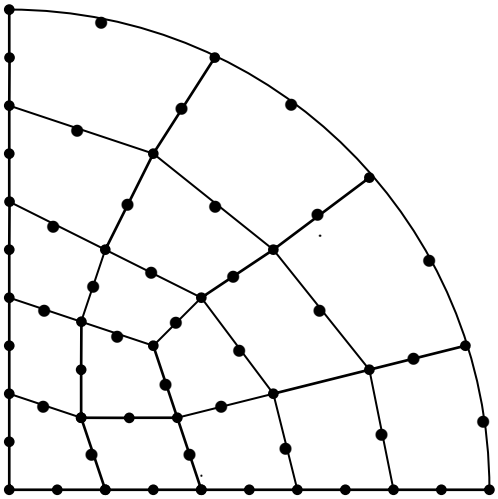

Mesh (4): 16 elements

Fig. (5.22): *Finite element meshes for circular plate due to symmetry only one quadrant is discredited*

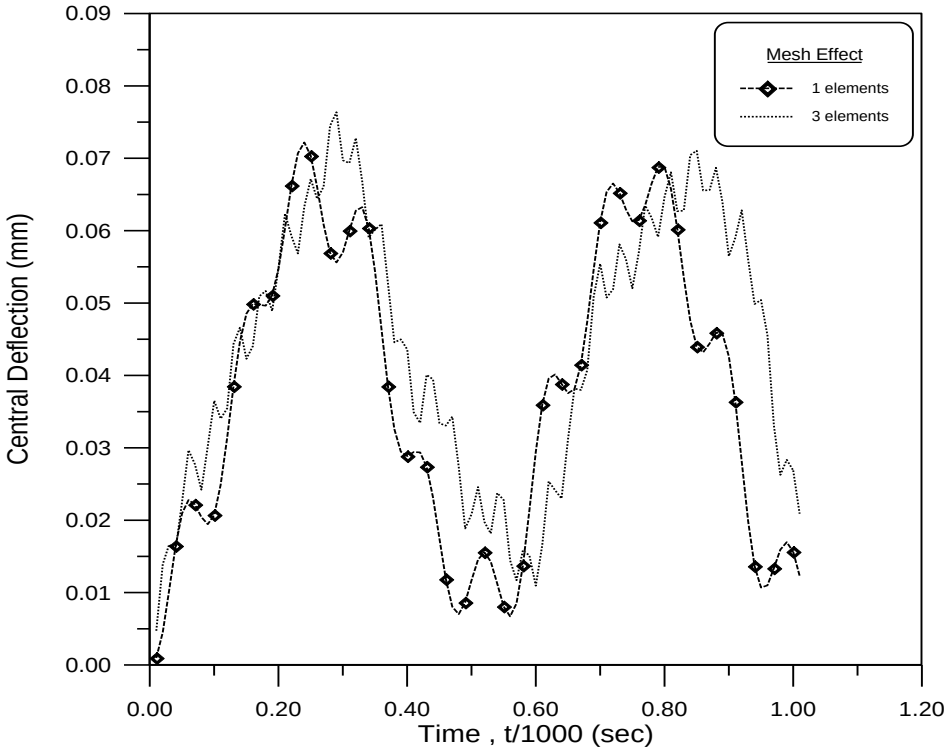

(a)*For 1 element and 3 elements*

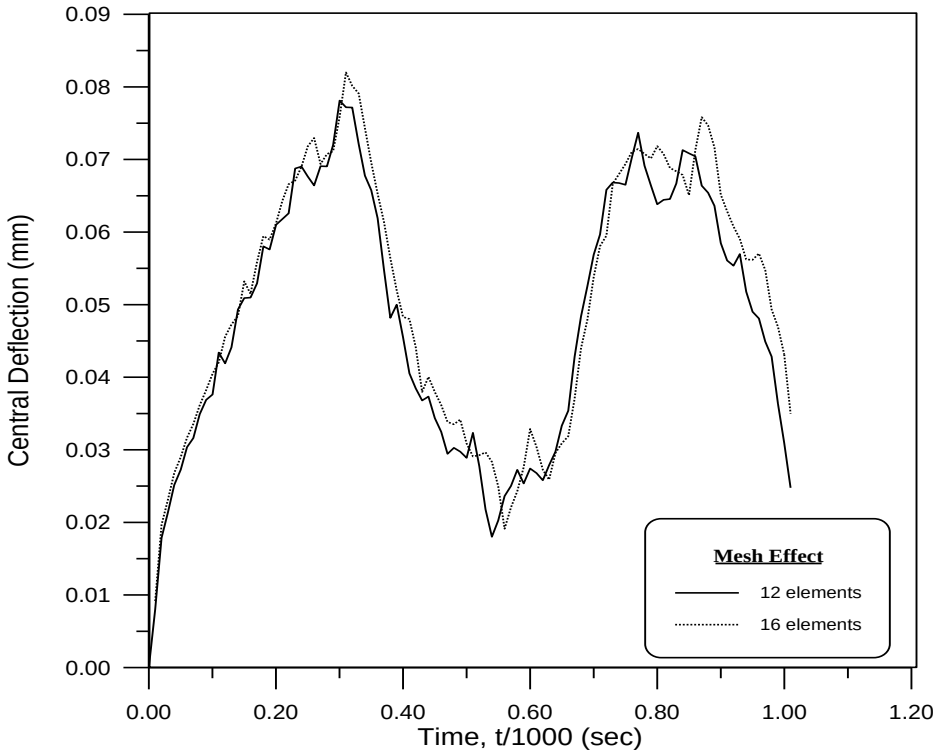

(b) *For 12 elements and 16 elements*

Fig.(5.23) : *Nonlinear transient response for a clamped supported circular plate subjected to suddenly applied concentrated load for different mesh size (R_0=2.5).*

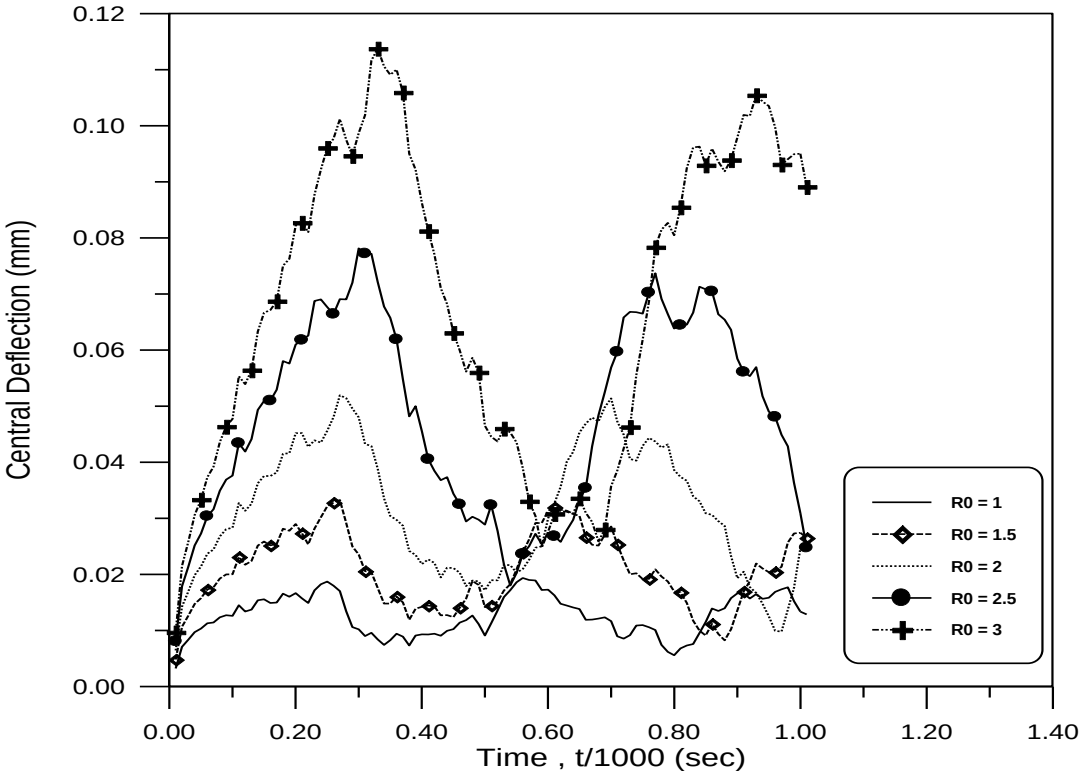

Fig.(5.24) : *Nonlinear transient response for a clamped supported circular plate subjected to suddenly applied concentrated load for different values of R_0 .*

5.5 Parametric study

5.5.1:ExampleNo.7 : ***square plate subjected to suddenly applied uniformly distributed load***

A square plate subjected to a suddenly applied uniformly distributed load of (300 psi = 2.07 Mpa) (see Fig.(5.8.b)) is analyzed using 9 elements (mesh 3 in Fig.(5.9)) to model a symmetric quadrant of this plate.

The plate geometry, material properties are as follows:-

length (a) = 18 in = 0.4572m

modulus of elasticity (E) = $0.1 * 10^8$ psi = $69*10^3$ MPa

the mass density (ρ) = 0.2589 Ib/in^3 = $7.157*10^3$ Kg/m^3

Poisson's ratio (υ) = 0.3

the yield stress = 57971.0149 psi = 400MPa

The results obtained by using time step equals to 0.00001 sec.

5.5.1.a :The effect of length(a)/ thickness(h) ratio

The effect of (L_0 = a/h) ratio on the nonlinear behavior for plates can be shown in figures (5.25), (5.27) for simply supported plate and figures (5.26), (5.28) for clamped supported plate. Where figures (5.25), (5.26) plot the central deflection vs. time and show that the deflection for the central point of the plate is greater for thin plates, while for thick plates the vibration will be very small but with more cycles. While figures (5.27), (5.28) plot the central normal stress (σ_x) vs. time and explain that when plate thickness increases the normal stress decreases, where the increasing in the thickness of plate make it more stiff.

Fig.(5.29) represents the central normal stress vs. time for the 6 Gauss points through the thickness. It is clear from this figure that the stress distribution is symmetrical above and under the middle surface and this was expected because only the bending effect is included in the present work.

5.5.1.b :The effect of boundary condition on the damping

Figures (5.30) and (5.31) show the damping effect on the nonlinear behavior for simply supported and clamped supported plate respectively with L_0 = 2 using damping ratio equal to 0.0, 0.01, 0.05and 0.09.

Figures (5.32) and (5.33) plots for the nonlinear behavior for simply supported and clamped supported plate respectively with L_0 = 2 using damping ratio equals to 0.0 and 0.07.

From these figures one can conclude that the damping effect with fixed supported plates leads to stop the vibration with less time comparing with simply supported plates. This can be related to the stiffness of the structure.

Since the clamped plate can be considered as stiffener structure in comparison with simply supported plate, so the effect of the damping for clamped plate will be greater comparing with the simply supported plate because of the mutual effect between stiffness and damping.

Also, from figures(5.32) and (5.33) one can noted that the damping for clamped plate can stop the vibration with time lesser by about 33.3% with respect to the simply supported plates when the same plate dimension and same load is used.

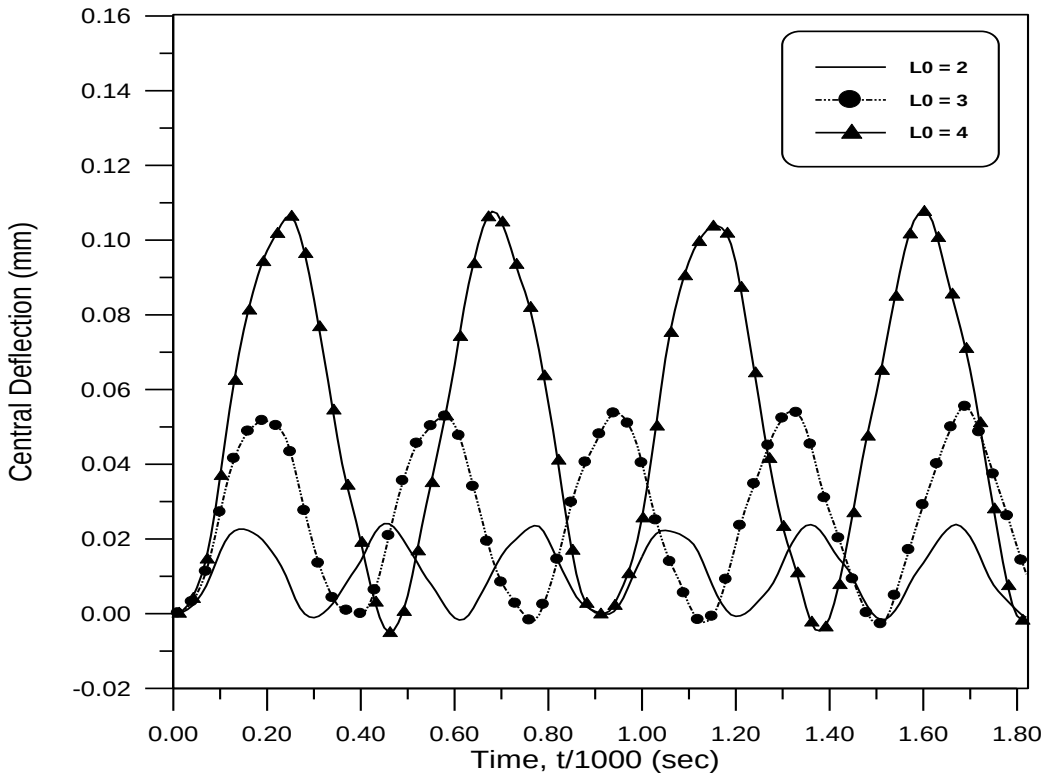

Fig.(5.25): *Nonlinear transient response of a simply supported square plate subjected to suddenly applied uniformly distributed load for different values of* L_0.

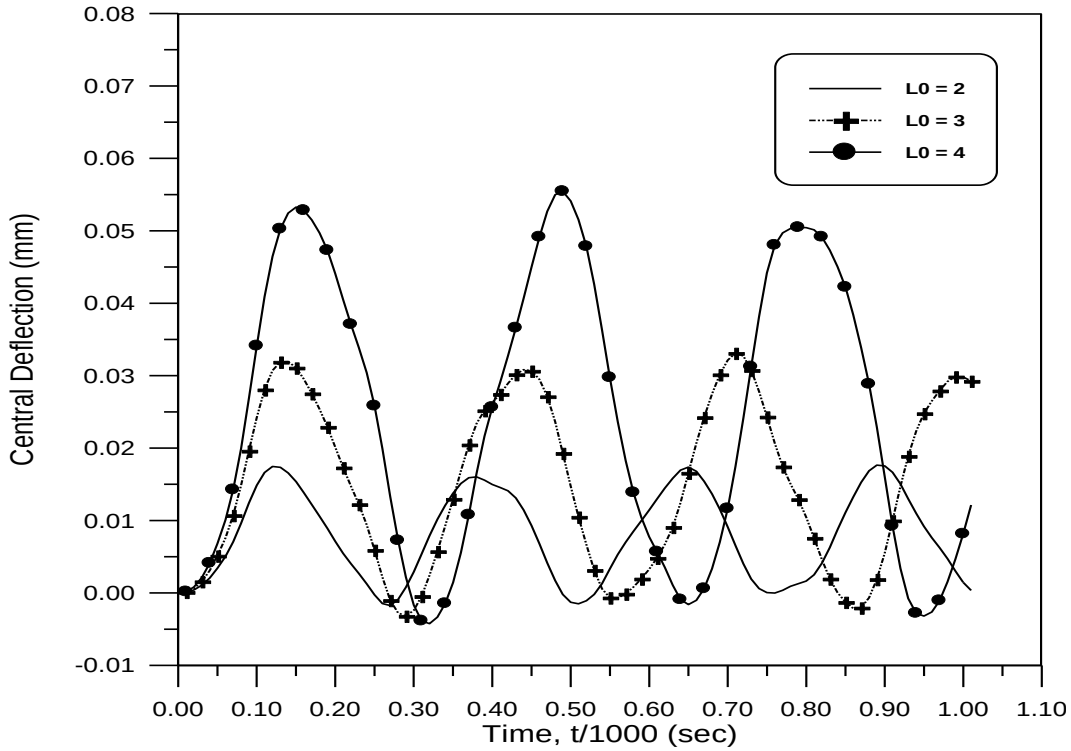

Fig.(5.26): *Nonlinear transient response of a clamped supported square plate subjected to suddenly applied uniformly distributed load different values L_0.*

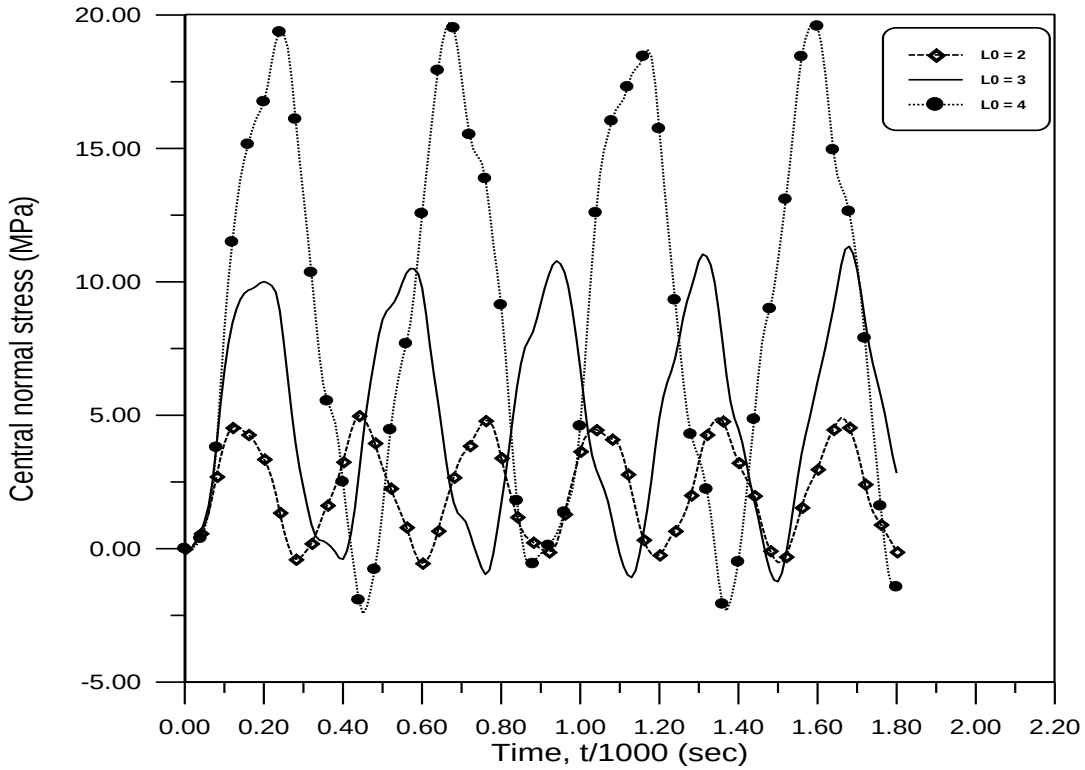

Fig.(5.27): *Central normal stress at distance 0.9324695 from the middle surface of a simply supported square plate subjected to suddenly applied uniformly distributed load for different values of L_0.*

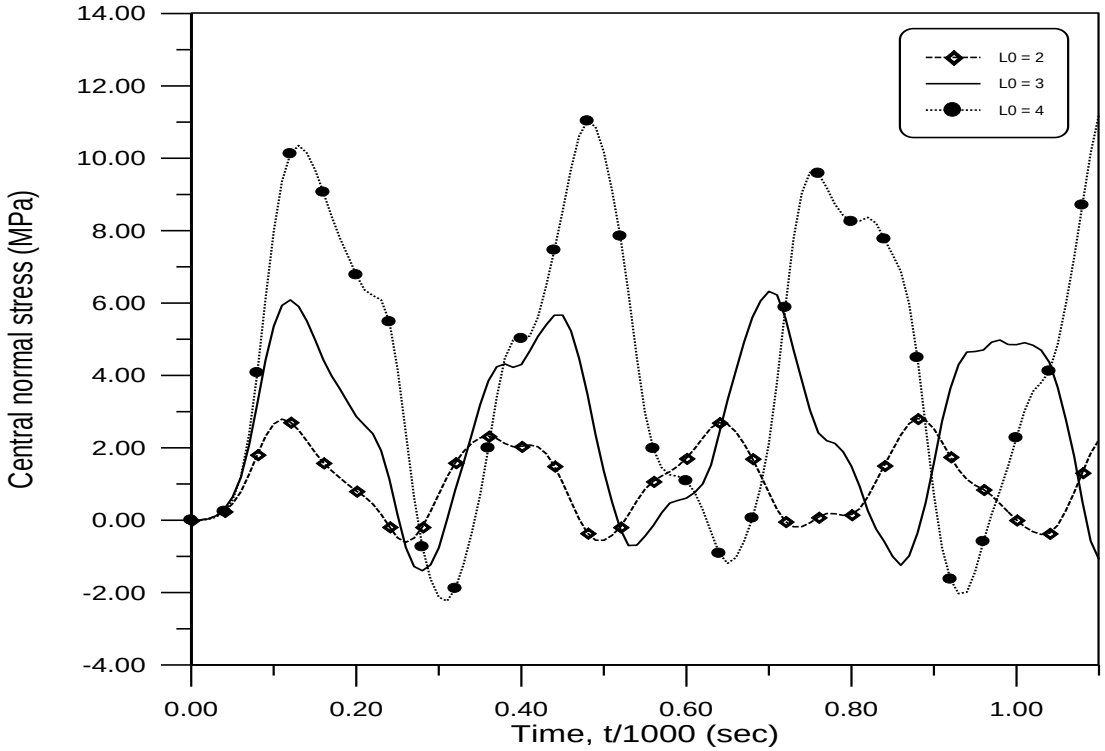

Fig.(5.28): *Central normal stress at distance 0.9324695 from the middle surface of a clamped supported square plate subjected to suddenly applied uniformly distributed load for different values of L_0.*

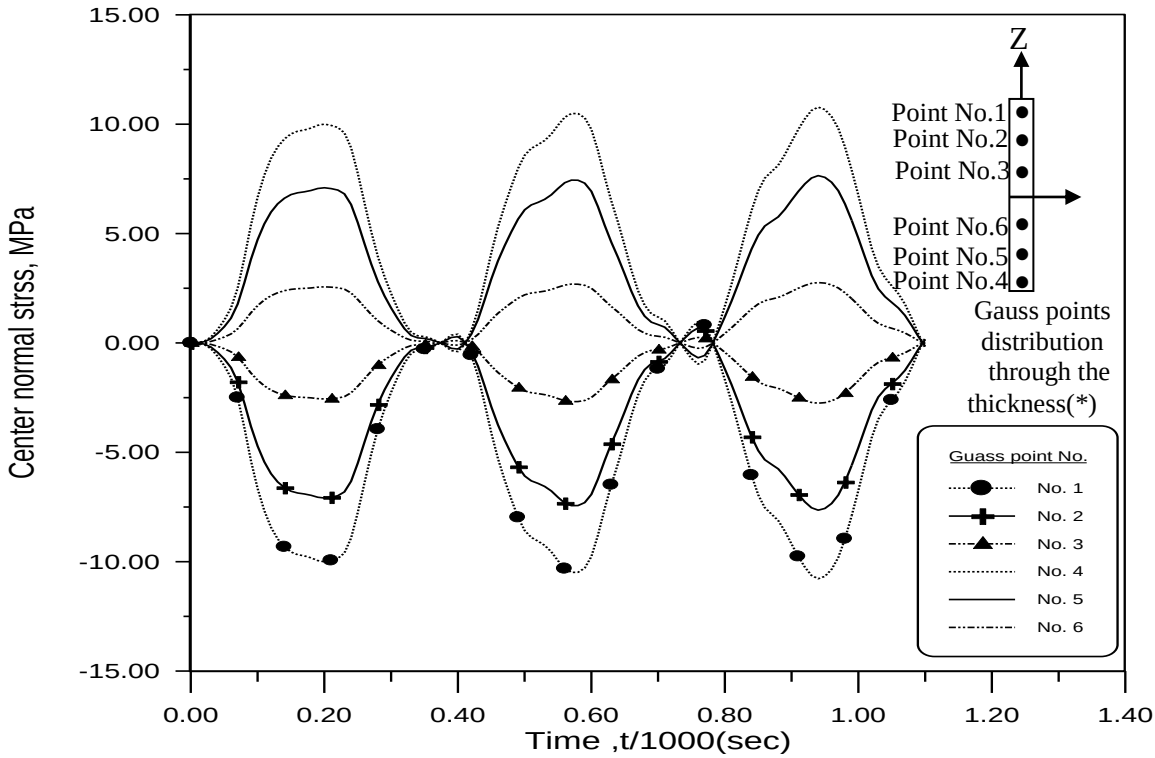

Fig.(5.29): *Central normal stress of a simply supported square plate subjected to suddenly applied uniformly distributed load for different Gausses points location.*(distances between Gauss points explained in table (A.1))*

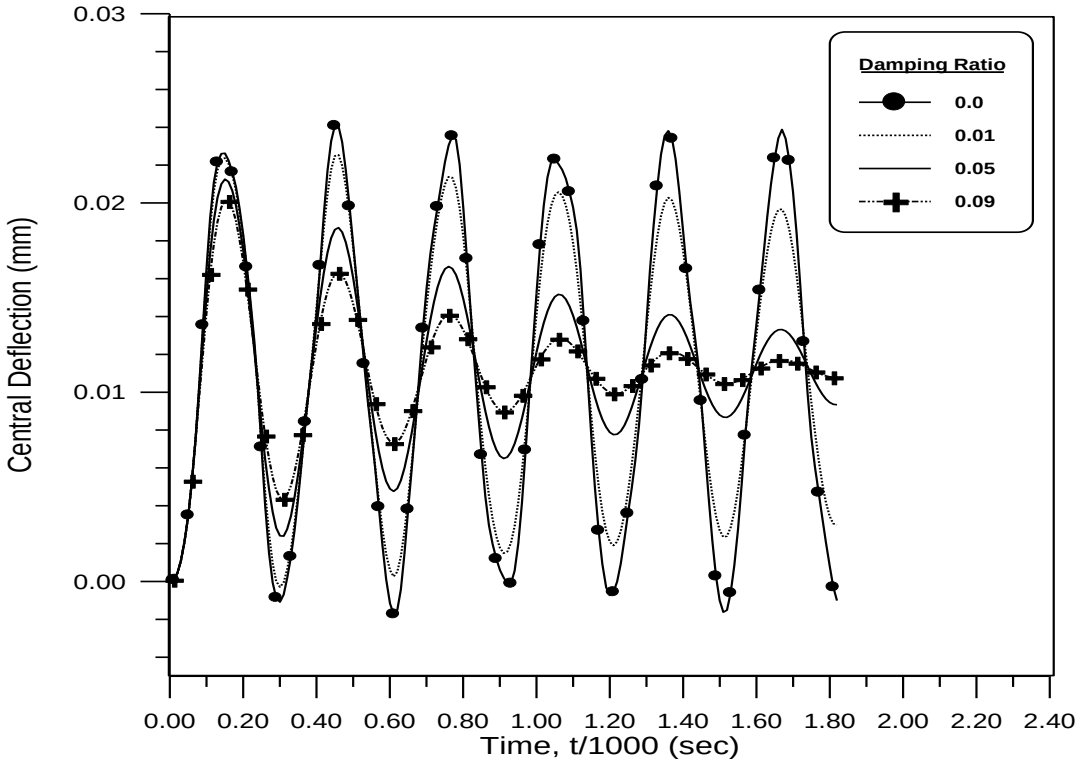

Fig.(5.30): *Nonlinear transient response of a simply supported square plate (L_0=2) subjected to suddenly applied uniformly distributed load for different damping ratio (ζ_1).*

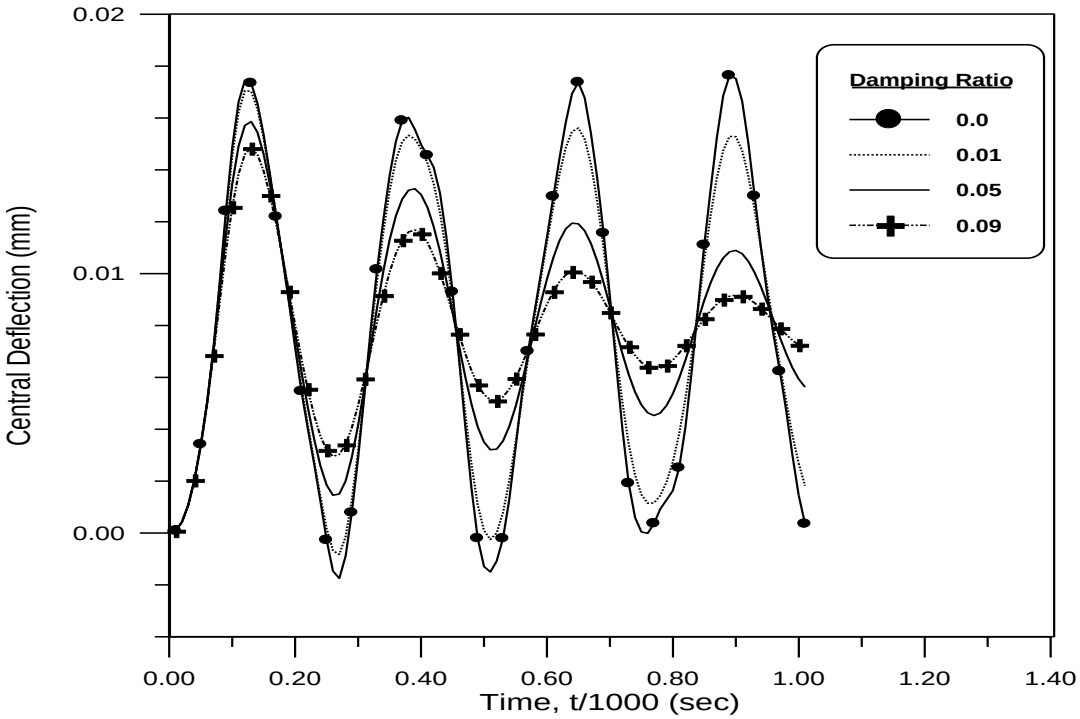

Fig.(5.31):*Nonlinear transient response of a clamped supported square plate (L_0=2) subjected to suddenly applied uniformly distributed load for different damping ratio (ζ_1).*

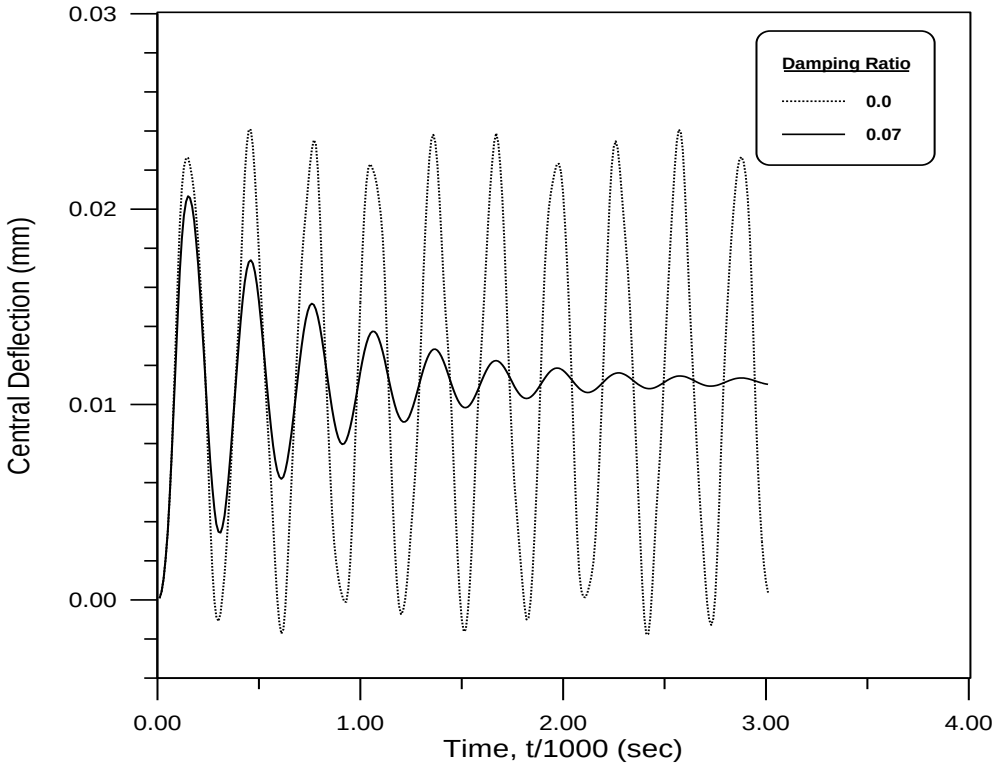

Fig.(5.32): *Nonlinear transient response of a simply supported square plate (L_0=2) subjected to suddenly applied uniformly distributed load*.

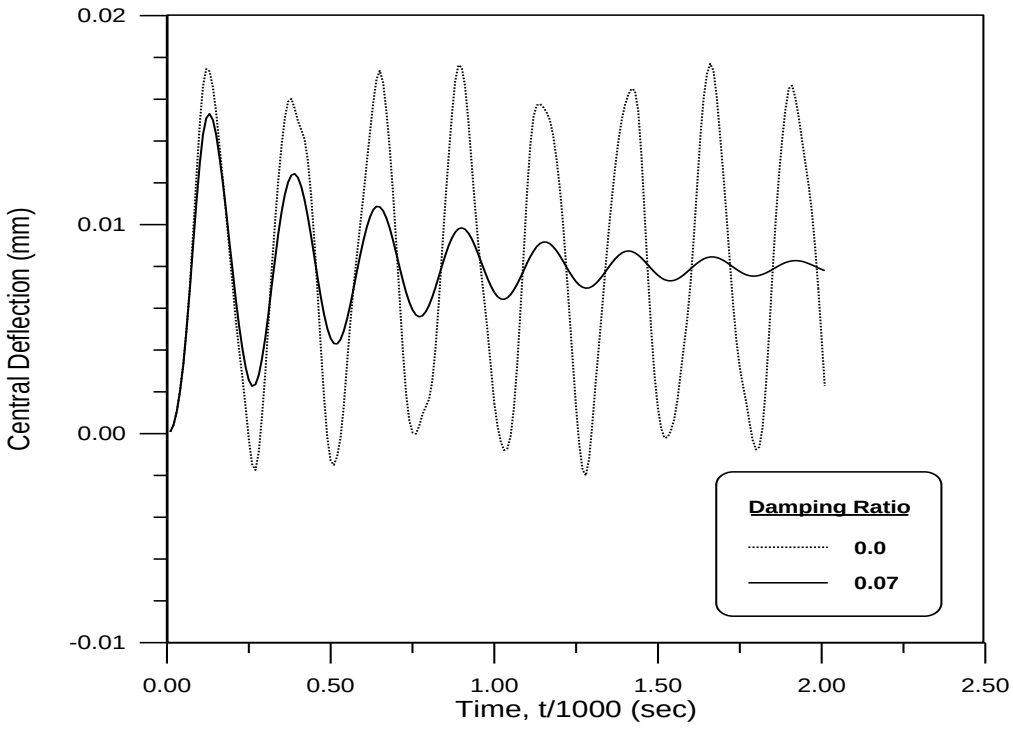

Fig.(5.33):*Nonlinear transient response of a clamped supported square plate (L_0=2) subjected to suddenly applied uniformly distributed load.*

5.5.2 ExampleNo.8 : ***square plate with varying thickness subjected to transverse uniformly distributed static load***

A square plate subjected to an increasing uniform load is analyzed to study the effect of the varying in the thickness of the plate using 16 elements (mesh(4) in Fig.(5.9)),[16 elements used here instead of 9 elements to represent the jump in the thickness due to the adding a cover plate], to model a symmetric quadrant of this plate.

The plate geometry and material properties are as follows:-

length (a) = 18 in = 0.4572m

modulus of elasticity (E) = $0.1 * 10^8$ psi =$69*10^3$ MPa

the mass density (ρ) = 0.2589 Ib/in^3 = $7.157*10^3$ Kg/m^3

Poisson's ratio (υ) = 0.3

the yield stress = 57971.0149 psi = 400MPa

the thickness of the plates is assumed to be varying with five cases as shown in figure (5.34) , where the thickness of the plates varying in one direction (case 1,3) , two direction (case 4,5) and uniformly thickness (case 2).

where:

h = 8 in = 0.2032 m

h(ave) = (h + h/2)/2 = (8 + 4)/2 = 6 in = 0.1524 m

The load versus central deflection curves are shown in figures (5.35) and (5.36) for simply supported and clamped plates respectively

For the simply supported square plate (Fig. (5.35)), case (2 and 4) can be considered as the best. It is clear that case -2- give the maximum value for the collapse load about (200 Mpa for this example). But for the range (q = 0 to q ≈ 190Mpa), one can see that the central deflection for case -4- (which

gives the maximum volume) is smaller than that for cases -2- when the two cases subjected to the same amount and type of loading, where the difference may be reach to about 10%.

For the clamped plate, figure (5.36) explain that case -4- provides the best load capacity and smaller deflection comparing with the other cases.

Figures (5.37) and (5.38) show the shape of the deflection along the line C—— C (see Fig.(5.34)) for the five cases for the simply supported and clamped plates respectively.

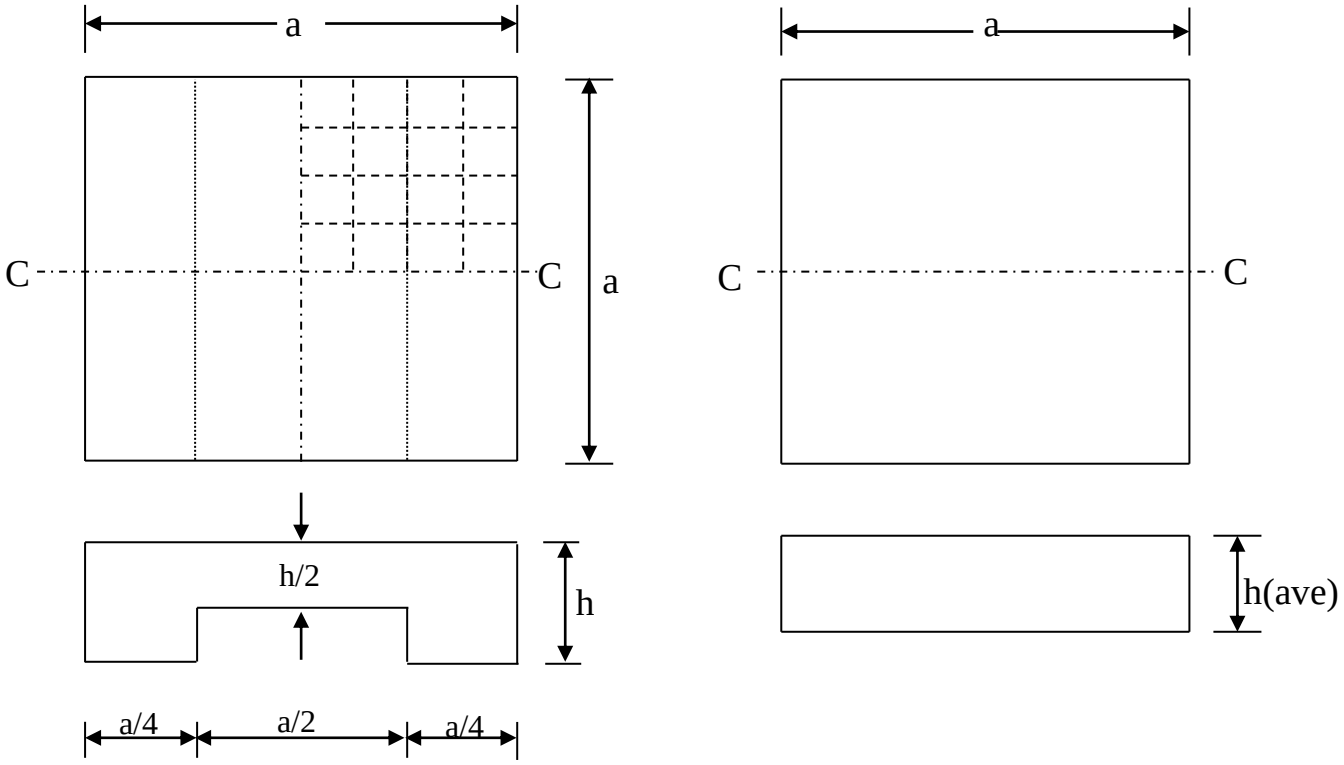

a. Case -1- b. Case -2-

Fig. (5.34): *square plate with varying thickness*

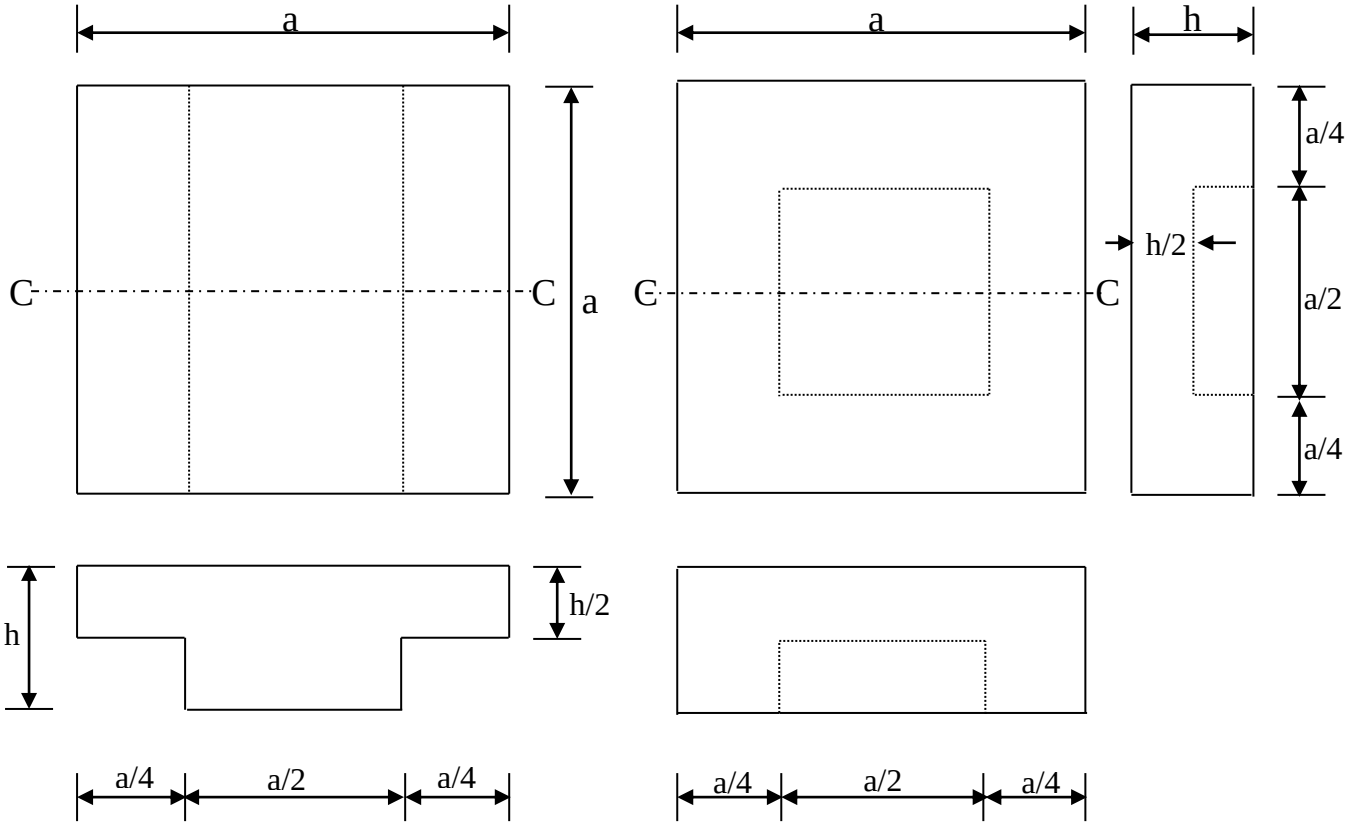

c. Case -3- d . Case -4-

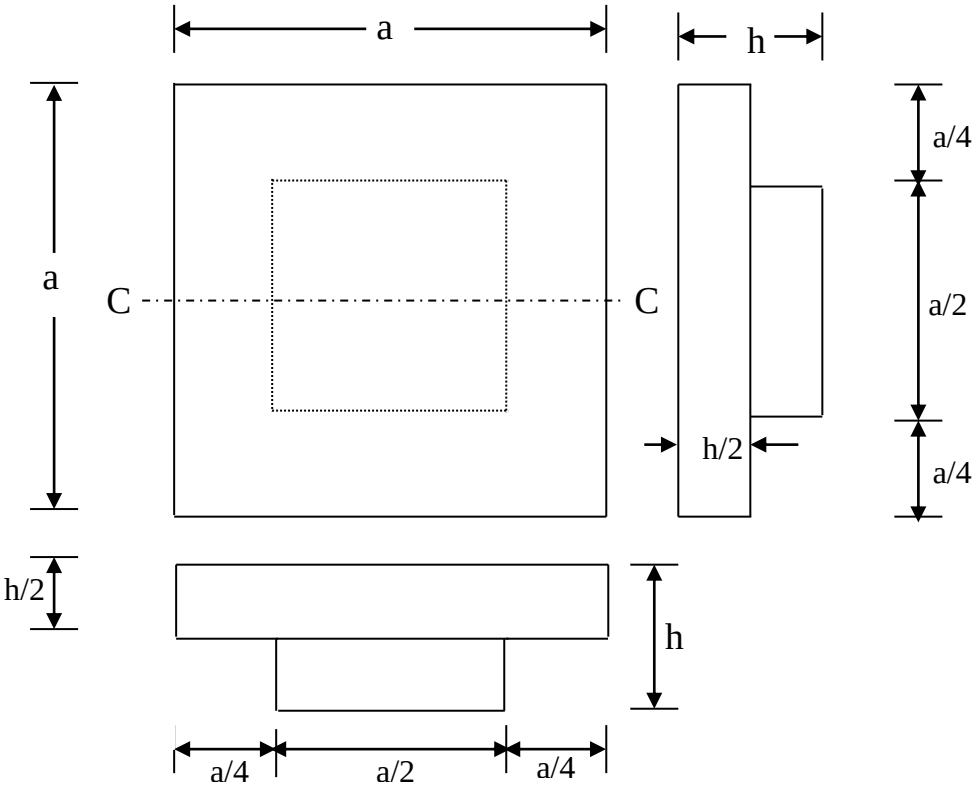

e. Case -5-

Fig.(5.34): *continued*

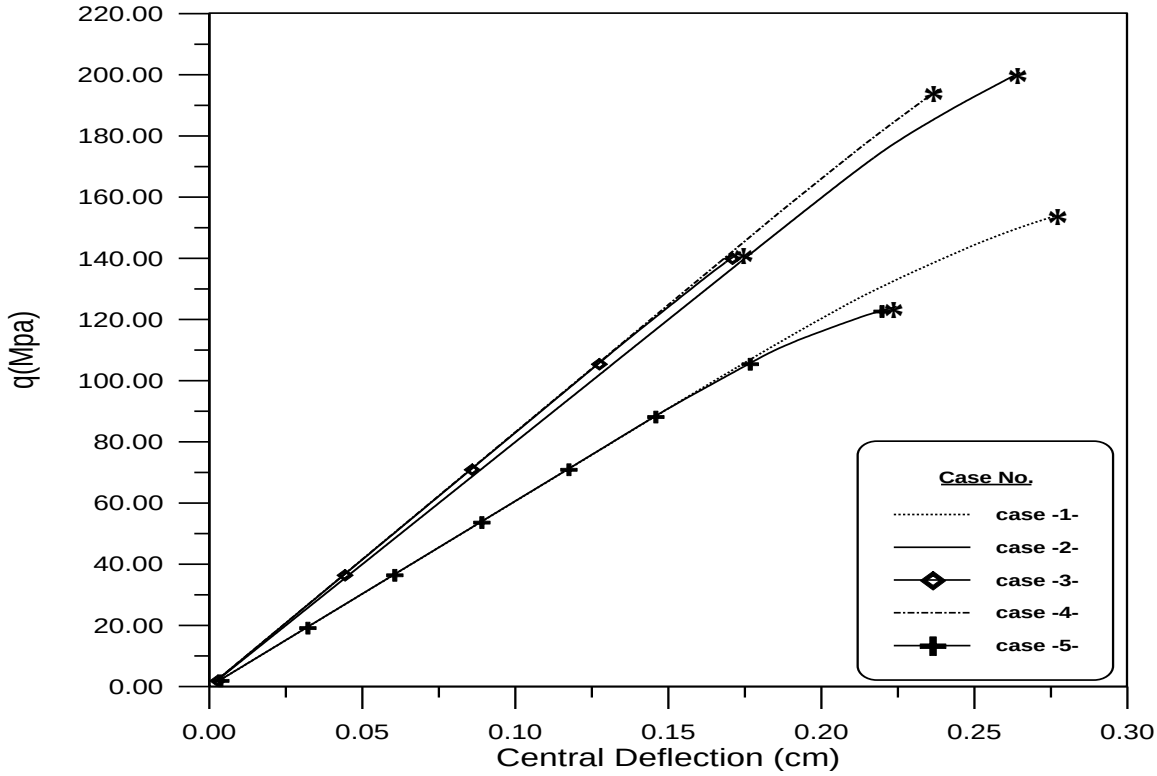

Fig.(5.35) *: Load versus central deflection for a simply supported square Plate using different cases of varying in the thickness(the sample * represent the collapse point) .*

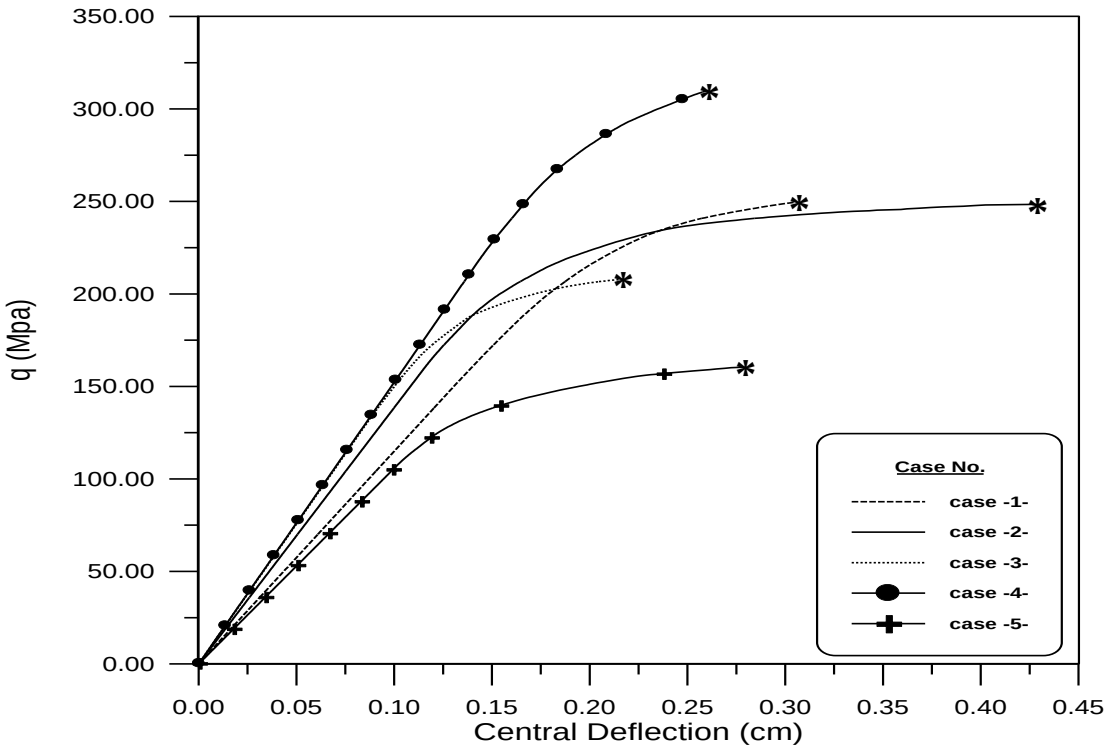

Fig.(5.36) *: Load versus central deflection for a clamped square plate using different cases of varying in the thickness(the sample * represent the collapse point) .*

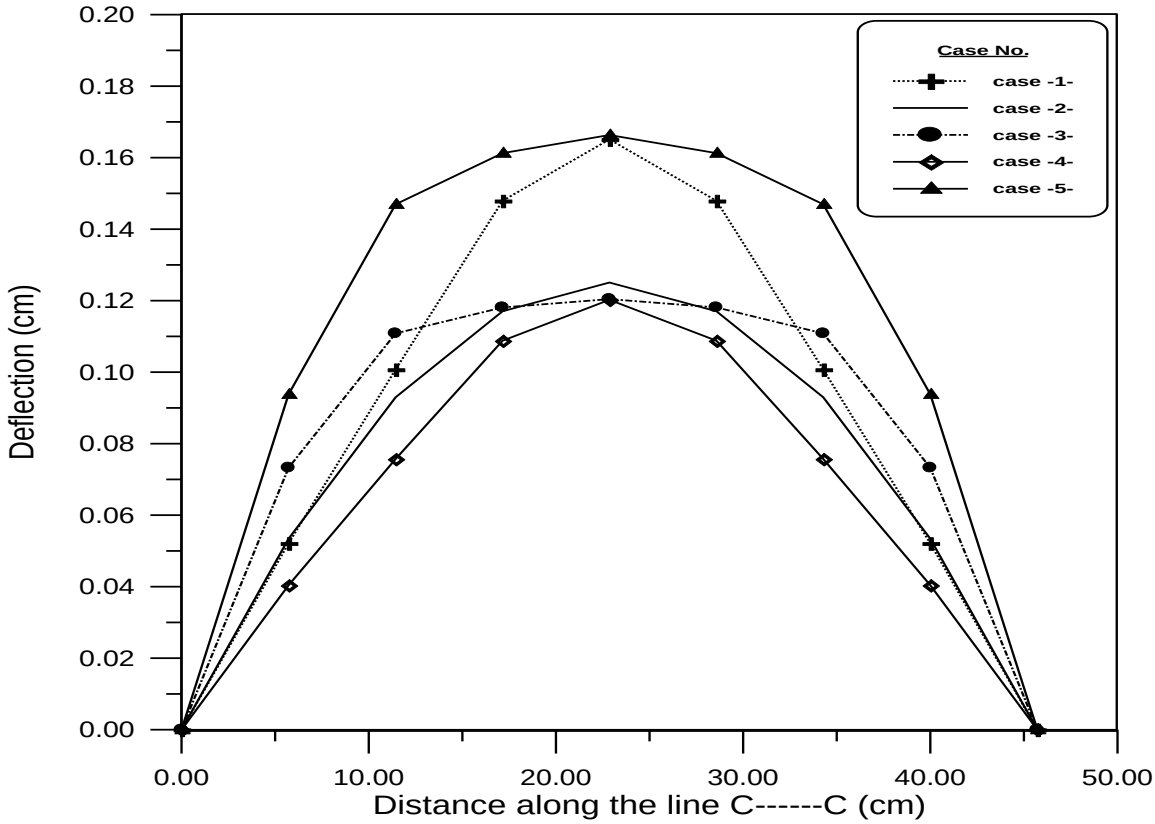

Fig.(5.37) : *Shape of the deflection along a line in the middle of simply supported plate using different cases of varying in the thickness.*

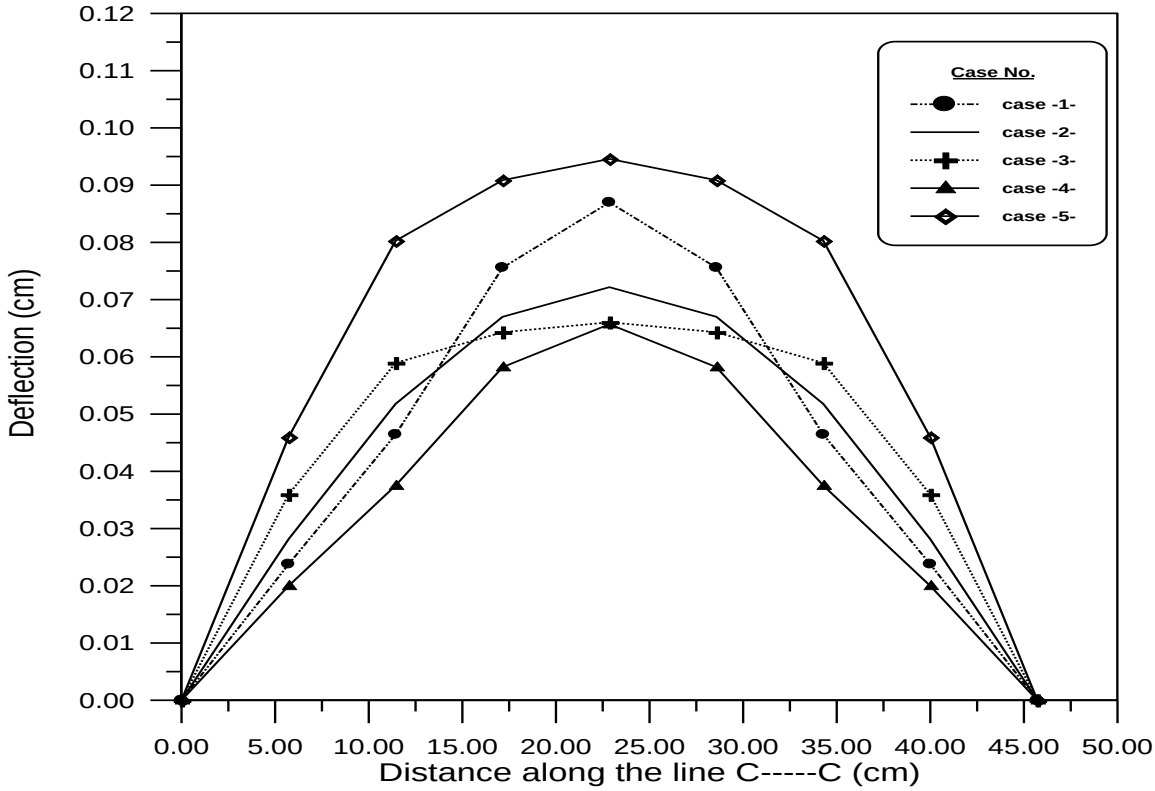

Fig.(5.38) : *Shape of the deflection along a line in the middle of clamped plate using different cases of varying in the thickness.*

5.5.3:ExampleNo.9 : ***square plate with varying thickness subjected to suddenly applied uniformly distributed dynamic load***

A square plate (the same plate in example no.8) subjected to a suddenly applied uniformly distributed dynamic load of (300 psi = 2.07 Mpa) (see Fig.(5.8.b)) is analyzed using 16 elements,[16 elements used here instead of 9 elements to represent the jump in the thickness due to the adding a cover plate], to model a symmetric quadrant of this plate.
The plate geometry and material properties are as explained in example no.8. The thickness of the plates is assumed to be varying with five cases as shown in figure (5.34).

The results obtained using time step equal to 0.00001 sec.

The dynamic response can be seen in figures (5.39),(5.40)for a simply supported plate and (5.41),(5.42) for clamped plate .

Figure (5.39),(the thickness varying in one direction),for simply supported plate, shows that the deflection for case -1- was larger than that ones which are obtained for case -2- and 3, and the difference between case -2- and -3- in amplitude is small, where the all cases 1,2 and 3 give the same volume. So, case -2- can be chosen as the best case , where it is of a uniform thickness and it is easier in working.

Figure (5.40) show a comparing between case 2, 4 and 5, and it is explain that the difference between case 2 and 4 was small in amplitude. Since the volume of case 2 less than that for 4. So, case -2- represents the best distribution for the thickness of the simply supported plates.

When the fixed edges used instead of the simply support, the dynamic response for the plate plots in figures (5.41) and (5.42).

Figure (5.41) shows that the difference between case -2- and -3- becomes grater than that for simply supported plate and reach to 15% in the amplitude. So, case -3- can be chosen as the best case. Now, when a comparing is making between cases 3,4 and 5 in figure (5.42) , the results show that case -5- gives the larger deflection, while the difference between 3 and 4 is less than 5% in the first peak value and after that the difference becomes very small. Since case -4- provides a load capacity larger than case -3- as shown before in Fig.(5.36). So, case -4- will be the best case for the thickness distribution for the clamped square plates.

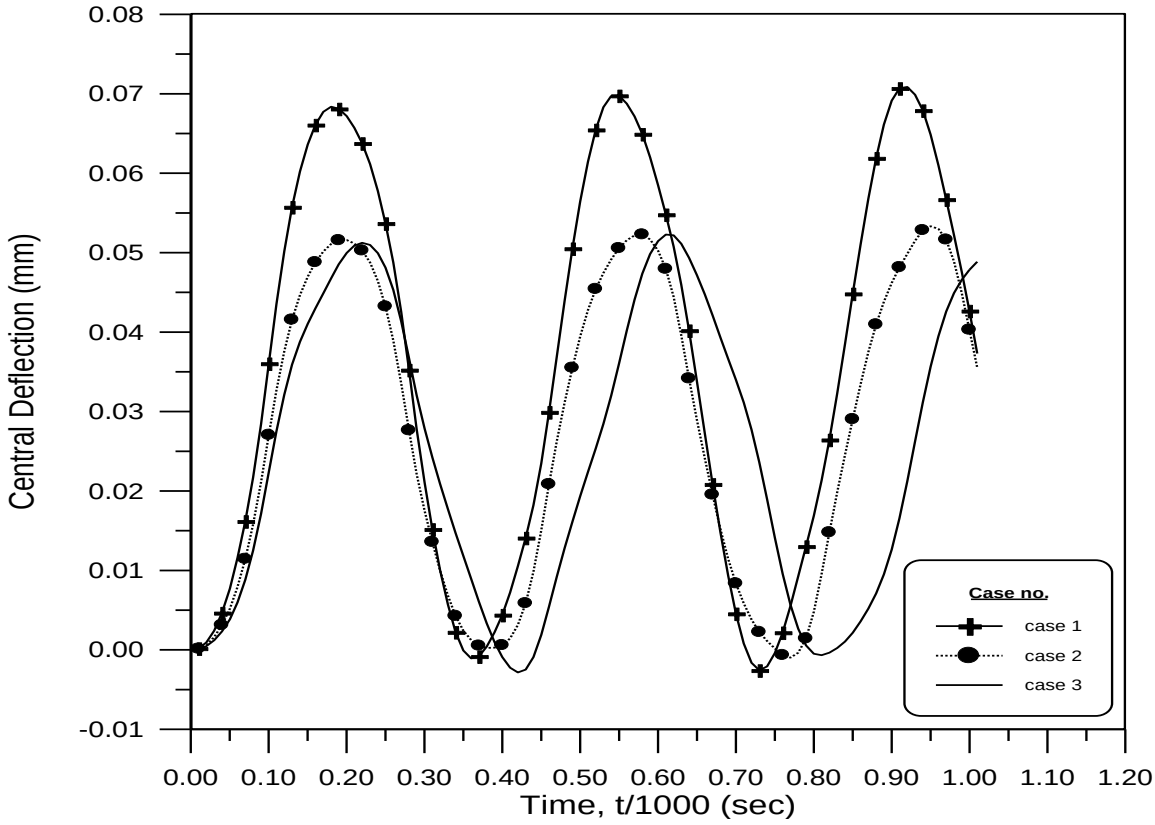

Fig. (5.39): *dynamic response for simply supported plate with varying thickness in one direction subjected to suddenly applied load.*

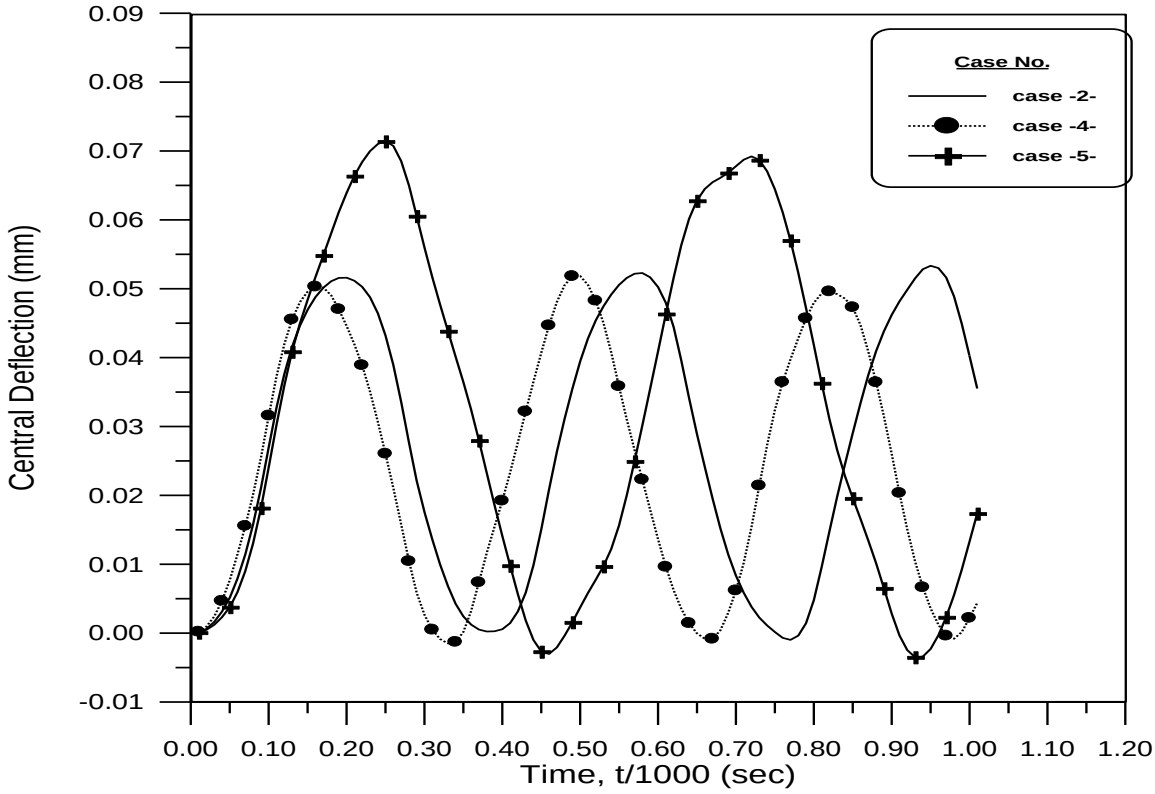

Fig. (5.40): *dynamic response for simply supported plate with varying thickness in two direction subjected to suddenly applied load.*

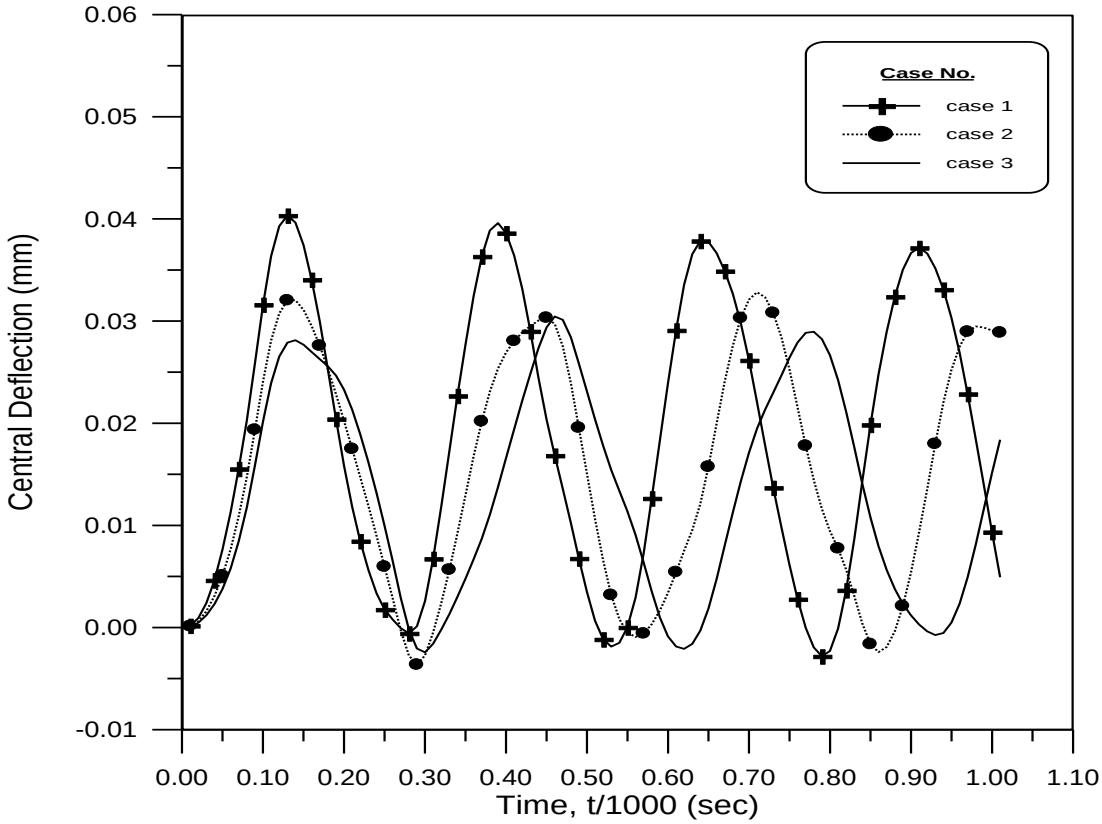

Fig. (5.41): *dynamic response for clamped plate with varying thickness in one direction subjected to suddenly applied load.*

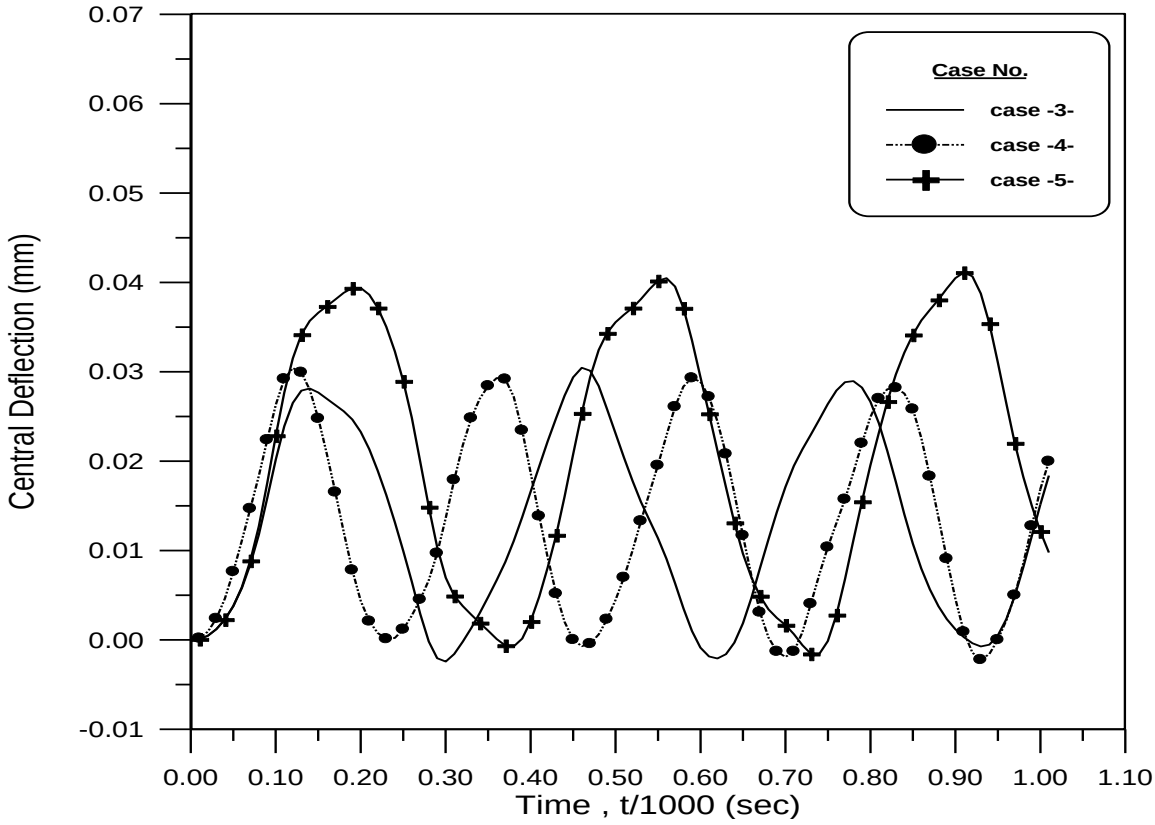

Fig. (5.42): *dynamic response for clamped plate with varying thickness in two direction subjected to suddenly applied load.*

5.5.4:ExampleNo.10 : ***square plate with opening subjected to suddenly applied uniformly distributed dynamic load***

A square plate with opening (see Fig.(5.43.b)) subjected to a suddenly applied uniformly distributed dynamic load of (300 psi = 2.07 Mpa) (see Fig.(5.8.b)) is analyzed using 8 elements to model a symmetric quadrant of this plate. The same plate but without opening(see Fig.(5.43.a)) is analyzed using 9 elements mesh size, the plate(a) is loaded in two ways: the first, the load (300 psi = 2.07 Mpa) is distributed on the whole plate. The second, the load is assumed to be zero on the central area (1/3 a * 1/3 a).

The plate geometry, material properties are as follows:-

length (a) = 18 in = 0.4572m

the thickness (h) = 6 in = 0.1524 m

modulus of elasticity (E) = 0.1 * 10^8 psi =69*10^3 MPa

the mass density (ρ) = 0.2589 Ib/in^3 = 7.157*10^3 Kg/m^3

Poisson's ratio (υ) = 0.3

the yield stress = 57971.0149 psi = 400MPa

The results obtained using time step equal to 0.00001 sec.

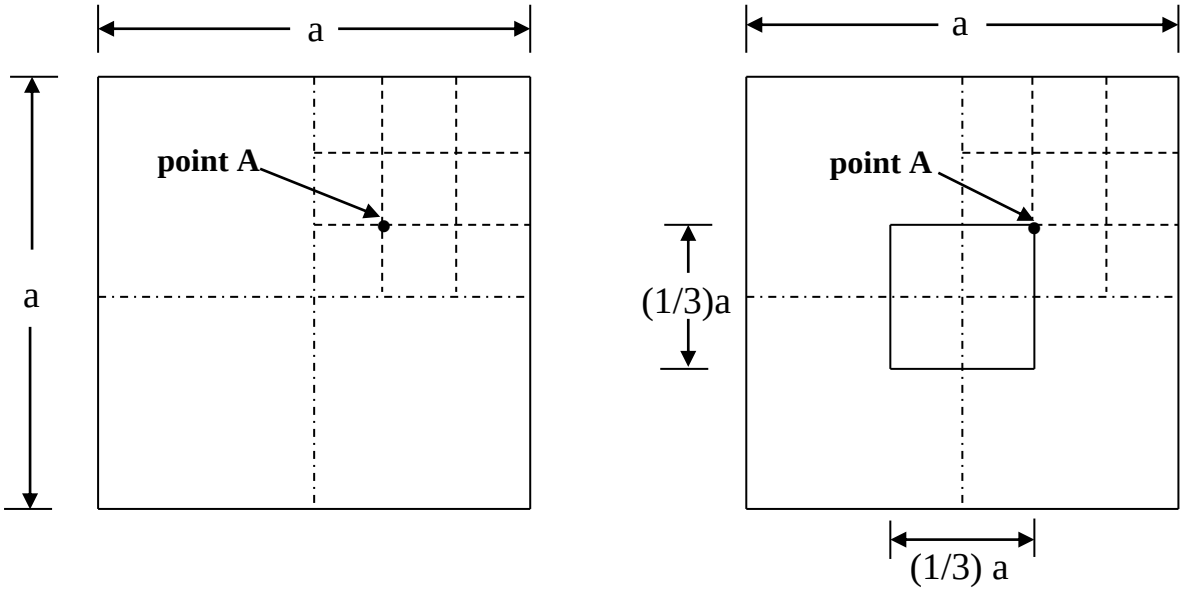

a. *square plate without opening* b. *square plate with opening*

Fig. (5.43): *square plate with and without opening*.

The dynamic response can be seen in figures (5.44) for a simply supported plate and (5.45) for clamped plate .

From figure (5.44), its clear that the deflection for the plate without opening is lesser than that for the same plate with opening, where the opening decreases the plate stiffness.

But, when a clamped supported plate is used in figure (5.45), the results show that the deflection for the plate without opening is larger than that for the plate with opening, due to the effect of lager total load applied on plate without opening. But, when the load assumed to be zero on the central area (1/3 a * 1/3 a) for the plate which is without opening, the effect of the decreasing in the stiffness for the plate with opening appears where, the deflection for the plate with opening become large comparing with the plate without opening (the load on the central area is zero).

So, the effect of opening on the simply supported plate is of more important, where the deflection may be increased by about (39%) when the plate contains opening. But, the effect for the clamped plates is lesser in comparison with the simply supported plate where the deflection increases by about (19%).

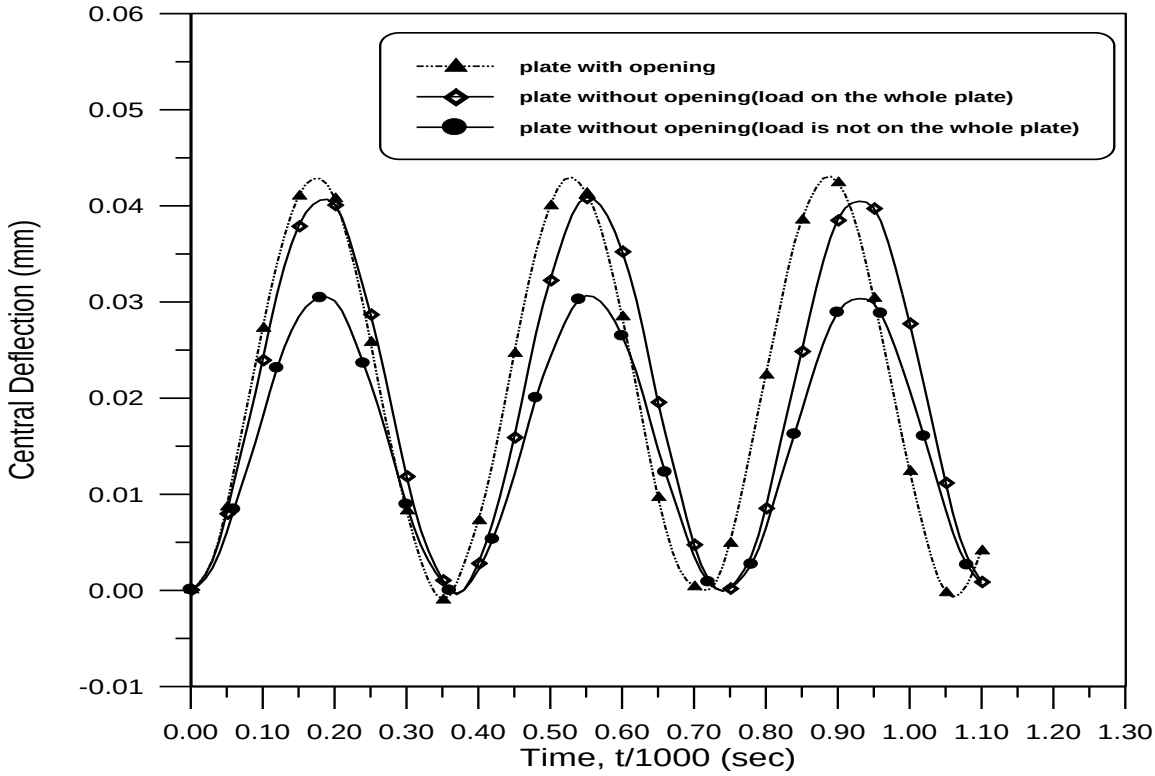

Fig.(5.44) : *Deflection at point A for a simply supported square plate with opening and without opening.*

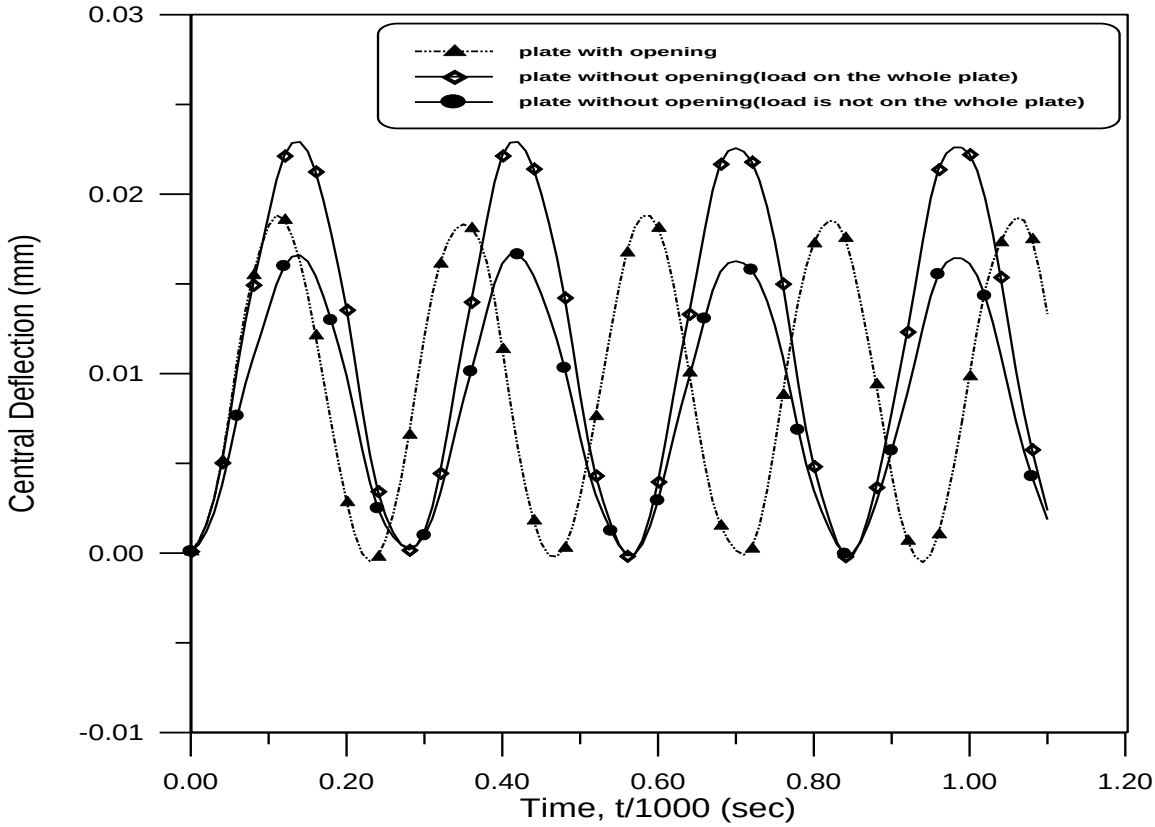

Fig.(5.45) : *Deflection at point A for a clamped supported square plate with opening and without opening.*

CHAPTER SIX

CONCLUSIONS AND RECOMMENDATIONS

6.1 Conclusions

Based on the results obtained from the present analysis procedure, the following conclusions can be drawn:

1. The results of the present elasto-plastic analysis by finite element method including the effect of transverse deformations shear show that this method is suitable for the prediction of the static and dynamic behavior of thin and thick plates. This is proved through a comparison with previous studies with difference not more 10% in results.

2. The elasto-plastic behavior for the plates under dynamic loads is of significant importance in the analysis and design. This is concluded from the results obtained in this research in which, it is clear that the displacements of the elasto-plastic system is greater than that of the assumed purely elastic system for the same amount and type of excitation force, and the difference becomes greater when the yield stress reduced.

3. The vibration for thick plates is really small but with more cycles in comparison with the vibration of thin plates, so thick plates can be used in places which are subjected to a high intensity impact load and need to damp this wave in a shorter time duration.

4. The damping effect for clamped plate is greater than that of the same plate but with simple supports, where in clamped plates, including the damping effect leads to stop the vibration with lesser time in comparison with the simply supported plate(the time reduce by about 33.3%).

5. From the point of view of economy with safety for square plates, prismatic simply supported plate is the best. But, for clamped plates, using stepped plates (through adding cover plate at the edges) may be a good choice.

6. The effect of opening on the simply supported plate is of more important, where the deflection may be increased by about (39%) when the plate contains opening. But, the effect for clamped plates is lesser in comparison with the simply supported plate where the deflection increases by about (19%).

6.2 Recommendations

The following topics are suggested for future studies:

1. This subject requires to be supplemented by experimental results to be obtained from laboratory tests under dynamic loads.

2. The present study has been concerned mainly with the effect of material nonlinearity. A good field for extending the present work is to include the geometrical nonlinearity.

3. Studying the effect of elasto-plastic behavior on the laminated composite plates.

4. Extension the present study to include the effect of the transverse direct stress.

5. Study the thick plate with movable boundary conditions.

References

1. Al-Bidairi S. H. (1998) ,"***Large Displacement Elastic Stability Analysis of Plane Steel Frames Including Shear and Damping Effects***", M.Sc. thesis, University of Babylon, Iraq.

2. Albarwary J. H. (2006) , "***Dynamic Analysis of Plates Using Finite Layer Method***" ,M.Sc. thesis, University of Mosul, Iraq.

3. Ali N. H. (2004), "***Finite Element Dynamic Analysis of Laminated Composite Plates Including Damping Effect*** ", M.Sc. thesis, University of Babylon, Iraq.

4. Al-Saeq H. M. (2005), "***Optimal Design of Plate and Shell Structures Based on Nonlinear Finite Element Analysis*** " ,M.Sc. thesis, University of Babylon, Iraq.

5. Alwash N. A. (1989), "***Elasto-Plastic and Limit Analyses of Thick Plates***", M.Sc. thesis, University of Baghdad, Iraq.

6. Alwash M. F. (2002), "***Structural Behavior of Piles During Driving***", M.Sc. thesis, University of Babylon, Iraq.

7. Argyris J. ,Papadrakakis M. ,Mouroutis Z. and Papachrisitidis A. G. (2002) , "***Nonlinear Dynamic Analysis of Shells with the TRIC Shell Element*** ", Computational Mechanics, pp. 1-11.

8. Bathe K. J. (1982),"***Finite Element Procedures in Engineering Analysis***", Prentice –Hall Inc., Englewood Cliffs, New Jersey.

9. Bathe K. J. (1996),"***Finite Element Procedures***", Prentice –Hall Inc., Englewood Cliffs, New Jersey.

10. Bert Ch. W., Jang S. K. and Striz A. G. (1989), "***Nonlinear Bending Analysis of Orthotropic Rectangular Plates by the Method of Differential Quadrature*** ", Computational Mechanics, Vol. 5, pp.217-226.

11. Biggs J. M. (1964), "***Structural Dynamics***", 1st Edition, McGraw-Hill Inc., USA.

12. Chen X. and Austin M. (1995), "***A system Approach to Nonlinear Finite Element Analysis of Shell Structures*** ", Technical Research Report, Sponsored by the National Science Institute Foundation, Engineering Research Center Program, University of Maryland, Harvard University, and Industry.

13. Chen H. ,Hong M. and Liu Y. (2004), "***Dynamic Behavior of Delaminated Plates Considering Progressive Failure Process***", Composite Structures, Vol.66, pp.459-466.

14. Cheung Y. K., Zhu D. S. and Iu V. P. (1998), "***Nonlinear Vibration of Thin Plates with Initial Stress by Spline Finite Strip Method***", Thin-Walled Structures, pp.275-287.

15. Cheung M. S. and Chan M. Y. T. (1981), "***Static and Dynamic Analysis of Thin and Thick Sectorial Plates by the Finite Strip Method***", Computers& Structures, Vol.14, pp.79-88.

16. Clough R. W. and Penzien J. (1982), "***Dynamics of Structures***", McGraw-Hill.

17. Cook, R. D., Malkus D. S., and Plesha M. E.(1989)," ***Concepts and Applications of Finite Element Analysis***", 3rd Edition, John Wiley & Sons Inc., New York, London.

18. Craig R.R. (1981), "***Structural Dynamics***", John Wiley & Sons Inc., USA1.

19. Haitham I. (2003), "***Nonlinear Dynamic Analysis of Reinforced Concrete Stiffened Shells Using The Finite Element Method***", PhD. dissertation, University of Mosul, Iraq.

20. Hart G.C., and Wong K. (2000), "***Structural Dynamics for Structural Engineers***", John Wiley & Sons Inc., USA.

21. Hughes T. J. R., Taylor R. L. and Kanoknukulchai W. A. (1977), "***Simple and Efficient Finite Element for Plate Bending***", I. J. N. M. E. Vol.11, 1529-1543.

22. Hurty W.C., and Rubinstein M.F. (1964), "***Dynamics of Structures***", Prentice –Hall Inc., Englewood Cliffs, New Jersey.

23. Johnson W. and Mellor P. B. (1978), "***Engineering Plasticity***", van Nostrand Reinhold Company Ltd.

24. Karkush M. O. (1998), "***Non-Linear Behavior of Folded Plate Structures***", M. Sc. thesis, University of Babylon, Iraq.

25. Kocak S. and Hassis H.(2003), "***A higher Order Shear Deformable Finite Element for Homogeneous Plates***", Engineering Structures, Vol.25, Issue 2, pp.131-139.

26. Kwak, H. G., and Flippou, F. C.(1990). "***Finite Element Analysis of Reinforced Concrete Structures Under Monotonic Loads***", Report No.UCB/SEMM-90/14 Structural Engineering,Mechanics and Materials Department of Civil Engineering University of California,Berkeley.

27. Moshaiov A. and Vorus W. S. (1986), "***Elasto-Plastic Plate Bending Analysis by a Boundary Element Method with Initial Plastic Moment***", Int. j. Solids Structures, Vol.22, No.11, pp.1213-1229.

28. Newmark N. M. (1962), "***A method of Computation for Structural Dynamics***", Transaction, ASCE, Vol.127, Part I, Paper No.3384, pp.1406-1435.

29. Norris C. H., Hanssen R. J., Holley M. J., Nameyt S. and Minami J. K. (1959) , "***Structural Design for Dynamic Loads***", McGraw-Hill Company, USA.

30. Owen D. R. J. and Figueiras J. A. (1983), "***Elasto-Plastic Analysis of Anisotropic Plates and Shells by the Semiloof Element***", International Journal of Numerical Methods in Engineering, Vol.19, pp.521-539.

31. Owen D . R. J and Figueiras J. A. (1983), "***Anisotrapic Elasto-Plastic Finite Element Analysis of Thick and Thin Plates and Shells***", International Journal for Numerical Methods in engineering, Vol.19, pp.541-566.

32. Petyt M. (1990) "***Introduction to Finite Element Vibration Analysis***", Cambridge University Press.

33. Providakis C. P. ,Beskos D.E. and Sotiropoulos D.A (1994), "***Dynamic Analysis of Inelastic Plates by the D/BEM***", Computational Mechanics Journal, Vol.13, No.4, pp.276-284.

34. Raghavan K. S. and Rao S. S,(1978), "***Influence of Elasto-Plastic Transition on the Inelastic Response of Beams and Plates***", Journal of Applied Machanics, Vol.45, pp.521-526.

35. Reddy J. N. (1984), "***An Introduction to the Finite Element***", First Edition, McGraw-Hill, Inc., USA.

36. Reddy J. N. and Haung C. L. (1981), "***Non Llinear Axisymmetric Bending of Annular Plates with Varying Thickness***", Int. j. solids and structures, Vol.17, pp.811-825.

37. Ross C. T. F. (1990), "***Finite Element Methods in Engineering Science***", 1st Edition, Ellis Horwood Limited, England.

38. Roy P.K and Ganesan N.(1995), "***Studies on the Dynamic Behavior of a Square Plate with Varying Thickness***", Journal of Sound and Vibration, Vol.182, Issue 3, pp.355-367.

39. Sladek J., Sladek V., and Mang H. A. (2003), "***Meshless LBIE Formulations for Simply Supported and Clamped Plates under Dynamic Load*** ", Computers and Structures, Vol.81, pp.1643-1651.

40. Striz A. G., Jang S. K. and Bert Ch. W. (1988) "***Nonlinear Bending Analysis of Thin Circular Plates by Differential Quadrature***", Thin-Walled structures, Vol.6, Issue 1, pp.51-62.

41. Subbaraj K., and Dakainish M.A. (1989), "***A Survey of Direct Time – Integration Methods in Computational Structural Dynamics – II. Implicit Methods*** " , Computers and Structures, Vol. 32, No.6, pp. 1387-1401.

42. Zhao-ping J., Chang-Chun W. and Pian T. H. H., (1994), "***Geometrically Nonlinear Analysis of Mindlin Plate using the Incompatible Bending Elements with Internal Shear Strain*** ", Applied Mathematics and Mechanics, Vol. 15, No.6, pp.507-516.

43. Zhou sh. J. (2002), "***Load-induced Stiffness Matrix of Plates***", Con. J. Civ. Eng., Vol.29, PP.181-184.

44. Zienkiewiez O.C. (1977), "***The Finite Element Methods***", 3rd Edition, McGraw-Hill Book Company, London.